Engaging the Immune Response to Normalize the Tumor Microenvironment

by

Nina Chi Sabins

B.S., Villanova University, 2003

M.B., University of Pennsylvania, 2005

Submitted to the Graduate Faculty of

School of Medicine in partial fulfillment

of the requirements for the degree of

Doctor of Philosophy

University of Pittsburgh

2013

UNIVERSITY OF PITTSBURGH

SCHOOL OF MEDICINE

This dissertation was presented

by

Nina Chi Sabins

It was defended on

July 19, 2013

and approved by

Lisa Butterfield, Ph.D., Associate Professor, Department of Medicine

Olivera Finn, Ph.D., Distinguished Professor, Department of Immunology

Adriana Larregina, M.D., Ph.D., Associate Professor, Department of Dermatology

Hideho Okada, M.D., Ph.D., Professor, Department of Surgery

Donna Beer Stolz, Ph.D., Associate Professor, Department of Cell Biology

Dissertation Advisor: Walter J. Storkus, Ph.D., Professor, Department of Dermatology

Engaging the Immune Response to Normalize the Tumor Microenvironment

Nina Chi Sabins, Ph.D.

University of Pittsburgh, 2013

Solid tumors exist as heterogeneous populations comprised not only of malignant cells, but various other cell types, including cells that make up the vasculature, that can strongly influence tumorgenicity. Many forms of solid cancers are highly vascularized due to dysregulated angiogenesis. The tumor vasculature is classified by leaky, chaotic blood vessels consisting of several components including vascular endothelial cells and pericytes, as well vascular progenitors, resulting in vascular permeability and high interstitial pressure. As a result, the tumor vasculature limits the access of immune effector cells to the tumor, and may in part be responsible for the modest success observed in many current anti-cancer immunotherapies. Current first-line therapeutics in the advanced stage disease setting include anti-angiogenic small molecule drugs that have yielded high objective clinical response rates, however these responses tend to be transient in nature, with most patients becoming drug-refractory. Anti-tumor vasculature vaccines may promote the reconditioning of the tumor microenvironment by coordinately promoting a pro-inflammatory environment and the specific immune targeting of tumor-associated stromal cell populations that contribute to vasculature destabilization. Implementing a vaccine with these therapeutic effects is a promising treatment option that may extend disease-free intervals and overall patient survival. I show that vaccines specifically targeting tumor vasculature populations can "normalize" the tumor microenvironment, as shown by upregulation of proinflammatory molecules within the tumor as well as vascular remodeling promoting enhanced recruitment of $CD8^+$ T cells, resulting in superior anti-tumor efficacy.

TABLE OF CONTENTS

LIST OF TABLES

LIST OF FIGURES

PREFACE

I must first thank my advisor, Dr. Walter Storkus, for accepting me into his lab and providing me knowledge, insight, guidance, and support in all aspects of my life for the past five years. I want to specifically thank Walt for continuing to believe in me when my experiments weren't working, for staying positive throughout my paper submission process, and for encouraging and supporting me in my career choices as a scientist. I would like to thank my Thesis Committee for their feedback on my project because it truly helped shape my paper into what it is today. I would also like to thank my friends in the Storkus lab for making the lab such an enjoyable place.

I want to acknowledge my father who defeated Hodkins Lymphoma more than twenty years ago, and to my mother who lost her battle to non-small cell lung adenocarcinoma twelve years ago. They have been my inspiration in entering the field of cancer research so that one day no one has to lose this battle.

And lastly I want to thank my husband, Erik, who encouraged me to pursue a Ph.D., who moved with me to build a life in Pittsburgh, who supported me through all the ups and downs of graduate school, and who gave me the greatest treasure of my life, my daughter CeCe.

To you all, I dedicate this dissertation.

1.0 INTRODUCTION

Functional immunity protects the body from a broad span of dangers through different processes, from destroying external pathogenic microbes to controlled killing of abnormal cells arising from genetic mutation. Countless studies have been performed showing the adaptive response as the dominant mechanism in the rejection of tumors, particularly the activation of $CD4^+$ helper T cells, $CD8^+$ cytotoxic T cells, and antibodies (Ab), thus prompting extensive efforts in the development of immunotherapies that can activate T cells against cancers (1). The first cancer antigen (Ag) discovered to be recognized by T cells was MAGE1 found to be expressed in melanoma over two decades ago (2). Since then many more markers have been identified to be expressed on solid tumors of various tissue origin that are recognizable by the immune system (3).

While the findings in this thesis are applicable to all forms of vascularized solid cancer, we adopted renal cell carcinoma (RCC) as our model due to its intrinsic immunogenic nature (4). RCC accounts for approximately 3% of all cancers in adults, with metastases identified in 20-30% of patients at the time of initial diagnosis. Metastatic RCC, if left untreated, has a 5-year disease-free survival rate of only 2-11% (5). Following nephrectomy, conventional treatments with standard chemotherapeutic agents, hormones, and radiotherapy have exhibited minimal success. This has prompted extensive evaluation of alternate treatment strategies, including immunotherapies, in advanced stage disease settings.

1.1 IMMUNE TARGETING OF RCC

Although administration of high-dose interleukin-2 (IL-2) has yielded durable complete responses in a small minority of treated patients with metastatic RCC, severe toxicities have also been observed with this approach (5), suggesting the need to identify more specific and focused immunotherapy approaches.

1.1.1 Cellular vaccines for RCC

Reports have shown that Type-2 T cell responses (typically characterized by IL-4 and IL-5 production and associated with humoral immunity and allergic reactivity) may be repolarized towards Type-1 [*i.e.*, producing interferon-γ (IFN-γ) and capable of mediating the cytotoxic death of tumor cells] immunity *in vitro* by stimulation with antigen-pulsed dendritic cells (DC) that were pre-conditioned with pro-inflammatory cytokines, toll-receptor ligands (TLR), and other costimulatory adjuvants (6-8). In humans, Type-1 effector T cells have exhibited extended survival, function and conversion into the memory cells when provided signals from $CD16^+$ monocyte-derived DC (9). Furthermore, Type-1 polarized DC appear superior to alternate antigen presenting cell (APC) types in their capacity to activate and drive naïve T cell differentiation into Type-1 $CD4^+$ and $CD8^+$ T effector cells *in vitro* and *in vivo* (8, 10, 11). While much of this data has been developed clinically in the context of cell (*i.e.*, DC)-based therapeutics, it would also be predicted that cell-free vaccine formulations including the appropriate tumor antigens and conditioning adjuvants would activate APC *in situ* with similar Type-1-polarizing potential (12-14).

Several vaccine formats have been designed to promote specific adaptive immunity against RCC. One format of vaccine is the RCC cells themselves (either autologous or allogenic cells that express unique and shared tumor-associated antigenic proteins). The first attempt was made over twenty years ago when one group trialed autologous RCC tumor cells using C. *parvum* as adjuvant (15). Later, other investigators modified the autologous tumor cell vaccine by using granulocyte macrophage-colony stimulating factor (GM-CSF) or other inflammatory cytokines as adjuvant (16). Soon thereafter, others used genetically modified patient tumor cells that expressed inflammatory cytokines including GM-CSF, IFN-γ, and IL-2 (17). Another tumor vaccine formulation is represented by RCC-APC fusion hybrids, which generate APC that are capable of expressing RCC gene products and presenting their derivative peptide epitopes to T cells. Using serial electrical pulses, autologous RCC tumor cells could be fused to DC from normal donors (18). Another approach involves RCC-derived total mRNA or cDNA (encoding the complete repertoire of RCC-associated antigens). While most published work using these vaccines has been limited to preclinical models (19, 20), there has been one clinical report using autologous DC transfected with total RCC RNA (21).

More recently, several labs have been moving towards a more specified vaccine format using peptides, protein, mRNA or cDNA derived from or encoding one or more molecularly-defined RCC-associated antigens (RCCAA). In one trial, RCC patients were vaccinated with autologous DC loaded with carbonic anhydrase-IX (CA-IX) peptides, and while the treatment was well tolerated, patients did not show CA-IX specific immunity and there was no observable clinical response (22). In another RCC trial, however, where patients received MUC1 pulsed-DC, several patients exhibited MUC1-specific T cell reactivity along with objective responses (23). Just last year, it was reported that patients receiving a vaccine consisting of multiple

RCCAA peptides, administered intradermally with GM-CSF, exhibited immune responses to multiple RCCAA with decreased regulatory T cells, correlating with improved disease control and overall survival (24). These mixed results indicate the therapeutic potential of DC-peptide based vaccines in RCC, but also highlights the need for fine-tuning of antigen selection and vaccine formulation. In general, vaccines based on specific RCCAA or their derivative peptides that can be presented on major histocompatibility complexes (MHC) have lagged behind due to the comparatively recent molecular identification of these antigens.

1.1.2 Genetic vaccines for RCC

An alternative approach to cellular-based vaccines is *in situ* genetic vaccination using recombinant viral-based deliver systems. Various reports have shown virus-based vaccinations possess therapeutic advantages over protein antigen/adjuvant-based approaches (25, 26), presumably due to the intrinsic pro-inflammatory properties of viruses (*i.e.*, via activation of TLR expressed by APC) and their ability to infect professional APC, allowing for ectopic expression of the vaccine antigen within patient dendritic cells (27-29). Additionally, high-titer recombinant viruses are easy to produce and when compared to cell-based therapies that require costly time-consuming methods due to their patient-specific nature, viral vectors can be administered to any given patient as an "off-the-shelf" treatment modality. Thus, despite minor concerns for replication-competent contaminant virus or for insertional mutagenesis in the case of retroviruses (30), genetic vaccines remain attractive treatment options in the cancer setting.

The recombinant modified vaccinia virus Ankara (MVA) encoding RCC antigen 5T4, (TroVax®) has been tested in several clinical trials. Initial trials in RCC patients showed some objective clinical responses after administration of the TroVax® vaccine (31, 32), however in

phase III trials employing TroVax® with or without cytokines (IFN-α and IL-2) in combination with the approved first-line treatment tyrosine kinase inhibitor, sunitinib, no significant difference in survival between the experimental and control groups could be demonstrated (33). A second MVA vaccine was developed containing the recombinant MUC1 and IL-2 transgenes, administered with or without cytokines. Although some RCC patients exhibited anti-MUC1 T cell responses, treatment with this vaccine formulation did not result in objective clinical responses based on RECIST criteria (34).

It is important to note there are non-viral molecular vaccines under development for RCC. One such approach a direct intradermal injection of multi-antigen mRNA-based vaccine encoding MUC1, CEA, Her-2/neu, telomerase, survivin, and MAGE-A1 has been evaluated in a phase I/II clinical trial involving 30 RCC patients. The reported results were promising, with some vaccinated patients exhibiting stable disease and coordinately increased tumor antigen-specific T cell responses (35).

1.1.3 Clinical responses to current vaccine treatment for RCC

Despite recent discussions that immunotherapies should not be evaluated based on the "acute" RECIST criteria defined for chemotherapeutic agents because immunotherapies may depend on the gradual build up of adaptive immunity over a protracted period of time (36, 37), virtually all reported RCC vaccine trials currently still do so. Therefore, I have depicted objective clinical response frequencies based on partial responses (PR), complete responses (CR) or stabilization of disease (SD) per RECIST criteria as reported by the primary investigators (**Figure 1**). The consensus of such information suggests that current RCC vaccines are generally safe and well-tolerated (38), but are curative in only a very minor subset of treated patients.

While partial responses increase somewhat after vaccine treatment, the major benefit of these cancer vaccines is reflected in the many patients that exhibit stable disease, translating into increased progression-free and overall survival when compared to control groups (38-41). Notably, each of the various vaccine formulation categories listed yielded similar clinical impact based on RECIST criteria (**Figure. 1**) with roughly 50% of treated patients exhibiting stable disease, 20% showing partial response and <20% developing complete responses.

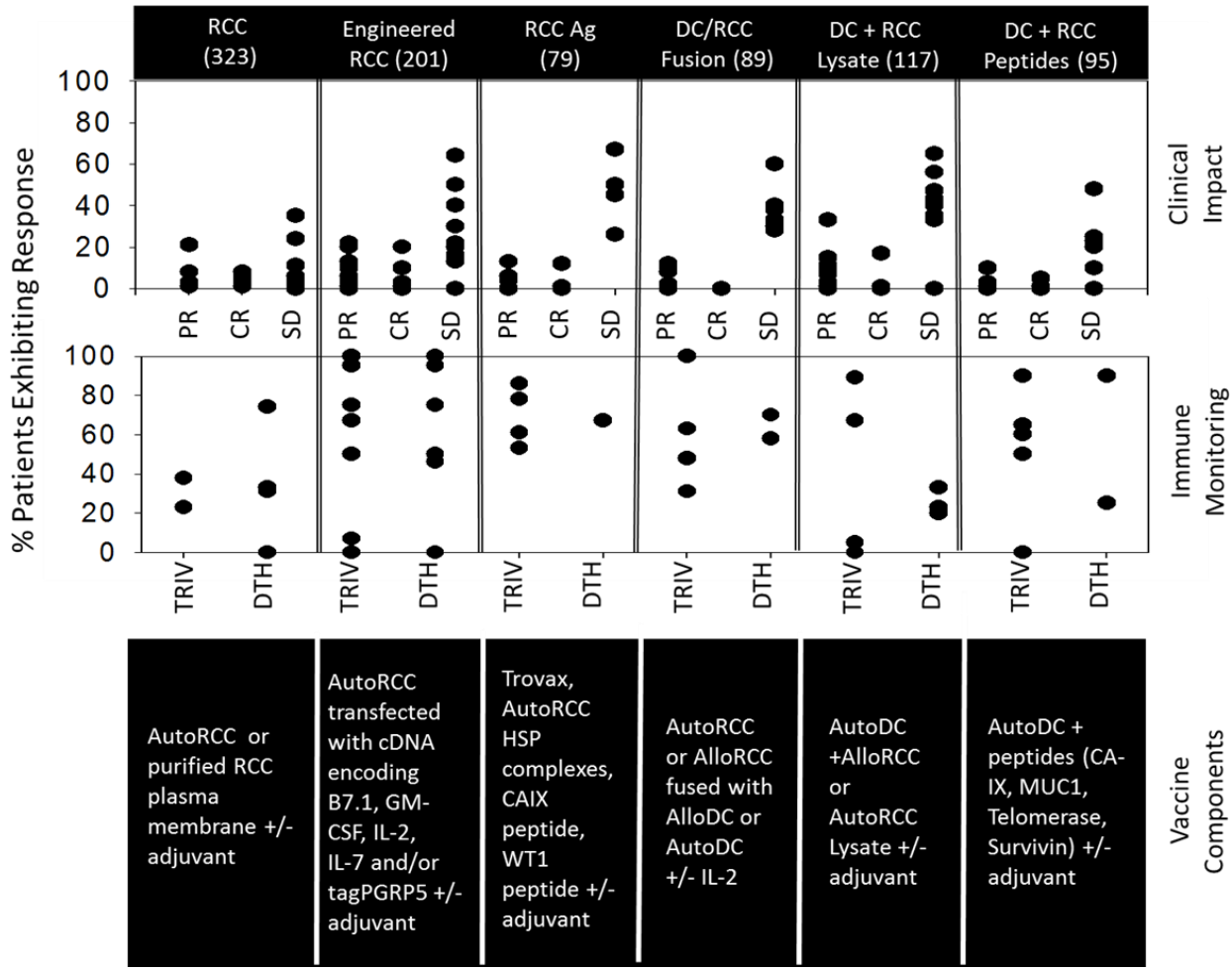

Figure 1. Trial outcomes based on the clinical and immunologic endpoints.
Objective clinical response frequencies based on partial responses (PR), complete responses (CR) or stabilization of disease (SD) per RECIST criteria and patient tumor-specific T cell responses in vitro (TRIV) and delayed-type hypersensitivity (DTH) responses to vaccine components in vivo as reported by the primary investigators.

1.1.4 Immune responses to current vaccine treatment for RCC.

Since these represent immunotherapies rather than chemo- or radiotherapies, immunologic endpoint analyses are critical in determining the biologic efficacy of these approaches and how such strategies may be improved based on our current understanding of RCC immunobiology. In this regard, the diverse array of RCC vaccine trials performed over the past 15 years has implemented a number of immune assessment assays to determine specific immune response to active vaccination; including analyses of patient tumor-specific T cell responses *in vitro* (TRIV) and delayed-type hypersensitivity (DTH) responses to vaccine components *in vivo*. Assays for TRIV have dramatically evolved over the past decade, with established proliferation (*i.e.*, ^{3}H-thymidine incorporation) and cytokine (*i.e.,* ELISA) assays now being supplemented by additional methods capable of discerning the frequency and/or functionality of clonal T cell responses [*i.e.,* cytokine ELISPOT assays, intracellular staining of T cells for cytokines (predominantly IFN-γ) production and reactivity of T cells with fluorescently-labeled, recombinant MHC-tumor peptide multimers]. The merits and perceived weaknesses of these various methods have been well discussed in the past (42-44).

In **Figure 1**, I include a sampling of the reported clinical trial data that supports the capacity of RCC vaccines to promote an increase in RCC-specific T cell responsiveness. Although the frequency of immunologically-responsive patients was highly variable within a given treatment format, in many cases the majority of treated patients exhibited detectable increases in TRIV at some point post-vaccination. Similarly, DTH analyses suggest that RCC vaccines have been generally competent to promote tissue inflammation at sites of vaccination (mediated by Type-1 T cells). Unfortunately, detectable TRIV and DTH as determined by current methods, even at high percentages, do not appear to directly correlate with clinical

outcome (**Figure 1**), implying that other factors within the TME may inhibit vaccine efficacy and that tumor cells (and their associated antigens) may not serve as the most effective targets for immunotherapy, thus reinforcing the need for improved treatments against RCC.

1.2 THE TUMOR MICROENVIRONMENT

Within the tumor microenvironment (TME) is a heterogeneous population of various cell types that are distinct from the tumor cells themselves. Among the non-tumor (*i.e.*, stromal) cells of the TME are fibroblasts, mesenchymal stem cells (or cancer stem cells), vascular cells, such as neutrophils, myeloid-derived suppressor cells, mast cells, and lymphocytes (45). These cells serve various functions that could be either pro- or anti-tumor, depending on signals that are systemic or within the TME.

1.2.1 Adaptive T cell response against tumor

To activate potent anti-tumor immunity, APC, particularly DC, are required to undergo several processes. Dendritic cells are a professional type of APC specialized in the detection of tissue damage, pathogen entry, and inflammation (46), and the first step involves their capture and processing of tumor protein antigens. DC can acquire antigens by various endocytic routes such as phagocytosis, macro/micro-pinocytosis, and receptor-mediated endocytosis (*e.g.*, Ab-Ag complexes via Fc receptors or C-type lectins.) These antigens are then processed through the MHC class II pathway for presentation to $CD4^+$ T cells, or translocated to the cytosol to enter the MHC class I pathway for "cross-presentation" to $CD8^+$ T cells (47). Immature DC present the

antigenic peptides, and are activated by pro-inflammatory cytokines, such as IFN-γ and TNF-α, to express costimulatory molecules, such as CD80/86, as well as increased expression of MHC on their surface. The next step is for tumor-specific naïve T cells to differentiate into effector T cells. This event occurs as a result of the combination of signaling from T cell receptor (TCR) binding to the antigen peptide-loaded MHC on the DC and the binding of costimulatory molecules expressed by the T cells and the DC, such as CD28 and CD80/86, respectively. Activated cytotoxic T lymphocytes (CTL) will then recognize cells expressing the specific antigens to which they were primed against and induce target cell lysis. However, despite the comprehensive list of tumor-associated antigens found to be immunogenic, solid tumors continue to progress and metastasize in generally immune-competent individuals (**Figure 1**) (48). Tumor cells possess the ability to adapt and evade the immune response by down-regulating MHC molecules on their surface, abrogating the ability for T cell recognition and inducing T cell anergy. Additionally, solid tumors can secrete immunosuppressive factors [*i.e.*, tumor growth factor-β (TGF-β), IL-10] into their local environment or systemically that can thwart the immune response.

1.2.2 Immune dysfunction within the tumor microenvironment

Optimism for the use of biologic response modifiers and vaccines has been buoyed by past findings suggesting that RCC progression/regression may be regulated by immunologic mechanisms (49). Patients with RCC exhibited a low but significant incidence of spontaneous regression (50), and patients under chronic immunosuppression regimens to retain kidney allografts displayed an increased risk of developing RCC (51). The degree of tumor infiltration by lymphocytes has been used as a prognostic indicator for patient survival (52). In particular, T

cells with a Type-1 polarization profile and high proliferative potential (53), have proven to represent primary immunologic mediators of objective clinical responses.

However, patients with RCC are frequently characterized with a state of "immune dysfunction" (53-56), where Type-1 responses directed against RCCAA are muted in comparison to Type-2 and/or T-regulatory (Treg) responses, which favor humoral responses in nature (57-60). Furthermore, when they can be identified, Type-1 anti-RCCAA T cells may be pro-apoptotic given a chronic state of stimulation with specific tumor antigens in the cancer-bearing patient (61, 62).

Additional factors in solid tumors can lead to impaired effector T cell and DC function, including hypoxia (63). Upregulated hypoxia inducible factor (HIF) expression leads to increased vascular endothelial growth factor (VEGF) expression, which can generate regulatory/tolerogenic DC and/or attenuate DC differentiation. VEGF can also increase STAT3 activation via VEGF receptor-2 (VEGFR2)-mediated signaling, thus promoting the intrinsic expression of immunosuppressive factors including IL-10 and TGF-β in these regulatory DC (64). In many cancer patients, Type-1 pro-inflammatory responses required for tumor destruction are inhibited or functionally dysregulated by the suppressive influence of Treg or myeloid-derived suppressor cells (MDSC) with or without the addition of Type-2 inflammatory molecules (59-62).

It has recently been shown that tumors can inhibit the Notch pathway in T cells through reductions of Delta like ligand (DLL)-1 and -4 expression, thereby suppressing their function and allowing for tumor immune escape (65). Additionally, reduced Notch activation within the TME has been reported to promote accumulation of IL-10 producing M2 macrophages in tumors and reducing the number of IL-12 producing M1 anti-tumor macrophages (66, 67). Such immune-

evasion tactics assumed by the tumor serve to limit the protective host immunological responses and allow for tumor survival and progression. In addition, the destabilized vasculature in progressively growing tumors can further abrogate effective immune responses by preventing circulating Type-1 anti-tumor T effector cells to traffic efficiently to sites of tumor (68). These limitations observed in anti-tumor immunotherapy alert the need for alternative approaches towards solid cancer treatments, including targeting of the vasculature within the tumor microenvironment.

1.2.3 Angiogenesis and the vasculature

The cancerous features of tumor cells cannot manifest without the important interplay between cancer cells and their environment. Various cell populations reside within the TME including the cancer cells themselves and self-renewing cancer stem cells (CSC), as well as cells the make up the vasculature (*i.e.*, VEC and pericytes). Blood vessels in the TME support cancer progression by: i.) delivering oxygen and nutrients, ii.) providing a conduit by which primary tumors can metastasize, iii.) recruiting/supporting cancer stem cells and vascular cell precursors that promote tumor neovascularization, and iv.) recruiting immune regulatory cell populations (*i.e.*, Treg, MDSC, M2 macrophages). Solid tumors of various tissue types, including renal, ovarian, and lung, are typically highly-vascularized, with dysregulated angiogenesis resulting from excessive growth-promoting signals and a lack of sufficient cues to spatially and temporally coordinate vessel growth, remodeling, maturation, and stabilization. Under physiological conditions, angiogenesis is a vital process that supplies normal organs and tissue with oxygen and nutrients while disposing of catabolic products (69). Multiple steps are necessary for functional angiogenesis, the first being the partial degradation of the extracellular

matrix (ECM) and opening and migration of existing capillaries, allowing for migration of endothelial cells towards avascular areas. VEC are guided by VEGFA, which is induced by hypoxia, via their expression of VEGFR2 on their cell surface (70). A VEGFA gradient promotes the infiltration of a subset of VEC, tip cells, toward the avascular, hypoxic region, with high VEGFA concentrations inducing stalk cell proliferation to form a new vessel sprout (71). These tip cells become proteolytic in function and begin breaking down the vascular basement membrane with matrix metalloproteinases (MMP), triggering a series of signaling cascades that result in cytoskeleton reorganization and sprouting morphogenesis of VEC. VEGF also induces expression of Notch ligand DLL4 along Notch1 and Notch4 receptors. DLL4-Notch interactions limit excess angiogenesis and promote the orderly development of new blood vessels (72). This resolution step turns off VEC proliferation and signals the recruitment of pericytes and vascular smooth muscle cells, which provide stabilization and maturation to the vessel (73). Pericytes originate from arterioles and possibly from bone marrow-derived progenitors and are primarily recruited by platelet-derived growth factor (PDGF) that is secreted by endothelial cells, via expression of PDGF receptor β (PDGFRβ). Pericytes also express angiopoetin-1 (Ang-1) on their surface, which binds to Tie2 receptors on VEC. Contact between VEC and pericytes switches off the proteolytic activity of the VEC and leads to the tight junctions and adherens junctions that seal the vessel. Pericytes can also inhibit endothelial cell division via TGF-β activation (74). As new capillaries mature, pruning of excess or unnecessary vessels promote optimal perfusion. There is controversy regarding the role of pericytes in tumor vasculature, with some reports suggesting preventing pericyte recruitment through PDGFRβ inhibition may have anti-tumor benefits, while other studies have shown that decreased pericyte coverage leads to increased metastases (75, 76). In addition, pericytes are believed to possess pluripotent

characteristics of stem cells with the ability to differentiate into various cell types (77, 78). These confounding findings emphasize the need for better understanding of the role pericytes play is vessel homeostasis and maturation within the TME.

1.2.4 Abnormalities of the tumor vasculature

Under normal physiological conditions, the cellular processes that occur during angiogenesis are turned off once vascular perfusion is achieved. However, during tumor pathogenesis, the angiogenic cascade of events persists and fails to resolve in a controlled manner. The vasculature in the TME is typically characterized as "abnormal," here defined as tortuous, irregular networks of blood vessels with highly unstable and permeable capillaries branching from the main vessel bed. Instability in the tumor vasculature increases interstitial pressure within the tumor, preventing the delivery of tumoricidal drugs and immune effector cells into the TME (73, 79). Many cancers have increased VEGF expression due to various environmental cues (*i.e.,* hypoxia, gain of oncogene and/or loss of tumor suppressor function), which contribute to the abnormal vasculature observed in solid tumors. Inhibition of the Ang-Tie2 interaction between VEC and pericytes has also shown to be a factor contributing to tumor angiogenesis (80). It has been reported that tumor VEC may have genetic abnormalities, including aneuploidy, multiple chromosomes and multiple centrosomes (69) leading to irregular phenotypes. These abnormal VEC within the tumor exhibit differential gene expression when compared to VEC isolated from healthy tissue, with such transcripts believed to underlie tumor blood vessel destabilization. Silencing these genes using siRNA approaches has been shown to block VEC migration and vascular tube formation (81), thus supporting tumor VEC as a highly relevant therapeutic target. Another characteristic of the tumor vasculature is the aberrant

pericyte coverage of the blood vessels. Tumor pericytes are typically immature and loosely attached to the capillary, and may even be absent in some areas, leading to vessel destabilization (73, 82). Regulator of G protein-5 (RGS5) has been found to be highly upregulated in PDGFRβ^+ pericytes isolated from murine tumors (83). These pericytes exhibited an immature phenotype and were associated with highly angiogenic vasculature. RGS5 is transiently expressed throughout development, with one of the earliest reports showing RGS5 expression restricted to pericytes in mouse embryos (84). More recently, RGS5 has been found to play a key role in vascular maturation and vessel remodeling during tumorigenesis. In a study where *RGS5*-deficient mice were intercrossed with a mouse model for spontaneous insulinoma, tumors lacking RGS5 exhibited dramatically altered vessels that appeared more regular and homogeneous, with significantly reduced leakiness and hypoxia, similar to vasculature seen in normal healthy tissue. These vascular changes were associated with an increased infiltration of adoptively-transferred tumor-specific T cells into the TME, with coordinate prolonged survival of treated animals. On the other hand, the vasculature observed in *RGS5*-competent insulinomas displayed the hallmark characteristics of tumor angiogenesis, as depicted by a disorganized network of tortuous and leaky vessels with poor oxygen perfusion (68).

1.2.5 Hypoxia in the tumor microenvironment

Hypoxia is associated with various physiological processes, including cell survival and proliferation, tissue vasculogenesis and angiogenesis, all of which are necessary for normal functions such as wound healing (85). However, in cancer, these hypoxic events lead to tumor development and progression. Clinically, hypoxia has been shown to cause resistance to radiotherapy and chemotherapy, leading to increased risk of tumor recurrence and metastases,

with poor patient outcome and lower overall survival (86). Inadequate blood supply due to dysfunctional vessel formation is the major contributor to hypoxia in the TME. The rapid expansion of tumor cells can surpass the rate of angiogenesis leaving large regions within the TME without access to oxygen (87). Given other genetic modifications resulting in adaptation, tumor cells have superior survival compared to normal cells in such hostile, hypoxic environments, favoring tumor progression. This adaptation is largely controlled by the transcriptional changes in the genome, of which it is estimated that up to 1.5% is responsive to hypoxia, with hypoxia-induced factors (HIFs) playing a critical role in transcriptional regulation (87). In addition to hypoxia, aberrations in other pathways can pathologically upregulate HIF1α (69). For example, mutations in the tumor suppressor gene Von Hipple Lindau (*VHL*) is known to increase the expression and activity of HIF1α, particularly in renal cell carcinoma, by preventing its normal process of polyubiquitylation and proteosomal degradation of the HIF1α protein (88).

In recent years, there has been increasing evidence of hypoxia playing a role in the development and maintenance of cancer stem cells (CSC) and epithelial-to-mesenchymal transition (EMT) (86). CSC are a population of cells within the tumor with the ability of self-renewal with high resistance to many forms of anti-cancer therapies (89), providing one explanation as to why tumor regression may not correlate with patient outcome/survival. It has been shown that under hypoxic conditions, CSC have increased capacity to retain an undifferentiated state (90). Indeed, several reports have shown that upregulation of HIF1α and HIF2α promotes expression of HIF-target gene CD133, a CSC marker (86). EMT was originally described in embryonic development when epithelial cells with a cobblestone phenotype become mesenchymal cells with a spindle-shaped fibroblast-like morphology (91). More recently, EMT

has been implicated in cancer cell invasion and migration, and promoting CSC phenotype and function, leading to chemo- and radiotherapy resistance. Several studies have demonstrated that epithelial cells, when grown under hypoxic conditions, evolve to a more mesenchymal phenotype, leading to increased tumor aggressiveness (86). While the crosstalk between the HIF and EMT signaling pathways is not fully understood, it has been proposed that HIFs can upregulate EMT-associated transcription factors (63) as well as play a role in certain EMT-associated signaling pathways such as TGF-β, Notch, NF-κB, Wnt/β-catenin, and Hedgehog (86, 92).

1.3 TARGETING THE TUMOR STROMA

1.3.1 Small molecule drugs targeting angiogenesis and the vasculature

Over a decade ago, Judah Folkman presented the novel idea of angiogenesis as a therapeutic target in cancer (93). His theory spurred the development of several anti-angiogenic therapies including monoclonal antibodies reactive against angiogenic growth factors (and their cognate receptors) and small molecule inhibitors of pro-angiogenic receptor tyrosine kinases (RTK). Later it was suggested that normalization of the tumor vasculature could be achieved via administration of anti-angiogenic agents and that this would actually be a desirable therapeutic outcome in cancer therapy (94, 95) as this approach would coordinately allow for the improved delivery of co-applied chemotherapeutic agents into the TME.

The humanized monoclonal antibody bevacizumab (Avastin®) been shown to induce a transient normalization of the tumor vasculature in treated patients, which when coupled with

chemotherapy, promoted enhanced anti-tumor effects (96). Targeting soluble VEGF increases the preponderance of PDGF in the TME, thus inducing pericyte recruitment and activation and capillary stabilization (97). Huang *et al.* recently reported that at low doses of anti-VEGFR2 antibody, the tumor vasculature became normalized in mice. Furthermore, this treatment reprogrammed the TME to be more proinflammatory and receptive to T effector cell infiltration (98). Alternatively, pharmacological agents targeting VEGF receptors (*i.e.*, VEGFR1-3), as well as other pro-angiogenic RTK (*i.e.*, PDGFRβ), can also inhibit dysregulated angiogenesis leading to a temporary normalization of the vasculature.

Due to the highly-vascularized nature of RCC, several clinical trials have utilized tyrosine kinase inhibitors (TKI) that antagonize angiogenesis as a means to treat this disease. One such inhibitor is sunitinib malate (Sutent®) (99), which has exhibited pronounced (albeit temporary) efficacy in phase I/II clinical trials and is approved as a first-line treatment for patients with RCC (100-103). However, a phase III trial showed that while progression-free survival early on was higher in patients receiving sunitinib (11 months) compared to interferon treatment (5 months), the overall survival benefit associated with this approach was not dramatically different between the two groups (26.4 months versus 21.8 months) (100). Direct anti-tumor effects have not been determined for sunitinib, as no somatic mutations in RTK have been identified in human RCC (103) and *in vitro* studies have shown that mechanism of action of sunitinib involves the induction of an apoptotic death for tumor-associated endothelial cells rather than human RCC cells themselves.

Although sunitinib was initially developed as an angiostatic agent, recent reports suggest that this TKI actually "normalizes" the tumor vasculature, similar as observed with bevacizumab (104), by selective pruning of immature and fragile vessels, leaving the more differentiated

vessels intact with mature pericyte coverage. This normalization event leads to a decrease in interstitial pressure and improved delivery of chemotherapeutic drugs and effector T cells into the TME (105). Corresponding results from a study by Ganss *et al.* show that inflammation of the TME induced by local radiotherapy, in conjunction with adoptive transfer of tumor-specific cells, can induce microvasculature remodeling towards a phenotype resembling normal tissue (106). The normalized endothelium exhibited increased expression of Type 1 chemokines CXCL9 and CXCL10 as well as their cognate receptor CXCR3. CXCL10 is an endogenous angiogenic inhibitor that acts as a chemoattractant for Type-1 T cells and has been shown to induce apoptosis in human $CXCR3b^{+}$ endothelial cells but not tumor cells (107).

Additionally, patients treated with sunitinib exhibit reductions in MDSC and Treg populations with normalized Type-1 T cell responses *in vitro* (101, 102, 108, 109). Murine tumor models suggest that sunitinib suppresses STAT3 activation and boosts the efficacy of immunotherapy by promoting tumor-specific effector T cells while also suppressing MDSC and Treg *in vivo* (102, 108, 110). Sunitinib treatment has been shown to skew expression of chemokines and their receptors towards a Type 1 profile (111) as well as increased expression of VCAM1 and CXCL9 (MIG) with increased IFN-γ producing T cells within the TME and tumor draining lymph node implying this TKI may represent a potent immune adjuvant. We anticipate that a similar and potentially more durable impact of vascular normalization might result from the specific immune targeting of tumor-associated blood vessels and their cell sub-populations.

1.3.2 Vaccines targeting tumor stromal antigens

Genetic aberrations can potentially develop within the evolving and heterogeneous RCC lesion over many months to years under immune selective pressure (112). As previously

mentioned, vaccines based on whole tumor cells, tumor-APC hybrids, tumor-derived mRNA or cDNA, and/or tumor antigens derived from mutated or overexpressed proteins have thus far underperformed as therapeutic agents (**Figure 1**). These vaccine formulations may merely reinforce an existing, yet failing, immune repertoire given the immune dominance of certain tumor antigens over others and to immune evasion paradigms assumed by the heterogeneous TME. Competition between multiple peptide epitopes for loading on to MHC molecules expressed by APCs *in vivo* could also limit effective immune activation against a broad range of otherwise therapeutic tumor antigen targets.

Recently, several groups (113, 114) have shown that while treatment with anti-angiogenic agents may lead to the transient normalization of the tumor vasculature and to at least a temporary delay in tumor progression, ultimately, upon treatment cessation, the tumors recur and may even exhibit more aggressive behavior with regard to their invasiveness and metastatic potential. Since these drugs only limit angiogenesis (*i.e.*, via RTK signaling antagonism) rather than eradicating the vasculature outright, it is likely that tumor-associated vascular cells adapt to a state of drug-resistance. A possible means to circumvent this problem is to specifically induce immune-targeting of the tumor stroma providing a durable response capable of preferentially eliminating tumor-associated stromal cells, such as fibroblasts and vascular cells, while sparing the vasculature in normal, healthy organs in the patient. Indeed, multiple reports have already shown that vaccination with endothelial cells could effectively limit tumor growth *in vivo* (115, 116). There has been further evidence of therapeutic benefit with immune targeting of specifically defined vascular antigens (on VEC and pericytes) as a means to promote anti-tumor responses (117). However, as shown in **Figure 1**, while the frequency of antigen-specific T cells induced by a vaccine may indicate an active immune response, it is rarely indicative of patient

outcome. Indeed, induction of broad immunity to multiple antigens may confer better anti-tumor efficacy (118). By focusing Type-1 immune responses in the tumor vascular niche, one may also enhance the uptake of tumor antigens and induce epitope spreading within the TME, allowing for activation of tumor-specific T cells along with the tumor-associated antigen-specific T cells. Furthermore, this local Type-1 inflammation could activate the TME (*i.e.*, modulating the cytokine millieu and activation state and expression of adhesion molecules) leading to the enhanced recruitment and functionality of anti-RCCAA T effector cells.

We, and others, have recently advocated the implementation of vaccines promoting specific Type 1 T cell recognition of tumor vascular cell populations (119-121), however these vaccine formulations have been cellular-based, utilizing adoptive transfer of DC presenting stromal antigen-derived peptides. Rosenberg's group has recently shown that T cells engineered to express a chimeric antigen receptor specific for VEGFR2, which is overexpressed in the vasculature of many solid cancers, including RCC, were able to limit the growth of 5 different types of established, vascularized tumors in mice and to coordinately induce VEGFR2-specific host T cell responses (122). This treatment strategy is currently under investigation in Phase I trials for RCC as well as melanoma patients. It has also been shown that treatment with fibroblasts genetically altered to express endostatin, another molecule critical for tumor angiogenesis, leads to reduced tumor burden with increased infiltration of $CD4^+$, $CD8^+$, and CD49b/VLA-4^+ lymphocytes in a metastatic RCC mouse model when combined with rIL-2 administration, indicating an additive immunomodulatory effect of the vaccine (123).

Current genetic immunization strategies for RCC have been limited to those using recombinant vaccinia viruses encoding tumor antigens, which have thus far met with moderate clinical success (**Figure 1**). This muted efficacy may be, in part, due to the fact that vaccinia the

rapid host development of neutralizing antibodies can limit the booster capacity of repeated administrations of this vaccine modality (124). Given the ability of lentivirus to transduce endogenous DC *in vivo* in the absence of evoking neutralizing anti-viral immunity (125), and therefore the potential of reiterated dosing, I have developed a lentiviral-based vaccine designed to promote specific immune targeting of the tumor vasculature, and more specifically, an antigen our group recently discovered to be expressed specifically on tumor pericytes and immunologically relevant in multiple tumor models: Delta-like homolog-1 (DLK1).

1.4 NOTCH

1.4.1 Delta-like homolog 1 (DLK1)

DLK1, also known as Pre-adiposite factor 1 (Pref-1) and Fetal Antigen 1 (FA1), is a 50 kDa membrane-bound protein containing six tandem EGF-like repeats, a tumor necrosis factor-α converting enzyme (TACE)-mediated cleavage site, a transmembrane domain, and a cytoplasmic tail. ADAM17 is the TACE that cleaves DLK1 to yield the soluble form of DLK1 (126). While the structure DLK1 is similar to the canonical DLL ligands of Notch, it lacks the conserved Delta Serrate Lag (DSL) signaling domain, and is therefore considered a competitive inhibitor and negative regulator of Notch signaling (127). DLK1 has been reported to inhibit several Notch-dependent differentiation pathways including normal adipogenesis, muscular and neuronal differentiation, bone differentiation and hematopoiesis. DLK1 is widely expressed during embryonic development, with high amounts found in the placenta, adipose tissue, liver, skeletal muscle, and the pituitary and adrenal glands (127). In adults, expression is restricted to

neuroendocrine tissues, such as the pancreas, testes, prostate, and ovaries. While the expression pattern of DLK1 suggests an important role in tissue development and maturation, *Dlk*-null mice show relatively mild phenotype with increased adiposity, and defects in muscle development and B-cell differentiation, suggesting the existence of compensatory mechanisms (128-130). In cancer, DLK1 modulation of Notch activation has been reported to either promote or suppress tumor development/progression based on dynamic (temporally and spatially) context in which Notch signaling is involved (127, 131, 132).

1.4.2 Notch signaling

The Delta-Notch signaling pathway has been highly conserved through evolution, covering a broad range of developmental processes including cell differentiation and proliferation (133). Mammals possess four Notch receptors (Notch1-4) with five activating canonical ligands (Jagged1, Jagged2, Dll1, Dll3, and Dll4). These ligands are characterized by their DSL domain (a cryptic EGF-like repeat) and specialized tandem EGF repeats. Upon ligand-binding of the Notch receptor, two enzymatic cleavage events occur. The TACE, ADAM10, cleaves the extracellular portion of the receptor while a γ-secretase cleaves the Notch intracellular domain (NICD) that can then translocate to the nucleus. Within the nucleus the NICD displaces co-repressors bound to the DNA-binding transcriptional repressor CBF1, converting it into a transcriptional activator, and recruit co-activators (such as MamL1), thus inducing transcription of target genes, including the HES family of transcription factors (134). Here I provide a simplified schematic of the key players involved in Notch signaling (**Figure 2**).

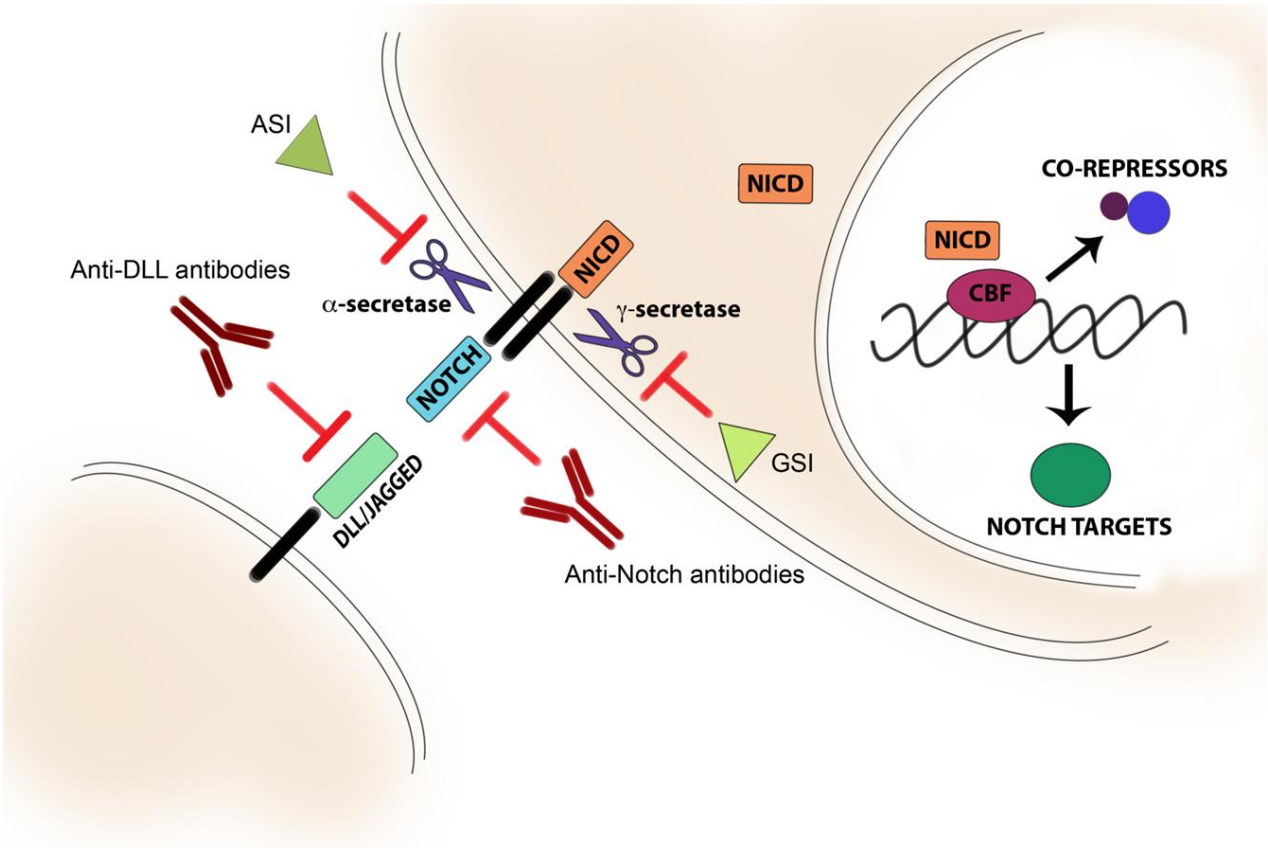

Figure 2. Notch signaling and its antagonism.
Canonical Notch signaling with Delta-like ligands (DLL) and Jagged ligands through Notch receptors leads to cleavage of Notch intracellular domain (NICD) and its translocation into the nucleus where it induces transcription of Notch target genes by displacing co-repressors of transcription factor CBF-1. Notch activation can be pharmacologically inhibited by anti-DLL and anti-Notch antibodies as well as α-secretase inhibitors (ASI) and γ-secretase inhibitors (GSI).

Many studies have shown that Notch signaling plays an important role in tumorigenesis through its regulation of cell proliferation, survival, and invasion (135). Indeed, Notch was first observed as an oncogene in T cell acute lymphoblastic leukemia (T-ALL) (136), and later found to be implicated in several solid tumors including breast cancer, colorectal cancer, non-small cell lung carcinoma, and melanoma (132, 137, 138) and as an activator of tumor invasion (139). There has also been evidence of Notch involvement with the induction of EMT and CSC maintenance and function (140, 141). Hypoxia has been shown to promote Notch activation in a HIF-1α-dependent manner, leading to increased cell survival, Notch-induced EMT, CSC

maintenance, and tumor cell invasion and migration (86). More recently, HIF-2α has also been found to induce Notch activation in stem cells (142).

Although Notch activation can promote tumorigenesis, there has been growing evidence of a tumor suppressive role as well, particularly in the skin. Indeed, it has been reported that loss of *NOTCH1* resulted in spontaneous basal cell carcinoma, increased sensitivity to chemically induced skin carcinogenesis, and defects in the integrity of the skin barrier promoting tumorigenesis (143, 144). Recent studies have revealed Notch to also be a tumor suppressor in hepatocellular carcinoma, chronic myelomonocytic leukemia, head and neck squamous cell carcinoma, gastrointestinal stromal cancer, endometrial cancer, and B cell malignancies (134, 145-148).

As mentioned briefly earlier, Notch also plays a crucial role in the regulation of angiogenesis. It has been shown that Notch signaling during normal physiological conditions limits excessive angiogenesis as a negative feedback mechanism and to promote the formation of an intact, functional, mature vascular network (149). Inhibition of DLL4 in the tumor vasculature results in a significant increase in the number of new vessel sprouts and branches, however these vessels are non-functional resulting in a disrupted vasculature. In certain models, DLL4 inhibition led to reduced tumor growth, while other studies observed severe toxicities and development of vascular tumors with chronic DLL4 blockade (150, 151), indicating the delicate balance of Notch signaling during angiogenesis.

Given the role Notch plays in such diverse cellular processes during embryonic development and in adult tissues, it may be expected that abnormalities in Notch signaling could result in such a wide range of pathologies. Evidence shows that depending on the cellular

context, Notch can promote stem cell maintenance or induce terminal differentiation, and that the mechanism behind this duality of Notch signaling in cancer requires further investigation.

1.4.3 Notch inhibition

As previously discussed, canonical Notch signaling involves an enzymatic cleavage event following ligand binding involving γ-secretase. Inhibiting this process has been done in clinical trials for Alzheimer's disease and various cancers using small molecule γ-secretase inhibitors (GSI) (152). Aside from the four Notch receptors, GSIs also target the Notch ligands, Jagged and Delta-like ligands. Most GSIs are hydrophobic compounds that are cell-permeable that can act as reversible inhibitors of γ-secretase. The most commonly used GSI in the laboratory is N-[N-(3,5-Difluorophenylacetyl-L-alanyl)]-S-phenylglycine t-Butyl ester (DAPT). Early clinical trials have been testing the Merck GSI MK-0752 in patients with T-cell leukemia/lymphoma as well as solid cancers including glioma and breast cancer showing moderate success (152).

While GSI are the only form of Notch inhibitors available in clinical trials, there are other types of Notch inhibitors under development. Targeting the α-cleavage of the Notch receptor using small molecule inhibitors of ADAM10 and ADAM17 has also been shown to effectively shut down Notch signaling with the added advantage of not being required to enter the cell (153).

Another method of blocking Notch activity is the use of antibody inhibitors that can physically block the protein-protein interactions between receptor and ligand. Studies have shown that anti-DLL4 antibodies can effectively inhibit Notch signaling resulting in chaotic, dysfunctional vasculature (149-151). There have also been reports describing antibodies to specific Notch family members, and even specific functional regions, such as cleavage sites

(152), that allow for fine-tuning of Notch inhibition. These methods of Notch inhibition are depicted in **Figure 2**.

1.5 STATEMENT OF THE PROBLEM

Despite the recent developments in vaccine therapy for RCC, with the vast majority targeting antigens expressed on tumor cells, these treatments have yet to show any prolonged clinical benefit. This is not entirely surprising given the ability of cancer cells to constantly adapt and evade immune recognition, thus rendering many of these tumor-specific vaccines ineffectual. Additionally, the aberrant vasculature of RCC tumors can further inhibit vaccine efficacy by limiting the trafficking of immune effector cells as well as promoting an inhospitable TME that abrogates effector cell function and favors tumor cell and CSC growth/maintenance. Current strategies to "normalize" the TME, specifically the vasculature, employ pharmacological agents, which have been shown to remodel the vasculature; however, these effects are transient at best, indicating a need for alternative therapies that could potentially induce a more durable effect.

The studies in this thesis were designed to assess the efficacy of anti-vascular/stromal targeted vaccines in reconditioning the TME. My findings show that tumor stroma-associated antigens can serve as promising targets for immunotherapy, and that by vaccinating against specific tumor stromal populations, the TME becomes "normalized" with corollary reduction in tumorigenesis. I believe these findings support a general therapeutic paradigm allowing for the immune targeting of various tumor stroma targets (*i.e.*, pericytes and VEC) thus rendering this approach versatile for the immunotherapy in most solid forms of cancer, including RCC.

2.0 INTRATUMORAL IL-12 GENE THERAPY RESULTS IN CROSSPRIMING OF TC1 CELLS REACTIVE AGAINST TUMOR-ASSOCIATED STROMAL ANTIGENS

Xi Zhao[1], Anamika Bose[1], Hideo Komita[1], Jennifer L. Taylor[1], Mayumi Kawabi[2], Nina Chi[2], Laima Spokas[1], Devin B. Lowe[1], Christina Golbach[3], Sean Alber[3], Simon C. Watkins[3], Lisa H. Butterfield[2,4,5], Pawel Kalinski[2,6], John M. Kirkwood[4.5], and Walter J. Storkus

From the Departments of [1]Dermatology, [2]Immunology, [3]Cell Biology and Physiology, [4]Medicine, and [5]Surgery. University of Pittsburgh School of Medicine, Pittsburgh, PA 15213, and the [6]University of Pittsburgh Cancer Institute, Pittsburgh, PA 15213.

These data have been reported in *Molecular Therapy* 2011 19(4): 805-814. Nina Chi Sabins *(Nina Chi)* developed the method to isolate the stromal cell targets and helped generate the reverse transcriptase - PCR and *in vitro* murine $CD8^+$ T cell response data. All authors contributed to the scientific discussion and constructive comments used in developing this manuscript.

2.1 ABSTRACT

HLA-A2 transgenic mice bearing established HLA-A2^{neg} B16 melanomas were effectively treated by intratumoral (i.t.) injection of syngeneic DC transduced to express high levels of IL-12, resulting in CD8$^+$ T cell-dependent antitumor protection. In this model, HLA-A2-restricted CD8$^+$ T cells do not directly recognize tumor cells and therapeutic benefit was associated with the crosspriming of HLA-A2-restricted type-1 CD8$^+$ T cells reactive against antigens expressed by stromal cells (*i.e.,* pericytes and VEC). IL-12 gene therapy-induced CD8$^+$ T cells that directly recognized HLA-A2$^+$ pericytes and VEC flow-sorted from B16 tumors based on IFN-γ secretion and translocation of the lytic granule-associated molecule CD107 to the T cell surface after coculture with these target cells. In contrast, these CD8$^+$ T effector cells failed to recognize pericytes/VEC isolated from the kidneys of tumor-bearing HHD mice. The tumor-associated stromal antigen (TASA)-derived peptides studied are evolutionarily conserved and could be recognized by CD8$^+$ T cells harvested from the blood of HLA-A2$^+$ normal donors or melanoma patients after *in vitro* stimulation. These TASA and their derivative peptides may prove useful in vaccine formulations against solid cancers, as well as, in the immune monitoring of HLA-A2$^+$ cancer patients receiving therapeutic interventions, such as IL-12 gene therapy.

2.2 INTRODUCTION

T cell-mediated antitumor immunity plays a role in regulating tumor growth, placing selective pressure on the heterogeneous cancer cell population throughout disease progression (154-156). To date, most tumor-associated antigens (TAAs) recognized by T cells have proven to be non-mutated, "self" antigens that may be quantitatively overexpressed by tumor cells of one or more histologic types (157). Clinical trials implementing vaccines and immunotherapies targeting such antigens have exhibited success in promoting increased numbers of specific $CD4^+$ and/or $CD8^+$ T cell populations in the peripheral blood of patients, but they have only rarely demonstrated therapeutic efficacy in the advanced disease setting based on RECIST criteria (**Figure 1**) (158-160). Although transient objective clinical responses have been reported in some instances, responding patients may relapse with progressor tumors that fail to express elements of the MHC antigen-presenting machinery and/or treatment-targeted antigens.

The modest success of current therapeutic vaccines targeting TAA suggests that alternate target antigens might instead be considered for integration into treatment designs in order to improve the efficacy of such approaches. In particular, a selection of antigens that are both crucial to tumor growth and survival, but which cannot be readily disposed of in the face of immune attack/selection (*i.e.*, the oncogenes HPV-E6/E7 in cervical carcinoma (161), etc.) would appear most prudent. As an alternative to developing immune-based strategies against dominant oncogenes, serious consideration should be given to the targeting of antigens that are expressed not by tumor cells themselves, but rather by cells comprising the tumor-associated stroma (162, 163). Treatment-induced, immune-mediated disruption of the tumor stroma would be expected to inhibit tumor growth and/or promote disease resolution (164).

In this context, we investigated whether the crosspriming of $CD8^+$ T cells reactive against TASA is a general paradigm for effective immunotherapy. We have previously shown that i.t. delivery of syngenic DC engineered to secrete interleukin (IL)-12p70 (*i.e.*, DC.IL12) results in potent $CD8^+$ T cell-mediated immunity against CMS4 sarcomas in Balb/c mice (121). Protection in this model was at least partially due to therapy-induced crosspriming of type-1 $CD8^+$ T (*i.e.*, Tc1) cells reactive against an H-$2L^d$-presented peptide derived from the β-hemoglobin (HBB) protein expressed by pericytes and/or VEC within the sarcoma TME (121). In the current report, we now show that delivery of DC.IL12 into B16 (HLA-$A2^{neg}$) melanomas established in HLA-A2 transgenic (HHD) mice results in the induction of protective HLA-A2-restricted $CD8^+$ T cells recognizing tumor-associated HLA-$A2^+$ pericytes and VEC, as well as an array of HLA-A2-presented TASA-derived peptide epitopes. Murine TASA-derived peptide epitopes share sequence identity with their human homologues, and human HLA-$A2^+$ normal donors and melanoma patients displayed anti-TASA $CD8^+$ T cell responses after *in vitro* stimulation (IVS). These data support the therapeutic targeting of TASA as a potential means to treat vascularized solid tumors that may be refractory to TAA-based therapeutics based on MHC/TAA expression heterogeneity and the progressive selection of immune escape variants.

2.3 MATERIALS AND METHODS

2.3.1 Mice

HHD mice were obtained from Dr François A. Lemonnier through Dr Pravin T.P. Kaumaya (The Ohio State University, Columbus, OH). HHD mice do not express H-2^b class I molecules, with their cells instead expressing an HLA-A*0201-hβ2 microglobulin single-chain (*HHD*) gene product (165). Ag-specific $CD8^+$ T cell responses in HHD mice recapitulate those observed in HLA-$A2^+$ human donors. Female 6–8-week-old mice were used in all experiments and were handled in accordance with an Institutional Animal Care and Use Committee-approved protocol. HLA-A2 expression on peripheral blood cells isolated from HHD mice via tail venipuncture was confirmed by coordinate positive staining as assessed by flow cytometry using two monoclonal antibodies (mAbs) MA2.1 (reactive against HLA-A2 and HLA-B17) and BB7.2 (reactive against HLA-A2 and HLA-Aw69) (both mAbs from the American Type Culture Collection, Manassas, VA).

2.3.2 Cell lines and culture

B16 is an HLA-$A2^{neg}$, mMART-1^+, $mgp100^+$ melanoma cell line (syngenic to the H-2^b background of HHD mice) and has been described previously (166). The T2 cell line is an HLA-$A2^+$, TAP-deficient human T-cell/B-cell hybridoma (57). Cell lines were free of mycoplasma contamination and were maintained in CM [RPMI 1640 supplemented with 10% heat-inactivated fetal bovine serum, 100 U/ml penicillin, 100 µg/ml streptomycin, and 10 mmol/l

-glutamine (all reagents from Life Technologies, Grand Island, NY)] in a humidified incubator at 5% CO_2 and 37 °C.

2.3.3 Reverse transcriptase-PCR

Reverse transcriptase – PCR was performed using the following primer pairs (**Appendix Table 1**). Cycling times and temperatures were as follows: initial denaturation at 94 °C for 2 minutes (1 cycle), denaturation at 94 °C for 30 seconds, annealing at 60 °C for 30 seconds and elongation at 72 °C for 1 minute (30 cycles), final extension at 72 °C for 5 minutes (1 cycle). PCR products were identified by image analysis software for gel documentation (LabWorks 4.6 Software; UVP, Upland, CA) following electrophoresis on 1.2% agarose gels and staining with ethidium bromide (Sigma-Aldrich, St Louis, MO).

2.3.4 Fluorescence imaging of tumor sections

Tumor tissue samples were prepared and sectioned as previously reported (121). For analysis of T cell subsets, sections were incubated with rabbit anti-mouse NG2 (Millipore, Bedford, MA) along with Alexa488-conjugated anti-CD4 or -CD8β antibodies or matching isotype controls (all from BD Biosciences, San Jose, CA) for 1 hour. After washing with 0.5% bovine serum albumin in phosphate-buffered saline (PBS), sections were stained with donkey anti-rabbit Ig Cy5 (Jackson ImmunoResearch, West Grove, PA) secondary pAb for 1 hour at room temperature. For analysis of CD31 versus NG2, sections were first incubated with rat anti-mouse CD31 (BD Biosciences) and rabbit anti-mouse NG2 (Millipore) Abs for 1 hour at room temperature and then washed. Sections were then treated with donkey anti-rat Ig Cy3 and donkey

anti-rabbit Ig Cy5 (both from Jackson ImmunoResearch) Abs for 1 hour and washed. For the analysis of target antigens in B16 tumor lesions, all sections received dilutions of rat anti-mouse CD31 (BD Biosciences) and guinea-pig anti-mouse NG2 (kindly provided by Dr. Bill Stallcup, The Burnham Institute for Medical Research, La Jolla, CA (167)) Abs. In addition, each slide received a pAb reactive against a given TASA: rabbit anti-mouse pAb for DLK1 (R&D Systems, Minneapolis, MN), EphA2 (Santa Cruz Biotech., San Diego, CA), PSMA (Thermo Fisher Scientific, Rockford, IL), RGS5 (Sigma-Aldrich), VEGFR1 (Thermo Fisher Scientific) or goat anti-mouse pAb for HBB (Santa Cruz), NRP1 (R&D Systems), NRP2 (R&D Systems), PDGFRβ (R&D Systems), VEGFR2 (Abcam, Cambridge, MA). Sections were then again washed five times with 0.5% bovine serum albumin (in PBS), before a 1-hour incubation with dilutions of a mixture of secondary antibodies: (i) donkey anti-rat Cy5 pAb, (ii) donkey anti-guinea-pig DyLight 488 pAb, and (iii) either donkey anti-rabbit Cy3 pAb or donkey anti-goat Cy3 pAb depending on the species of antibody directed against the TASA target (all secondary antibodies were purchased from Jackson ImmunoResearch). After secondary Ab staining, sections were then washed with three washes of PBS, coverslipped with Gelvatol mounting media (made in-house) and stored at 4 °C until imaging using an Olympus Fluoview 500 Confocal microscope (Olympus America, Center Valley, PA).

2.3.5 Synthetic peptides

Peptides (**Table 1**) were synthesized by 9-fluorenylmethoxycarbonyl (Fmoc) chemistry by the University of Pittsburgh Cancer Institute's Peptide Synthesis Facility (a shared resource). Peptides were >96% pure based on high-performance liquid chromatography profile and mass

spectrometric analysis performed by the University of Pittsburgh Cancer Institute's Protein Sequencing Facility (a shared resource).

TASA (ref.)	AA positions	Peptide sequence	HLA-A2 binding score[b]	Specific CD8$^+$ T cell response[a]		
				HHD mice treated with i.t. DC.IL12	HLA-A2$^+$ normal donors (of 8)	HLA-A2$^+$ melanoma patients (of 10)
DLK1	269–277	RLTPGVHEL	49	+	1	4
	310–318	ILGVLTSLV	118	+	2	6
	328–336	FLNKCETWV	1,760	+	2	4
EphA2 (ref. 27)	883–891	TLADFDPRV	1084	+	2	6
HBB	31–39	RLLVVYPWT	227	+	2	6
	105–114	RLLGNVLVCV	592	+	1	1
NG2 (ref. 15)	770–778	TLSNLSFPV	403	–	0	4
	2238–2246	LILPLLFYL	1,356	–	0	4
NRP1	331–339	GLLRFVTAV	2,249	+	2	7
	433–441	GMLGMVSGL	131	+	2	7
	869–877	VLLGAVCGV	1,006	+	2	1
NRP2	214–222	DIWDGIPHV	56	+	0	4
	328–336	YLQVDLRFL	249	+	0	4
	436–444	NMLGMLSGL	131	–	0	0
PDGFRβ	890–898	ILLWEIFTL	1,792	+	2	1
PSMA (ref. 21)	441–450	LLQERGVAYI	920	+	0	2
RGS5 (ref. 23)	5–13	LAALPHSCL	1	+	0	5
TEM1	691–700	LLVPTCVFLV	1,577	+	4	4
VEGFR1 (ref. 16)	770–778	TLFWLLLTL	182	+	1	3
VEGFR2 (ref. 17)	773–781	VIAMFFWLL	270	+	0	0

Table 1. TASA-derived peptides evaluated in this study: Summary of in vitro results.
CD8$^+$ T cell response data is summarized for (i) HHD mice treated with DC.IL12 gene therapy (as in **Figure 4C**) of (ii) HLA-A2$^+$ normal human donors and HLA-A2$^+$ patients with melanoma as displayed pictorially in **Figure 6**. Human (ELISA) responses were designated as + if CD8$^+$ T cell reactivity against T2 cells presenting the indicated peptide (IFN-γ) was >30 pg/ml and more than twofold higher than reactivity against T2 cells pulsed with negative control HIV-nef$_{190\text{-}198}$ peptide ($p<0.05$). Peptide sequences were submitted to an online algorithm predicting binding to HLA-A2 with the deduced scores provided. A higher number reflects the prediction of a more stable HLA-A2 peptide complex.

2.3.6 Generation of HHD bone marrow-derived DCs and DC.IL12

DC were generated from bone marrow precursors isolated from the tibias/femurs of mice using *in vitro* cultures containing 1,000 U/ml recombinant murine granulocyte/macrophage colony-stimulating factor and 1,000 U/ml rmIL-4 (both from Peprotech, Rocky Hill, NJ), as

previously described (121). The Ad.mIL-12p70 and Ad.ψ5 (empty) recombinant adenoviral vectors were produced and provided by the University of Pittsburgh Cancer Institute's Vector Core Facility (a shared resource), as reported previously (121, 168). Five million (day 5 cultured) DCs were infected at an multiplicity of infection = 50 with Ad.mIL-12p70 or the control, empty vector Ad.ψ5. While control DC produced <62.5 pg IL-12p70/ml/48 hour/10^6 cells, DC.IL12 cells produced 1–10 ng IL-12p70/ml/48 hour/10^6 cells.

2.3.7 Intratumoral (i.t.) DC.IL12 therapy

B16 melanoma cells (1×10^5) were injected subcutaneously in the right flank of HHD mice and allowed to establish for 7 days. Mice were then randomized into cohorts of five animals, with each cohort exhibiting an approximate mean tumor size of 30–50 mm^2. On days 7 and 14, tumor-bearing mice were untreated or treated with i.t. injections of 1×10^6 adenovirus-infected DCs (DC.ψ5 or DC.IL12) in a total volume of 50 µl PBS. Tumor size was then assessed every 3–4 days and recorded in mm^2, determined as the product of orthogonal measurements taken using vernier calipers. In some experiments, as indicated, *in vivo* antibody depletions (on days 6, 13, and 20 post-tumor injection) of $CD4^+$ T cells or $CD8^+$ T cells were performed as previously described (121). Data are reported as mean tumor area ± SD. On day 17–19 post-tumor inoculation, $CD8^+$ splenocytes and TIL were magnetic bead cell sorting-isolated from three mice/cohort, with cells pooled and assessed for reactivity against peptide epitopes or cell targets (pericytes, VEC, tumor cells) as described below.

2.3.8 Evaluation of murine $CD8^+$ T cell responses *in vitro*

To analyze Ag-specific responses, spleens and TIL were harvested (from two mice/group) 3–5 days after the second i.t. injection of control DC or DC.IL12 (*i.e.*, day 17–19 after tumor inoculation). Splenic lymphocytes were restimulated *in vitro* for 5 days with irradiated (2.5 Gy) naive peptide-pulsed HHD splenocytes at a stimulator:responder cell ratio of 1:1. Responder $CD8^+$ T cells were then isolated using magnetic bead cell sorting (Miltenyi Biotec, Auburn, CA) and analyzed for reactivity against unpulsed or peptide-pulsed T2 cells, as indicated. To analyze T cell response to stromal cell targets and tumor cells, untreated HHD mice bearing established day 17–19 B16 tumors were sacrificed and tumors and kidneys removed. Tissues were then minced manually and enzymatically digested as described by Crisan *et al*. (78) using collagenases IA, II, and IV (Sigma-Aldrich) and DNAse I (Sigma-Aldrich) for 30 minutes at 37 °C, with gentle shaking. Cells were then being passed through a 70-micron cell strainer (BD Biosciences), washed with PBS, and single-cell suspensions stained with anti-mouse CD31 FITC (BD Biosciences), anti-mouse CD140b (PDGFRβ) PE (eBioscience, San Jose, CA), and anti-mouse H-$2K^b$ APC (BD Biosciences). After washing with PBS, cells were sorted into enriched populations containing pericytes ($PDGFR\beta^+CD31^{neg}$H-$2K^{b(neg)}$) or VEC ($PDGFR\beta^{neg}CD31^+$H-$2K^{b(neg)}$) using a multicolor fluorescence-activated cell sorter (FACSAria; BD Biosciences). In all cases, cells were >95% pure for the stated phenotype. $CD8^+$ T cells (10^5) were then co-cultured with 10^4 pericytes or VEC in U-bottom 96-well plates (Sigma-Aldrich). To verify HLA-A2 restricted recognition of target cells by $CD8^+$ T cells, 10 µg of anti-HLA-A2 mAb BB7.2 or control anti-HLA-class II mAb L243 (both from ATCC) were added to replicate coculture wells. Forty-eight hours after initiating splenic $CD8^+$ T cell co-cultures, cell-free supernatants were collected and analyzed for mIFN-γ content using a

commercial ELISA (BD Biosciences) with a lower limit of detection of 31.3 pg/ml. Data are reported as the mean ± SD of triplicate determinations. Alternatively, freshly sorted $CD8^+$ TIL were cocultured with pericytes, VEC, T2 cells (±peptides) or B16 tumor cells at a T cell-to-target cell ratio of 3:2 for 4–5 hours at 37 °C and analyzed for intracellular levels of IFN-γ or cell-surface expression of CD107a/b using specific mAbs (APC-labeled anti-mouse CD8α from eBioscience; PE-labeled rat anti-mouse IFN-γ and FITC-labeled rat anti-mouse CD107a/b from BD Biosciences) and flow cytometry using the manufacturer's suggested protocol and ref. (169), respectively.

2.3.9 *In vitro* assessment of human $CD8^+$ T cells responses against TASA- or TAA-derived peptides

Peripheral blood mononuclear cells were obtained by venipuncture or leukapheresis from HLA-$A2^+$ normal donors or HLA-$A2^+$ melanoma patients with written consent under institutional review board-approved protocols. $CD8^+$ T cells were then isolated by magnetic bead cell sorting (Miltenyi Biotec) and either not stimulated or stimulated with autologous, TASA peptide-pulsed DC as previously described (57). Normal donor T cells were stimulated with TASA peptide-pulsed DC twice on a weekly schedule, with responder T cells harvested for analysis of their specificity 5 days after the booster stimulation (*i.e.*, day 12 of T cell-DC coculture). Melanoma patient $CD8^+$ T cells were analyzed after a single round of stimulation with TASA peptide-pulsed, autologous DC (*i.e.*, day 5 of T cell-DC coculture) as indicated in text. For DC-based stimulations, DC were pulsed with an equimolar (1 μmol/l each) pool of the TASA peptides (**Table 1**) for 4 hours at 37 °C at 5% CO_2 tension. These antigen-loaded DC were then used to stimulate autologous $CD8^+$ T cells at a T cell-to-DC ratio of 10:1 to generate a

bulk population of responder T cells. T cells were maintained in IMDM media supplemented with 10% human AB serum, 100 U/ml penicillin, 100 mg/ml streptomycin, 10 mmol/l -glutamine and MEM nonessential amino acids (all reagents from Invitrogen, except human AB serum that was purchased from Sigma-Aldrich, Carlsbad, CA). Responder $CD8^+$ T cells were analyzed for reactivity against control (HLA-$A2^+$) T2 cells or T2 cells pulsed with individual TASA or TAA peptides (1 µmol/l for 4 hours at 37 °C[50]) at a $CD8^+$ T cell-to-T2 cell ratio of 5:1 for 24 hours. Harvested cell-free supernatants were consequently assessed for hIFN-γ content using a specific ELISA (BD Biosciences) with a lower detection limit of 4.7 pg/ml.

2.3.10 Statistical analysis

Student's two-sided *t*-test and one-way analysis of variance were used to test for overall differences between groups (StatMate III; ATMS, Tokyo, Japan), with a *P* value <0.05 taken as significant.

2.4 RESULTS

2.4.1 Analysis of TASA expression in the TME.

We have previously reported that $CD8^+$ T cells responses against peptides derived from the murine HBB or EphA2 proteins inhibit the establishment and progression of HBB^{neg} or $EphA2^{neg}$ tumor cells, respectively, in syngeneic wild-type hosts *in vivo* (121, 166). The

"antitumor" efficacy of these Tc1 cells appeared to be due to their targeting of HBB^+ pericytes and/or $EphA2^+$ VEC within the TME. Based on these data, as well as, recent reports by other groups (170-173), we hypothesized that TASA might serve as "universal" targets allowing for $CD8^+$ T cell-mediated restricted growth of solid vascularized tumors. Among the known TASA expressed by pericytes and/or activated VEC (84, 121, 166, 170-178), we selected an initial panel of 12 antigens for evaluation in the current studies (**Table 2**). To validate that the chosen TASA were indeed expressed *in situ* by stromal cells in the TME, we performed immunohistochemistry analyses using specific pAbs on tissue sections isolated from day 14 ($HLA\text{-}A2^{neg}$) B16 melanomas growing progressively in untreated HLA-A2 Tg (HHD) mice. Using immunofluorescence microscopy, we determined coexpression patterns of specific stromal target antigens with $NG2^+$ pericytes and/or $CD31^+$ VEC within the TME. The resulting images are depicted in **Figure 3A**, with a summary of cellular protein expression profiles provided in **Table 2**. Based on these imaging analyses, we assigned the DLK1, HBB, NG2, PDGFRβ, RGS5, and VEGFR2 antigens as predominantly tumor pericyte-associated, and the EphA2 and TEM1 antigens as predominantly tumor VEC-associated. The NRP1, NRP2, PSMA, and VEGFR1 antigens appeared to be expressed by multiple cell types including pericytes, VEC, and alternate stromal cells and/or tumor cells within the progressive B16 TME. To further corroborate TASA expression by $NG2^+$ pericytes, $CD31^+$ VEC, or $H\text{-}2K^{b+}$ tumor cells within the TME, these cell populations were flow-sorted from enzymatically digested B16 tumors resected from untreated recipient HHD mice. To gauge potential overexpression of TASA in tumor versus normal tissues, pericytes and VEC were also flow-sorted from single-cell digests of tumor-uninvolved kidneys harvested from these same animals. Reverse transcriptase (RT)-PCR analyses were then performed on cDNA isolated from each of these sorted cell populations.

Quality control analyses supported the expression of NG2 transcripts only in pericytes, CD31 transcripts only in VEC and gp100 transcripts only in B16 cells (**Figure 3B**). These analyses also support: (i) tumor pericyte expression of all TASA transcripts with the exceptions of EphA2 and PSMA; (ii) tumor VEC expression of transcripts for DLK1, EphA2, HBB, PSMA, TEM1, VEGFR1, and VEGFR2; (iii) B16 expression of transcripts for NRP1, PDGFRβ, VEGFR1, and VEGFR2; (iv) higher levels of DLK1, EphA2, HBB, NRP1, NRP2, PDGFRβ, RGS5, TEM1, VEGFR1, and VEGFR2 transcript expression in tumor- versus normal kidney-derived stromal cells; and (v) comparable or greater levels of NG2, PSMA, and CD31 transcript expression in normal kidney- versus tumor-derived stromal cells (**Figure 3B**).

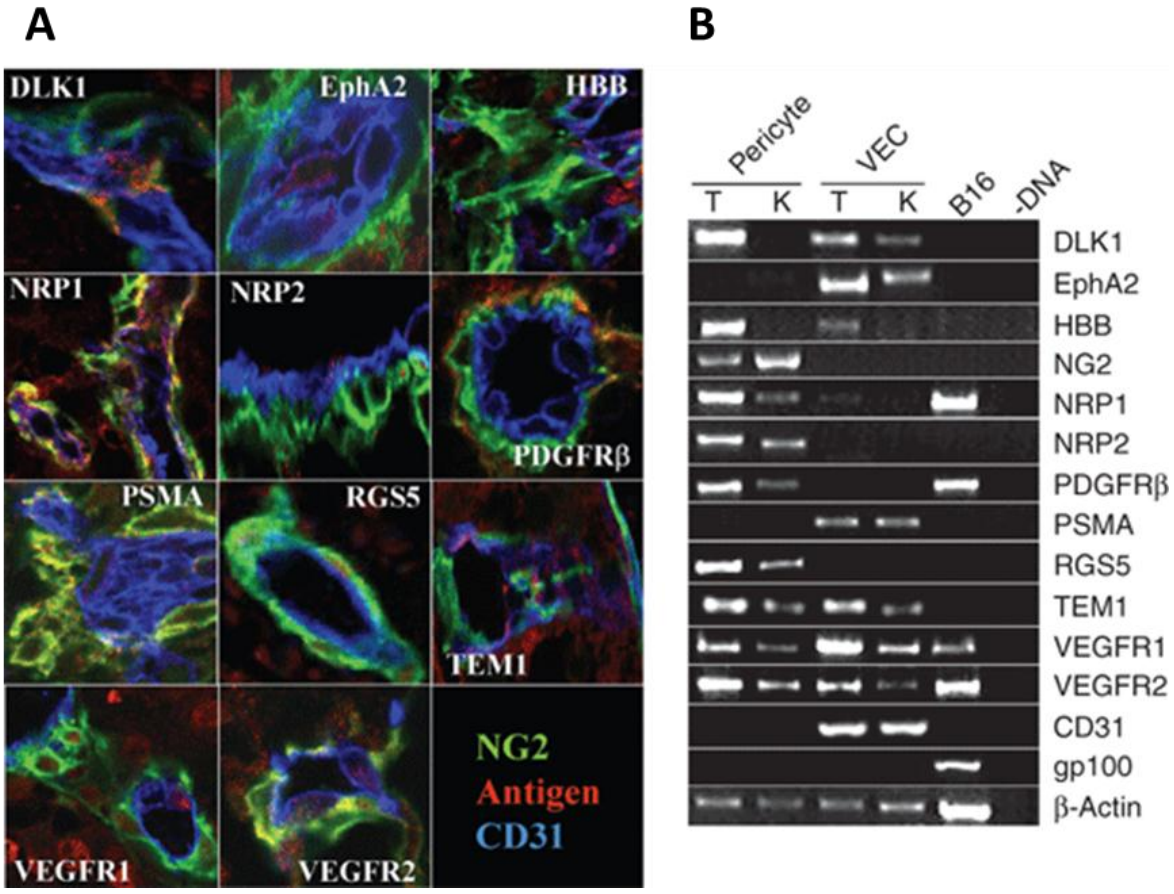

Figure 3. Expression of TASA in the established B16 TME.

(A) B16 melanoma cells were injected s.c. in the right flank of female HHD mice and allowed to establish/progress for 14 days at which time tumors were resected and analyzed for expression of the indicated antigens using specific Abs and fluorescence microscopy as outlined in Materials and Methods section. Specific pAb against NG2 (green), the indicated antigen of interest (red), and CD31 (blue) were used to distinguish preferential antigen expression in tumor-associated stromal pericytes, VEC, alternate stromal cells and/or tumor cells. **(B)** B16 melanoma cells, as well as, flow-sorted ($PDGFR\beta^{+}$, $CD31^{neg}$) pericytes and ($PDGFR\beta^{neg}$, $CD31^{+}$) VEC isolated from day 19 established B16 tumors and tumor-uninvolved kidneys were analyzed for expression of target genes using reverse transcriptase-PCR (RT-PCR) as described in Materials and Methods section. All data are reflective of three independent experiments performed for each tumor type.

TASA	Cells expressing TASA protein (IHC)	Cells expressing TASA mRNA (RT-PCR)
DLK1	P	P (Hi) > VEC (2.1)
EphA2	VEC	VEC (3.3)
HBB	P	P (Hi) > VEC (Hi)
NG2	P	P
NRP1	P, VEC, T/S (pericyte/VEC interface)	P (2.0), T > VEC
NRP2	P, VEC (intracellular)	P (1.6)
PDGFRβ	P > T/S	P (2.3), T
PSMA	VEC, P (vesiculated, punctuate)	VEC
RGS5	P > T/S (cytoplasmic)	P (1.7)
TEM1	T/S, VEC, P	P (1.5), VEC (1.6)
VEGFR1	VEC, P, T/S (intracellular/nuclear)	VEC (1.8) > P (2.6), T
VEGFR2	P > VEC, T/S	P (1.6) > VEC (4.5), T

Table 2. Cells expressing TASA in the TME.

Progressor B16 tumors (day 14) in untreated HHD mice were resected and analyzed for specific TASA expression by fluorescence microsopy, as described in Materials and Methods. Based on co-localization of TASA with NG2 and/or CD31 markers in fluorescence microscopy analyses, we assigned a pericyte (P) – and/or VEC-association with a given marker, respectively. In some cases, TASA were also expressed by $NG2^{neg}$, $CD31^{neg}$ cells (designated as T/S – tumor/stromal) in the TME, which could reflect either tumor cells or alternate stromal cell populations. Reverse transcriptase (RT) – PCR analyses were performed on flow-sorted tumor-derived pericytes and VEC and tumor cells as described in Materials and Methods. Numbers in parentheses reflect the fold increase in expression of transcripts in tumor versus normal kidney pericytes or VEC, as indicated, after first normalizing densitometry signals against β-actin. (Hi) indicates the TASA transcript is expressed by tumor pericytes/VEC, but not normal kidney pericytes/VEC.

2.4.2 Selection of TASA peptides for immunologic analyses

Of the selected TASA, HLA-A2-presented epitopes recognized by $CD8^+$ T cells have been previously reported for human EphA2, NG2, PSMA, RGS5, VEGFR1, and VEGFR2 (**Table 1**). Notably, these defined human epitopes share 100% sequence identity with their murine homologues. To identify novel HLA-A2-presented epitopes in the alternate six selected TASA, a prediction algorithm (http://www.bimas.cit.nih.gov/molbio/hla_bind/) was applied to each protein, and nonameric (9-mer) and/or decameric (10-mer) peptides were preferentially chosen for synthesis and corollary analyses based on two priority criteria: (i) a high algorithm predicted binding score to the HLA-A2.1 class I molecule, and (ii) identity in the human versus murine peptide sequences. This latter restriction was adopted for translational purposes; *i.e.*, to insure that specific therapy-induced T cell responses would need to break operational tolerance in HLA-A2 Tg recipient mice in order to provide antitumor protection (*i.e.*, as would also need to occur for protection in $HLA\text{-}A2^+$ patients with solid cancers). After selection, we showed that each of the chosen synthetic peptides was competent (to a varying degree) to bind and stabilize HLA-A2 complexes expressed by T2 cells (**Appendix Figure 1**), a prerequisite to their ability to be presented to specific, HLA-A2-restricted $CD8^+$ T cells.

2.4.3 Delivery of DC.IL12 into $HLA\text{-}A2^{neg}$ B16 tumors promotes the cross-priming of $CD8^+$ T cells reactive against tumor pericytes, VEC and an array of TASA-derived peptide epitopes in HHD mice

In order to assess the potential *in vivo* relevance of therapy-induced $CD8^+$ T cell responses against these TASA in the tumor setting, we strategically built upon our earlier work

that identified HBB as tumor pericyte-associated antigen (121). In that study, i.t. delivery of syngenic DC.IL12, but not control DC, was competent to break operational tolerance against HBB and to yield protective immunity. As a consequence, in the current studies, DC.IL12 were prepared and injected directly into subcutaneous ($HLA\text{-}A2^{neg}$) B16 melanomas growing progressively in HLA-A2 Tg HHD mice on days 7 and 14 post-tumor inoculation. On day 19 post-tumor inoculation, the mice were euthanized and $CD8^+$ splenic T cells were analyzed for their ability to secrete interferon (IFN)-γ in response to stimulation with TASA-derived peptides presented by the $HLA\text{-}A2^+$ T2 cell line. I.t. delivery of DC.IL12 resulted in dramatically reduced tumor growth (**Figure 4A**; $P < 0.05$ versus versus DC.ψ5-treated or untreated controls after day 11). Furthermore, splenic $CD8^+$ T cells isolated from the DC.IL12 (but not DC.ψ5)-treated cohort of animals directly recognized $HLA\text{-}A2^+$ pericytes and VEC flow sorted from single-cell digests of B16 tumors (but not kidneys isolated from these same tumor-bearing animals) or $HLA\text{-}A2^{neg}$ B16 tumor cells (**Figure 4B** and **C** and **Appendix Figure 2**). Tc1 recognition of tumor-derived pericytes and VEC was completely blocked in the presence of the anti-HLA-A2 mAb BB7.2 (but not an anti-MHC II mAb L243), supporting the HLA-A2-restricted nature of T cell reactivity. Splenic $CD8^+$ T cells from DC.IL12- (but not control DC-) treated animals also responded against an array of TASA-derived peptides when presented by $HLA\text{-}A2^+$ T2 cells *in vitro* (**Figure 4C**). The ability of these murine (HHD) $CD8^+$ T cells to recognize TASA-derived peptides in the context of the human T2 cell line suggests these Tc1 effector cells exhibit moderate-to-high avidity for specific epitopes, since the murine CD8 coreceptor interacts inefficiently with the human HLA class I α3 domain (179) expressed by T2 cells.

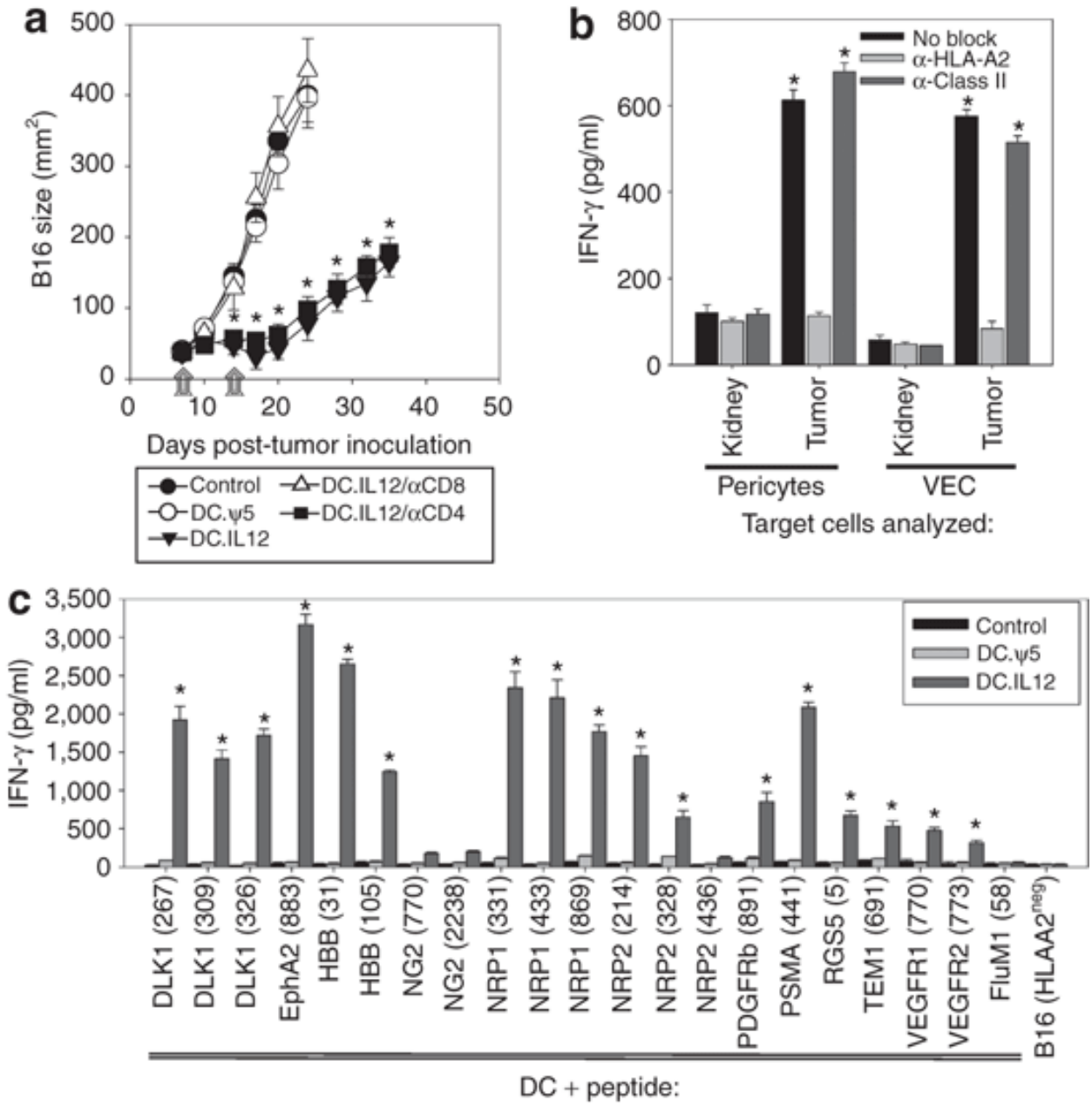

Figure 4. Induction of CD8⁺ T cells reactive against TASA after intratumoral delivery of DC.IL12.

(A) HLA-A2^{neg} B16 melanoma cells were injected s.c. in the right flank of female HLA-A2 Tg (HHD) mice and allowed to establish for 7 days upon which mice were randomized into three groups (n = 5 mice each) receiving no treatment (control), i.t. injection of DC.ψ5, or i.t. injection of DC.IL12. Animals were retreated using the same therapy on day 14 post-tumor inoculation. In replicate cohorts of animals receiving DC.IL12, depleting mAbs against CD4 or CD8 were provided as described in Materials and Methods section. Tumor sizes were assessed every 3–4 days and are reported as mean ± SD in mm^2. *$P < 0.05$ versus control or DC.ψ5-treated mice on days ≥14. **(B)** On day 19 post-tumor inoculation, the mice were euthanized and CD8$^+$ splenocytes isolated and cultured with flow-sorted pericytes or VEC as described in Materials and Methods.

After coculture ± anti-HLA-A2 mAb BB7.2 or anti-major histocompatibility complex (MHC) class II mAb L243, supernatants were analyzed for mIFN-γ content by ELISA. Data are mean ± SD for triplicate determinations, and are representative of two independent experiments performed. *$P < 0.05$ versus kidney cells (pericytes or VEC) and tumor pericytes/VEC in the presence of anti-HLA-A2 mAb BB7.2. (c) On day 19 post-tumor inoculation, the mice were euthanized and splenocytes and stimulated with stromal peptides as outlined in the Materials and Methods. On day 5, $CD8^+$ splenocytes were co-cultured with HLA-$A2^+$ T2 cells loaded with the indicated TASA-derived peptides or HLA-$A2^{neg}$ B16 tumor cells and analyzed for mIFN-γ production by specific ELISA. Data are mean ± SD for triplicate ELISA determinations. *$P <$ 0.05 versus FluM1 control peptide responses. All presented data are representative of three independent experiments performed.

We next analyzed the impact of therapy on the ability of $CD8^+$ TIL freshly isolated from day 17 tumors to recognize flow-sorted pericytes and VEC, as well as, TASA peptides presented by T2 cells. Using both intracellular IFN-γ staining (**Figure 5A**) and CD107 translocation (**Figure 5B**) assays, we observed that 3–12% of $CD8^+$ TIL isolated from animals treated with DC.IL12 mediated effector Tc1 responses against tumor (but not kidney)-derived pericytes and VEC. Similar frequencies of $CD8^+$ TIL from the DC.IL12-treated cohort of mice recognized TASA peptides presented by T2 cells (**Figure 5A and B**). The ability of target cells to elicit effector responses from $CD8^+$ TIL isolated from DC.IL12-treated mice was blocked by anti-HLA-A2 (but not anti-class II) mAb and these T cells display only background reactivity against HLA-$A2^{neg}$ B16 tumor cells (**Appendix Figure 3**). In contrast, the frequency of TASA-specific $CD8^+$ TIL isolated from untreated or DC.ψ5-treated melanoma was lower (versus DC.IL12 treatment) in all functional analyses performed (**Figures 4C**, **5A** and **B**, and **Appendix Figure 3**).

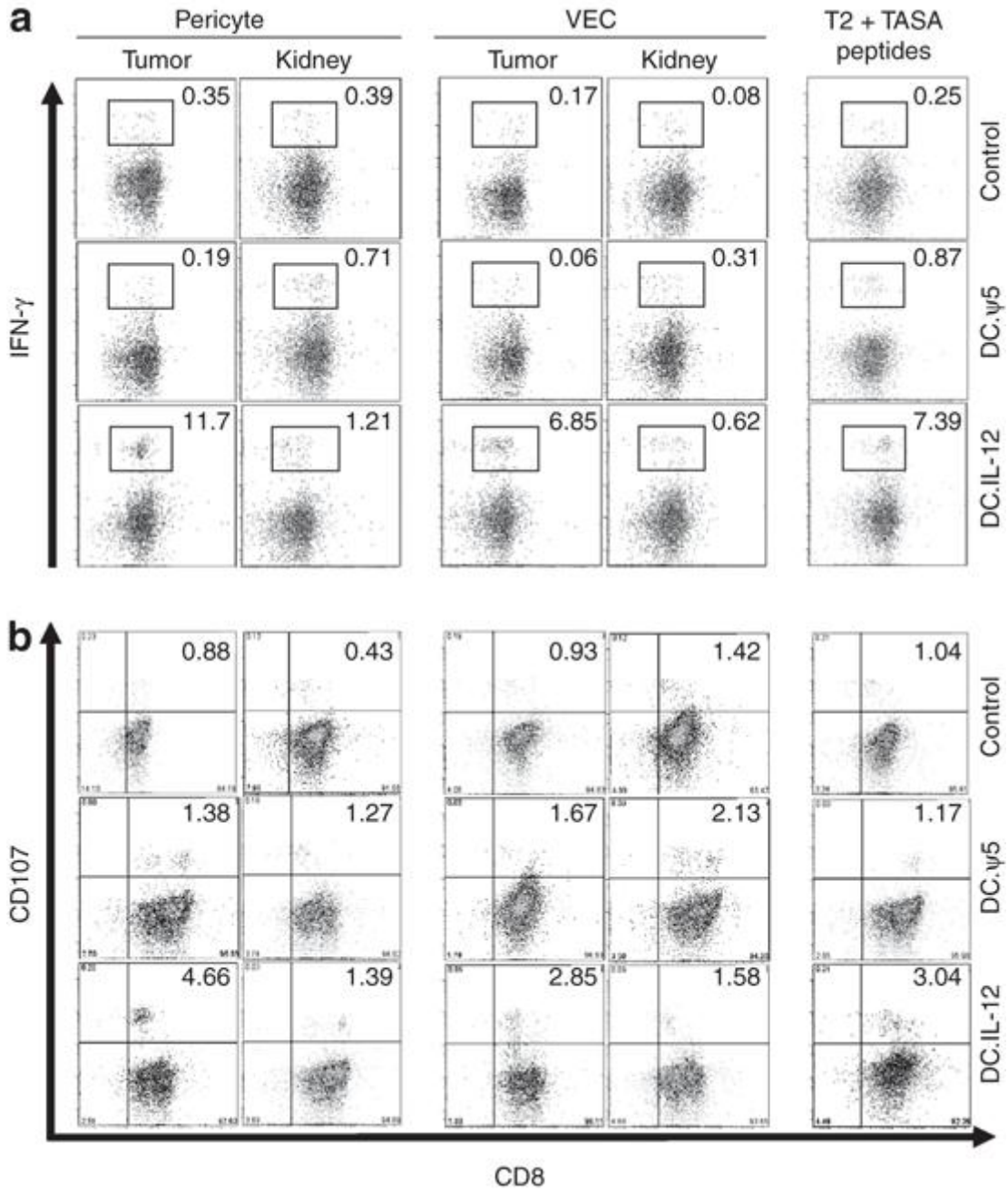

Figure 5. CD8$^+$ TIL from DC.IL12-treated mice are enriched in effector cells reactive against tumor pericytes and/or VEC, as well as TASA peptides.

B16 tumor-bearing mice were treated as described in **Figure 4**. On day 17 post-tumor inoculation, CD8$^+$ TIL were isolated from all cohorts of mice, and pericytes and VEC were isolated from the tumors and kidneys of untreated mice as described in the Materials and Methods section. Freshly sorted CD8$^+$ TIL were then co-cultured with pericytes, VEC, or T2 cells ± TASA peptides and analyzed for intracellular expression of **(A)** IFN-γ or cell-surface expression of **(B)** CD107a/b by flow cytometry. Inset numbers reflect the percentage of CD8$^+$ T cells expressing intracellular interferon (IFN)-γ or cell surface CD107a/b. Data are from one representative experiment of two performed.

2.4.4 $CD8^+$ T cells from HLA-$A2^+$ normal donors or HLA-$A2^+$ melanoma patients recognize TASA-derived peptides *in vitro*

To assess whether the TASA-derived peptides identified in our HHD tumor model were also capable of being recognized by human $CD8^+$ T cells, we performed IVS using T cells isolated from the peripheral blood of HLA-$A2^+$ normal donors or HLA-$A2^+$ patients with melanoma. DC were pulsed with peptides derived from a given TASA and used as stimulator cells for autologous $CD8^+$ T cells. In cases where more than one peptide existed for a given protein, we pulsed DC with an equimolar (10 μmol/l) mixture of each peptide. Based on our past experience using IVS protocols to elicit specific T cell responses against TAA (where the precursor frequency was far lower in normal donors versus cancer patients (57)), we applied two rounds of IVS using TASA for normal donors and a single-round of IVS using TASA for melanoma patients. Using this approach, we observed that HLA-$A2^+$ normal donors and melanoma patients (**Figure 6**; **Tables 1** and **3**) were each capable of recognizing many of the TASA-derived peptides.

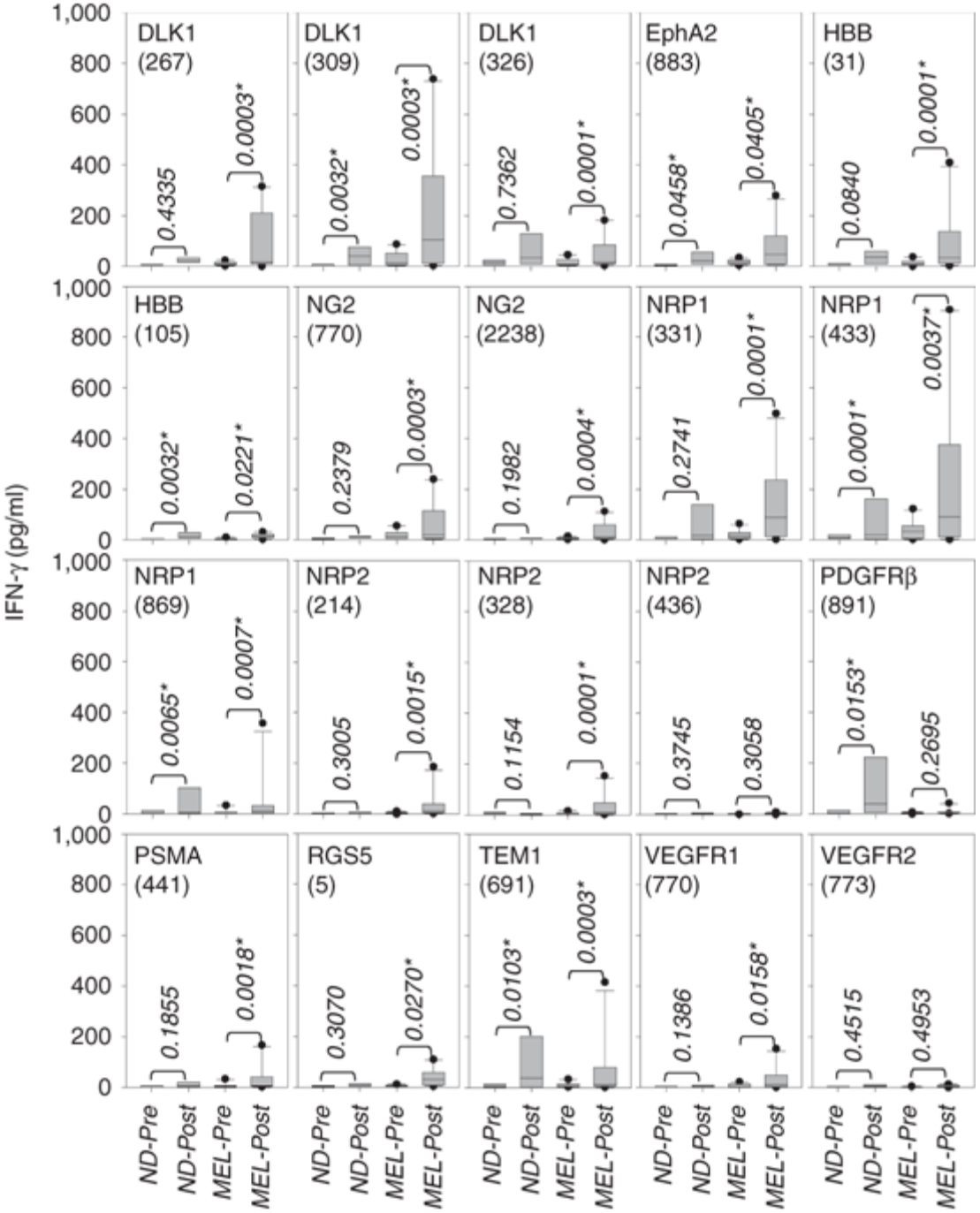

Figure 6. In vitro immunogenicity of TASA-derived peptides in HLA-A2$^+$ normal donors and patients with melanoma.

The indicated peptides were pulsed onto autologous DC and used to prime and boost CD8$^+$ T cells isolated from the peripheral blood of eight normal HLA-A2$^+$ donors or ten HLA-A2$^+$ patients with melanoma as described in the Materials and Methods section. Seven days after the primary IVS (melanoma patients) or a secondary IVS boost (normal donors), T cells were analyzed for their reactivity against HLA-A2$^+$ T2 cells pulsed with the relevant peptide versus the negative control HIV-nef$_{190–198}$ peptide and analyzed for levels of secreted IFN-γ by ELISA.

Data are reported in Bar and Whisker plots, with *P* values provided for paired pre- versus post-IVS data from normal donors and patients. In addition, we noted $P < 0.05$ for MEL-post versus ND-post for the following peptides: DLK1 (309), NG2 (770), NG2 (2238), PDGFRβ (891), and RGS5 (5).

						Specific $CD8^+$ T cell production of IFN-γ in response to TASA											
Donor	Age	Sex	Stage	Prior therapy	Status	DLK1	EphA2	HBB	NG2	NRP1	NRP2	PFGFRβ	PSMA	RGS5	TEM1	VEGFR1	VEGFR2
ND1	51	M	N/A	N/A	N/A	+	—	—	—	+	—	—	—	—	+	—	—
ND2	62	F	N/A	N/A	N/A	+	—	+	—	+	—	+	—	—	+	—	—
ND3	37	M	N/A	N/A	N/A	+	+	—	—	—	—	—	—	—	+	—	—
ND4	28	M	N/A	N/A	N/A	—	—	—	—	—	—	+	—	—	—	—	—
ND5	50	F	N/A	N/A	N/A	—	+	—	—	+	—	—	—	—	+	+	—
ND6	32	F	N/A	N/A	N/A	—	—	—	—	+	—	—	—	—	—	—	—
ND7	26	M	N/A	N/A	N/A	—	—	—	—	—	—	—	—	—	—	—	—
ND8	38	F	N/A	N/A	N/A	+	—	+	—	—	—	—	—	—	—	—	—
Mel1	62	F	IIA	S	NED	+	+	+	—	+	+	—	—	+	+	—	—
Mel2	69	M	IV	Anti-CTLA4	AD	+	+	+	—	+	+	—	—	+	—	—	—
Mel3	55	F	IIC	C	AD	—	+	+	—	+	—	—	—	—	—	—	—
Mel4	87	F	IIC	MAA-VAC, IL-2	AD	+	+	+	+	+	+	—	+	+	+	+	—
Mel5	65	M	IV	C, R	AD	—	—	—	—	+	+	—	—	—	—	—	—
Mel6	71	M	IV	GM2-KLH	NED	+	+	+	+	+	—	—	+	+	—	+	—
Mel7	56	F	IV	C	AD	—	—	+	—	+	—	—	—	—	+	+	—
Mel8	64	F	IV	C, IFN	NED	+	—	—	+	+	—	+	—	+	+	—	—
Mel9	62	F	IV	C, IFN	AD	+	+	—	+	—	—	—	—	—	—	—	—
Mel10	56	M	IV	C, IFN, IL-2	AD[a]	—	—	—	—	—	—	—	—	—	—	—	—

Table 3. Normal donor and melanoma patient demographics and responsiveness to TASA.

Abbreviations: AD, active disease; C, chemotherapy; CTLA-4, cytototoxic T-lymphocyte antigen-4; DC, dendritic cell; F, female; GM2, ganglioside M2; IFN, interferon-α; IRB, institutional review board; IL-2, interleukin-2; KLH, keyhole limpet hemocyanin; M, male; MAA, melanoma-associated antigen; NED, no evidence of disease; R, radiotherapy; S, surgery; VAC, vaccine. Peripheral blood was obtained from HLA-$A2^+$ normal donors and patients with melanoma with consent under IRB-approved protocols. Human responses were designated as + if T cell reactivity against T2 cells presenting the indicated peptide (IFN-γ ELISA) was >30 pg/ml and more than twofold higher than reactivity versus T2 cells pulsed with the negative control HIV-nef190–198 peptide (with $P < 0.05$ versus T2 + HIV-nef190–198). [A]Deceased at the time of this report.

2.5 DISCUSSION

The major finding of this chapter is that protective $CD8^+$ T cells induced as a consequence of effective i.t. DC.IL12 therapy recognize both tumor-associated stromal cells (*i.e.*, flow-sorted pericytes and VEC) and naturally processed and HLA-A2-presented peptides derived from TASA. $CD8^+$ T cell recognition of pericytes and VEC was tumor specific, since therapy-induced $CD8^+$ T cells did not recognize these same cell populations sorted from tumor-uninvolved "normal" kidneys. Based on our PCR analyses, such differential Tc1 recognition of tumor stromal cells may be directly related to the higher levels of TASA transcripts (and possibly protein) expressed by pericytes/VEC isolated from the TME versus the kidney. As expected, in our HHD recipient mouse model system, protective HLA-A2-restricted Tc1 cells failed to recognize HLA-$A2^{neg}$ B16 tumor cells, even though $CD8^+$ T cells appeared to be crossprimed against HLA-A2-presented B16 melanoma-associated antigens MART-1 and gp100 (**Figure 7**), presumably via cross-presentation mediated by HLA-$A2^+$ APC emigrating from the TME (163). Overall, protective immunity in our model was associated with polyspecific Tc1 responses against at least one peptide epitope derived from 11 of 12 TASA evaluated (with NG2 being the lone exclusion).

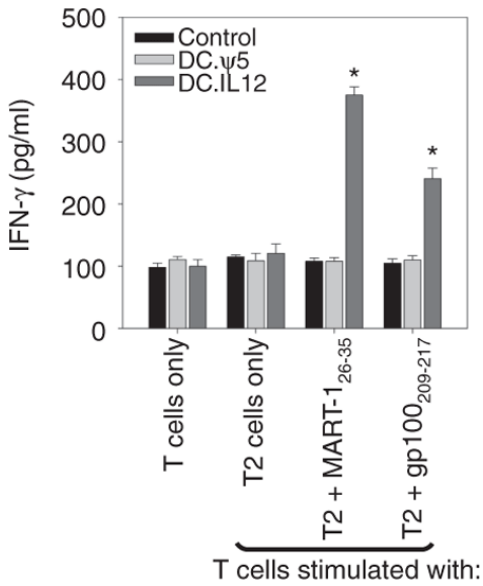

Figure 7. Splenic CD8$^+$ T cells from HHD mice effectively treated with DC.IL12 gene therapy develop HLA-A2-restricted responses against melanoma-associated antigens.

HHD mice bearing day 7 HLA-A2^{neg} (MART-1$^+$, gp100$^+$) B16 melanomas were left untreated or they were treated with i.t. injection of control DC.ψ5 or DC.IL12 as described in **Figure 4**. On day 19 post-tumor inoculation, CD8$^+$ spleen cells were isolated and analyzed for reactivity against the hMART-126–35 and h/mgp100209–217 peptide epitopes presented by the HLA-A2$^+$ T2 cell line. After 48 hours coculture of T cells and Ag-loaded T2 cells, cell-free supernatants were harvested and analyzed for IFN-γ content by ELISA. *P < 0.05 versus T2 only control.

Since the peptides analyzed in the current study are non-mutated and were chosen to be evolutionarily conserved sequences in humans and mice, i.t. DC.IL12 gene therapy must be capable of breaking operational tolerance in the T cell repertoire reactive against these "self" antigens/epitopes. Indeed, we observed that HHD mice and HLA-A2$^+$ normal human donors, as well as, HLA-A2$^+$ patients with melanoma exhibited detectable CD8$^+$ T cell responses against the vast majority of TASA evaluated. Although previous reports have characterized human CD8$^+$ T cell responses against HLA-A2-presented peptides derived from the TASA EphA2, NG2, PSMA, RGS5, VEGFR1, and VEGFR2 (57, 170-172, 176, 177), the current HHD model studies support the natural (tumor stromal cell) presentation of novel HLA-A2-presented epitopes derived from the DLK1, HBB, NRP1, PDGFRβ, and TEM1 gene products *in situ*.

Although our study of HLA-A2$^+$ normal donor and melanoma patient responses is small in size, these data suggest that melanoma patients and normal donors are capable of mounting type-1 CD8$^+$ T cell responses against many "self" TASA when appropriately stimulated (as a proof-of-principle for the development of future vaccines targeting such antigens). Although somewhat an unfair comparison given the application of two IVS cycles for normal donors and one IVS cycle for disease patients, post-stimulation CD8$^+$ T cell responses between these cohorts were statistically different for only a minor subset of TASA peptides (**Figure 6** legend). Such differences could reflect the differential presence of specific CD8$^+$ memory T cells in the peripheral blood of melanoma patients. Furthermore, given the diversity of prior therapies received by the evaluated melanoma patients and variance in their current disease status (*i.e.*, no evidence of disease versus active disease; **Table 3**), it is impossible to correlate T cell responsiveness to TASA with clinical outcome at the current time. Such information can only be determined with longitudinal immunomonitoring in prospective therapeutic trials. In this regard, our data argue for the translational utility of TASA peptides in the context of active vaccination protocols and/or clinical trials implementing immunotherapeutic/antiangiogenic approaches (including IL-12p70 gene therapy, TKI) for the treatment of solid cancers. While one could readily envision the development of phase I/II TASA peptide-based vaccines, it may ultimately be most attractive to consider recombinant TASA protein- or gene-based formulations. These latter agents would presumably have the capacity to promote polyspecific, polyfunctional T cell-mediated immunity in HLA-heterogeneous cancer patients, thereby obviating the need to restrict accrual to a given HLA allotype. Such approaches would also allow one to concomitantly elicit TASA-specific type-1 CD4$^+$ T cell-mediated immunity that may prove directly reactive against

MHC class II^+ pericytes or VEC in the proinflammatory TME and/or support optimal Tc1 functionality/durability in cancer patients (180).

Treatment-associated vascular "normalization," which has been reported to be a preferred clinical outcome in successful cancer therapies (68, 181-183), could also be the direct result of the $CD8^+$ T cell-mediated death/regulation of VEC or pericytes that are required to sustain VEC within the TME *in vivo*. In such a scenario, tumor-associated pericytes/VEC could be induced to undergo either apoptosis or granzyme/perforin-mediated lysis by effector Tc1 cells (115, 184, 185). Alternatively or additionally, the intimate communication between pericytes and VEC (*i.e.*, via PDGF, VEGF, TGF-β, etc.) could be disrupted by IFN-γ, TNF-α, and/or additional factors secreted by Tc1 in response to cognate Ag presented by tumor pericytes or VEC, or crosspresented by tumor-associated APC (186, 187). Such a pathway could be reinforced in an autocrine manner based on the expected upregulation of pericyte/VEC MHC class I expression by IFN-γ (188), allowing for improved $CD8^+$ T cell recognition of these target cells. Furthermore, it remains possible that IL-12 gene therapy-induced inhibition of vasculogenesis in the TME may be related to systemic T cell-mediated targeting and eradication of circulating $TASA^+$ pericyte and/or VEC progenitors that could otherwise have been recruited into, and co-opted to become components of the tumor vascular bed (189).

Beyond the predicted direct suppression of tumor growth by treatment-induced, TASA-specific $CD8^+$ T cells, these strategies would be presumed to reduce tumor interstitial pressure, thereby enhancing the "deliverability" of systemic therapeutic agents (such as chemotherapeutic drugs or even therapeutic T cells themselves) into the TME. Additionally, such treatments would be expected to promote loco-regional tumor cell death (necrosis and/or apoptosis), providing an enriched source of tumor antigen *in vivo* that may allow for secondary waves of

crosspriming and the "epitope spreading" of the antitumor T cell repertoire (168, 190-192). This diversification in the specificity of protective T cells would theoretically allow for enhanced therapeutic efficacy and more durable T cell-mediated protection against tumor recurrence or the progression of micro-metastatic disease.

Ultimately, the clinical success of therapies that evoke anti-TASA Tc1 responses will depend on whether such T effector cells are preferentially recruited into, and sustained within, the TME versus normal vascularized tissues. In this regard, recent reports studying peptide- or DNA-based vaccines targeting the TASA EphA2, NG2, or VEGFR2 have all exhibited some degree of antitumor effectiveness with little or no off-target disruption of the normal vasculature (121), the cutaneous wound-healing process (170-172) or normal fertility, gestational period, or litter size in treated mice. Thus far, we have not observed any acute behavioral or physical manifestations of toxicity in HHD mice cured of B16 tumors as a result of DC.IL12 therapy. Furthermore, our *in vitro* analyses suggest that therapeutic anti-TASA Tc1 cells do not recognize normal tissue-derived pericytes or VEC. Nevertheless, given our belief that "epitope spreading" [classically associated with the development of chronic autoimmune diseases (193)], underlies effective IL-12 gene therapy, we will continue to assess the health/performance status of treated animals for any signs of evolving autoimmune pathology.

In conclusion, our data suggest that therapies that promote $CD8^+$ T cell targeting of tumor-associated TASA, such as DLK1, EphA2, HBB, NRP1, RGS5, and TEM1, may be meritorious for translation into the clinic for the treatment of patients with solid, vascularized tumors. In particular, vaccines based on such TASA are of compelling interest and may prove effective in the treatment of a broad range of cancers regardless of the immunophenotype (MHC and tumor antigen) status of the patient's tumor cells *in vivo*.

3.0 VACCINES TARGETING TUMOR BLOOD VESSEL ANTIGENS PROMOTE CD8$^+$ T CELL-DEPENDENT TUMOR ERADICATION OR DORMANCY IN HLA-A2 TRANSGENIC MICE

Xi Zhao[1], Anamika Bose[1], Hideo Komita[1], Jennifer L. Taylor[1], Nina Chi[2], Devin B. Lowe[1], Hideho Okada[2,3,6], Ying Cao[4], Debabrata Mukhopadhyay[4], Peter Cohen[5], and Walter J. Storkus[1,2,6]

From the Departments of [1]Dermatology, [2]Immunology, and [3]Neurological Surgery, University of Pittsburgh School of Medicine, Pittsburgh, PA 15213, [4]Department of Biochemistry and Molecular Biology, Mayo Clinic Cancer Center, Rochester, MN 55905, [5]Departments of Hematology and Oncology, Mayo Clinic, Scottsdale, AZ, and the [6]University of Pittsburgh Cancer Institute, Pittsburgh, PA 15213.

These data have been reported in *Journal of Immunology* 2012 188(4): 1782-1788. Nina Chi Sabins *(Nina Chi)* developed the method to isolate the stromal cell targets and helped generate the *in vitro* murine CD8$^+$ T cell response data. All authors contributed to the scientific discussion and constructive comments used in developing this manuscript.

3.1 ABSTRACT

We have shown that effective cytokine gene therapy of solid tumors in HLA-A2 Tg (HHD) mice lacking murine MHC class I molecule expression results in the generation of HLA-A2-restricted $CD8^+$ T effector cells selectively recognizing tumor stroma-associated pericytes and/or VEC. Using an HHD model in which HLA-$A2^{neg}$ tumor (MC38 colon carcinoma or B16 melanoma) cells are not recognized by the $CD8^+$ T cell repertoire, we now show that vaccines based on TASA elicit protective Tc1-dependent immunity capable of mediating tumor regression or extending overall survival. Vaccine efficacy was not observed if (HLA-$A2^{neg}$) wild-type C57BL/6 mice were used as recipient animals. In the HHD model, effective vaccination resulted in profound infiltration of tumor lesions by $CD8^+$ (but not $CD4^+$) T cells, in a coordinate reduction of $CD31^+$ blood vessels in the TME and in the "epitope spreading" of $CD8^+$ T cell responses to alternate TASA that were not intrinsic to the vaccine. Protective Tc1-mediated immunity was durable and directly recognized pericytes and/or VEC flow-sorted from tumor tissue, but not from tumor-uninvolved normal kidneys harvested from these same animals. Strikingly, depletion of $CD8^+$, but not $CD4^+$, T cells at late time points after effective therapy frequently resulted in the recurrence of disease at the site of the regressed primary lesion. This suggests that the vaccine-induced anti-TASA T cell repertoire can mediate the clinically-preferred outcomes of either effectively eradicating tumors or policing a state of (occult) tumor dormancy.

3.2 INTRODUCTION

Cancer vaccines based on tumor-associated Ags (TAA) have been extensively evaluated in both translational models and in the clinic. Although by most accounts TAA-based vaccines have been found to be immunogenic in promoting increased frequencies of antigen-specific T cell responses in a large proportion of treated patients, they have only rarely proven curative (118, 158, 194). This limitation in efficacy may relate, at least in part, to the heterogeneity of cancer cells found within a given tumor lesion, particularly with regard to subpopulation "immunophenotypes" (195-197). Indeed, many times patients that have exhibited objective clinical responses to immunomodulatory therapies ultimately progress with tumors characterized by defects in their antigen-processing/presentation machinery and altered immunophenotypes (155, 160).

A theoretical means by which to promote antitumor immunity, while coordinately circumventing the (immuno)phenotypic "instability" of cancer cells themselves, involves the development of vaccines eliciting T cells capable of selectively targeting tumor-associated stromal cells, such as (myo)fibroblasts, vascular pericytes, and VEC (115-117, 119, 162, 198-204). Interestingly, prophylactic peptide-based and/or recombinant vaccines, based on TASA such as endoglin (CD105), NG2, PDGFRβ, VEGFR1, or VEGFR2, have been previously reported to provide partial protection against challenge with tumor cell lines that do not express these antigens, presumably on the basis of T cell-mediated antiangiogenic activity in the TME (170-173, 198-200, 205, 206). However, when applied therapeutically, such vaccines have only slowed the progressive growth of established tumors and modestly extended the overall survival period of treated mice (171, 172, 200).

In the previous chapter, I reported that IL-12 cytokine gene therapy of established HLA-A2^{neg} B16 melanomas growing in HLA-A2 trangenic (Tg) mice results in CD8^{+} T cell-mediated protective immunity directed against host HLA-A2^{+} stromal cells within the TME. In this chapter, I show that therapeutic vaccination of HLA-A2 transgenic mice (HHD) mice with TASA-derived peptides defined in this previous study results in CD8^{+} T cell-dependent regression of colon carcinoma and melanoma and long-term protection against disease relapse.

3.3 MATERIALS AND METHODS

3.3.1 Mice

HHD mice are D^{b} × β_2-microglobulin null Tg for the modified HLA-A*0201 human β_2-microglobulin single chain (*HHD* gene; (207)) and exhibit CD8^{+} T cell responses that recapitulate those observed in HLA-A2^{+} human donors (165, 207, 208). C57BL/6 wild-type mice were purchased from The Jackson Laboratory (Bar Harbor, ME). Female 6- to 8-wk-old mice were used in all experiments and were handled in accordance with an Institutional Animal Care and Use Committee-approved protocol.

3.3.2 Cell lines

MC38, a methylcholanthrene-induced (HLA-A2^{neg}) murine colon carcinoma cell line, and B16, an HLA-A2^{neg} melanoma cell line (syngenic to the H-2^{b} background of HHD mice), have been described previously (166, 209). The T2 cell line is a TAP-deficient T cell/B cell

hybridoma that constitutively expresses HLA-A2 (210). All cell lines were free of mycoplasma contamination.

3.3.3 Peptides

All peptides were synthesized using 9-fluorenylmethoxycarbonyl (Fmoc) chemistry by the University of Pittsburgh Cancer Institute's Peptide Synthesis Facility (a Shared Resource). Peptides were >96% pure based on HPLC profile and mass spectrometric analysis performed by the University of Pittsburgh Cancer Institute's Protein Sequencing Facility (a Shared Resource).

3.3.4 Production of murine bone marrow-derived DC and DC.IL12

DC were generated from bone marrow precursors, as described previously in Chapter 2 (208). The Ad.mIL-12p70 recombinant adenoviral vector was produced and provided by the University of Pittsburgh Cancer Institute's Vector Core Facility (a Shared Resource), as reported previously in Chapter 2 (121).

3.3.5 Vaccine experiments

For prophylactic experiments, HHD mice were immunized s.c. on the right flank with 100 µl PBS or PBS containing 10^6 syngenic DC.IL12 cells that had been untreated or prepulsed for 4 h at 37°C with 10 µM synthetic peptide(s). Immunizations occurred on days −14 and −7, with mice subsequently receiving injections of MC38 (2×10^6) tumor cells in the left flank on day 0. In all cases, treatment groups contained five mice per cohort. For analysis of tumor

cellular composition in repeat experiments, MC38 tumors were isolated by surgical resection 10 d after tumor inoculation and prepared for fluorescence imaging, as described below. For therapeutic experiments, MC38 (2×10^6) or B16 melanoma cells (1×10^5) were injected s.c. in the right flank and allowed to establish/progress for 7 d, at which time, the mice were randomized into cohorts of five mice each, with each group exhibiting an approximate mean tumor size of 50–75 mm^2. Mice were then untreated or treated with control, syngeneic DC.IL12 or DC.IL12 (10^6 cells injected s.c in the left flank on days 7 and 14) pulsed with synthetic TASA peptides. In some experiments, as indicated, *in vivo* Ab depletions (on days 6, 13, and 20 after tumor inoculation to assess early involvement or on days 60 and 67 or 180 and 187 to assess late involvement) of protective $CD4^+$ T cells or $CD8^+$ T cells were performed and monitored as described previously in Chapter 2 (208). In all cases, tumor size (area) was monitored every 3–4 d and is reported as mean ± SD in square millimeters.

3.3.6 Evaluation of specific $CD8^+$ T cell responses in HHD mice

MACS (Miltenyi Biotec) sorted $CD8^+$ splenocytes were harvested (from three mice per group) 7 d after the second round of DC-based vaccination (i.e., day 21 after tumor inoculation) and analyzed for reactivity against unpulsed T2 cells, TASA peptide-pulsed T2 cells, or day 19 (flow-sorted) B16-derived $PDGFR\beta^+CD31^{neg}H\text{-}2K^{b(neg)}$ pericytes or $PDGFR\beta^{neg}CD31^+H\text{-}2K^{b(neg)}$ VEC isolated as described previously in Chapter 2 (208). Where indicated, 10 μg anti–HLA-A2 mAb BB7.2 or control anti-class II mAb L243 (both from American Type Culture Collection, Manassas, VA) were added to replicate coculture wells. After 48 h, supernatants were analyzed for murine IFN-γ content by specific ELISA (lower detection limit = 31.3 pg/ml; BD Biosciences). Data are reported as the mean ± SD of triplicate determinations.

3.3.7 Reverse transcriptase-PCR

Reverse transcriptase (RT)-PCR was performed using primer pairs as described previously in Chapter 2 (208).

3.3.8 Fluorescence imaging of tumor sections

Tumor tissue samples were prepared and 6-μm sections prepared as reported previously in Chapter 2 (121).

3.3.9 Cutaneous wound healing assays

Wound-healing analyses were performed in HHD mice as described by Maciag *et al*. (170).

3.3.10 Statistical analysis

Two-tailed Student *t* test or two-way ANOVA were used to test overall differences between groups (StatMate III; ATMS, Tokyo, Japan) with $p < 0.05$ considered significant.

3.4 RESULTS

3.4.1 Vaccines incorporating peptide epitopes derived from TASA are immunogenic and protect HHD mice against HLA-A2^{neg} MC38 tumor challenge

To assess the immunogenicity of TASA-derived peptides, female HLA-A2 Tg mice were vaccinated twice on a weekly schedule with 10^6 peptide-pulsed (HHD) DC.IL12. One week after the booster immunization, CD8$^+$ splenocytes were isolated and analyzed for their ability to secrete IFN-γ in response to peptide-pulsed HLA-A2$^+$ T2 cells *in vitro*. As shown in **Figure 8A**, the majority (17 of 20; $p < 0.05$ versus T cells stimulated with DC only) of TASA-derived peptides analyzed primed Tc1 responses in vivo that could be detected *in vitro*. We noted that the DLK1, EphA2, HBB, NG2, NRP1, NRP2, PDGFRβ, PSMA, RGS5, TEM1, VEGFR1, and VEGFR2 antigens were expressed *in situ* by blood vessel cells in the MC38 colon carcinoma TME (**Appendix Figure 4**). These findings were similar to our previous observations in the B16 TME, shown in Chapter 2 (208). This led us to next analyze whether immunization with TASA-derived peptides on days −14 and −7 would protect HHD mice against a subsequent challenge with HLA-A2^{neg} MC38 tumor cells injected s.c. on day 0. As depicted in **Figure 8B**, vaccines incorporating peptides from the TASA DLK1, EphA2, HBB, NRP1, PDGFRβ, RGS5, or TEM1 were effective in preventing HLA-A2^{neg} MC38 tumor establishment or they resulted in the regression of tumors (after a transient period of establishment) in HHD mice. In contrast, vaccines based on the TASA NG2, NRP2, PSMA, VEGFR1 or VEGFR2 yielded minimal protection (**Figure 8B**). On the basis of the data provided in **Figure 8**, vaccine immunogenicity and efficacy were not always correlated with one another in the MC38 prophylaxis model

(**Appendix Figure 5**), a finding in accordance with reports for peptide-based vaccines in human clinical trials (118, 158, 194).

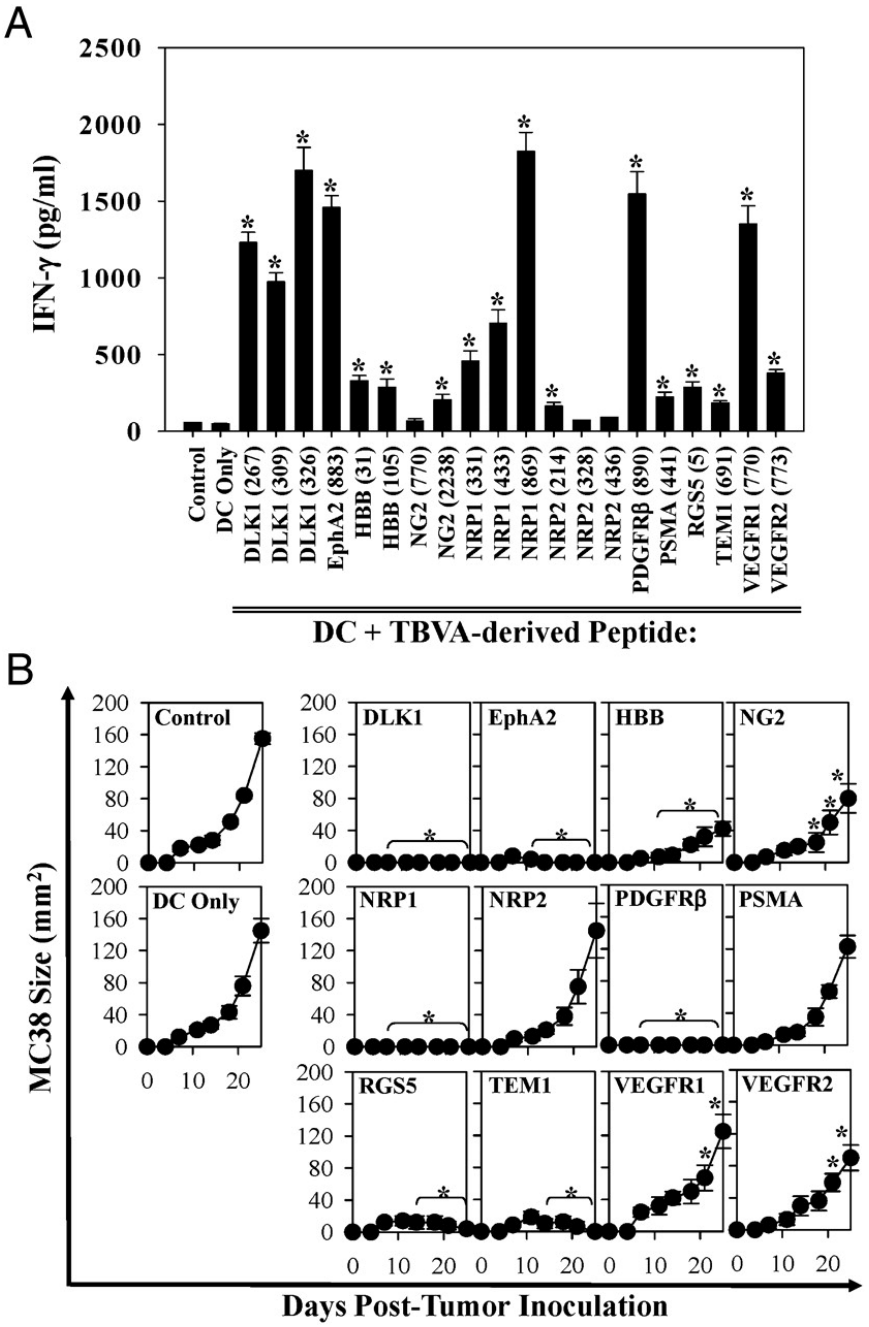

Figure 8. Induction of specific/protective CD8$^+$T cells reactive against TASA as a consequence of DC/peptide-based vaccination.

(A) HHD mice (five animals per cohort) were vaccinated twice (day 14 or 7) s.c. with PBS or with isologous DC.IL12 pulsed with PBS or synthetic peptides (**Appendix Table 2**) derived from the indicated TASA. In cases where more than one peptide was identified for a given target

Ag, an equimolar pool of the indicated peptides (each 10 μM) was pulsed onto DC.IL12 and used for vaccination in the relevant cohort. One week after the second immunization, splenic $CD8^+$ T cells were isolated and stimulated *in vitro* using the HLA-$A2^+$ T2 cell line pulsed with relevant TASA versus irrelevant HIV-$nef_{190\text{-}198}$ (171) peptides and analyzed for IFN-γ production by ELISA. Data are reported as mean ± SD for triplicate ELISA determinations, and are representative of three independent experiments performed. *$p < 0.05$ versus HIV-nef control peptide responses. **(B)** HHD mice were vaccinated twice (days −14 and −7; right flank) s.c. with PBS or with isologous DC.IL12 pulsed with or without TASA peptides as indicated in **A**. One week after the booster vaccine animals were challenged s.c. on their left flank with 2×10^6 MC38 colon carcinoma cells. Tumor growth was then monitored every 3–4 d through day 24. All data represent mean tumor area (in mm^2) ± SD determined from five mice/cohort, and are representative of three independent experiments performed. *$p < 0.05$ versus DC only on the indicated days.

3.4.2 Protective vaccines incorporating TASA peptides promote enhanced infiltration of the TME by $CD8^+$ T cells in association with an inhibition of tumor vascularity

Because a cohort of the protective vaccines allowed for a transient period of tumor growth prior to ultimate tumor regression, we isolated MC38 tumor lesions from all cohorts of animals with evidence of disease on day 14 (after tumor inoculation) and performed immunofluorescence microscopy on tumor sections. We observed that although control (untreated or vaccinated with DC.IL12/no peptide) mice contained few $CD8^+$ T cells in the TME, the majority of the peptide-vaccinated cohorts exhibited a variable but significantly elevated number of $CD8^+$ TIL (**Figure 9A and B**). In marked contrast, $CD4^+$ T cell infiltration in the TME was sparse, and the data were indistinguishable when comparing control versus vaccinated mice (data not shown). An analysis of vascular structures in these tumors revealed that mice pre-vaccinated with peptides derived from the TASA EphA2, RGS5, or TEM1 had the greatest degree of suppression in $CD31^+$ vessel counts in the MC38 TME, with somewhat less pronounced effects also noted for groups vaccinated against HBB or VEGFR2 ($p < 0.05$ versus

untreated mice or mice vaccinated with DC.IL12/no peptide; **Figure 9C and D**). Correlative analyses indicated an association between the antitumor efficacy of vaccines and their ability to promote $CD8^+$ T cell infiltration and reduced vascularity in the TME (**Appendix Figure 5**).

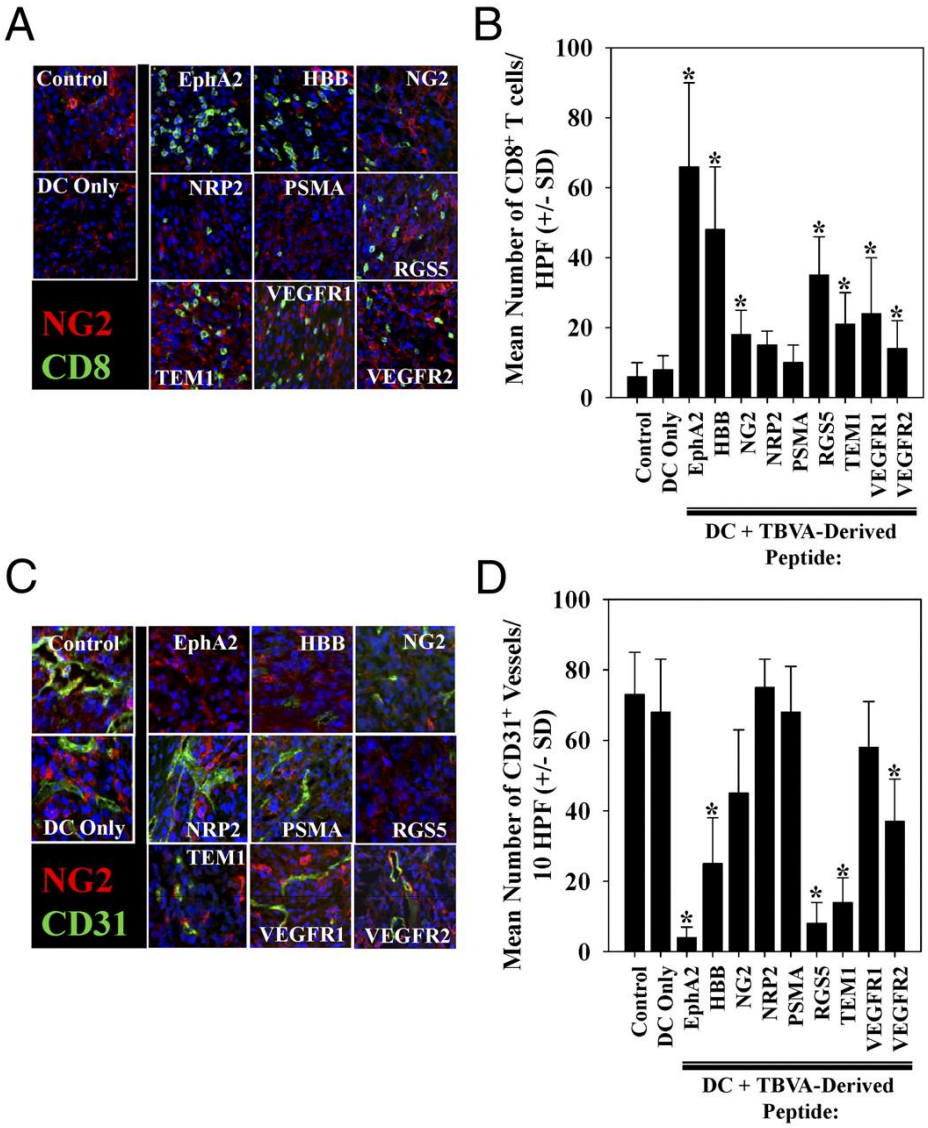

Figure 9. MC38 tumors in mice prevaccinated with TASA-derived peptides exhibit differential infiltration by $CD8^+$ T cells and alterations in vascular density.

On day 14 MC38 tumors were harvested from HHD mice that had been vaccinated as outlined in **Fig. 8B** with the indicated peptides (or control PBS or DC.IL12 alone). (**A**) 6μm tissue sections were costained with anti-CD8 (green) and anti-NG2 (red) Abs and imaged by fluorescence microscopy. Blue signal = nuclear counterstain using DAPI. Original magnification ×40. **B** provides a summary of the mean ± SD number of $CD8^+$ cells per high-power field (HPF) in MC38 tumors isolated from control or vaccinated mice as depicted in A. (**C**) Tissue sections were co-stained with anti-CD31 (green) and anti-NG2 (red) Abs and imaged by fluorescence

microscopy. Blue signal = nuclear counterstain using DAPI. Original magnification ×40. (**D**) The mean ± SD number of $CD31^+$ vessels per HPF of MC38 tumors in control or vaccinated mice are summarized. Representative data are depicted from one of three independent experiments performed. *$p < 0.05$ versus DC only or untreated control mice.

3.4.3 Therapeutic vaccines incorporating TASA-derived peptide epitopes are effective against established HLA-$A2^{neg}$ MC38 colon carcinomas and HLA-$A2^{neg}$ B16 melanomas in HHD mice

Given the robust antitumor activity noted for vaccines based on a subset of TASA in the prophylactic model, we next studied how well these vaccines would perform as immunotherapies in mice bearing established day 7 s.c. MC38 or B16 tumors. In the MC38 model, we treated HHD mice with DC.IL12 cells pulsed with (an equimolar mixture of) peptides derived from an TASA shown most capable of regulating tumor growth under prophylactic conditions (**Figure 8B**) and exhibiting the highest degree of immunogenicity, based on data provided in (**Figure 8A**) (*i.e.*, $DLK1_{326–334}$, $EphA2_{883–891}$, $HBB_{31–39}$, $NRP1_{869–877}$, $PDGFR\beta_{890–898}$, $RGS5_{5–13}$, and $TEM1_{691–700}$). As shown in **Figure 10A**, the combination peptide vaccine effectively promoted the regression of established MC38 tumors. Furthermore, on the basis of the antibody depletion analyses, therapeutic benefit was largely due to the action of $CD8^+$, but not $CD4^+$, T cells (**Figure 10A**). Therapeutic vaccines applied to mice bearing B16 melanomas were also effective in suppressing tumor growth if: 1) the vaccine incorporated peptides derived from the stromal antigens DLK1, EphA2, HBB, NRP1, RGS5 (and to a lesser extent TEM1); and 2) recipient mice were competent to respond to these peptides in an HLA-A2–restricted manner (**Figure 10B**). Hence, none of the vaccines evaluated perturbed B16 tumor growth in syngeneic B6 mice, which do not express the relevant HLA-A2 class I restriction element required for $CD8^+$ T cell recognition of the immunizing peptides. We did not evaluate therapeutic vaccines using the

NRP2 or PSMA peptides in the B16 model on the basis of their poor performance in the preliminary MC38 protection model (**Figure 8B**).

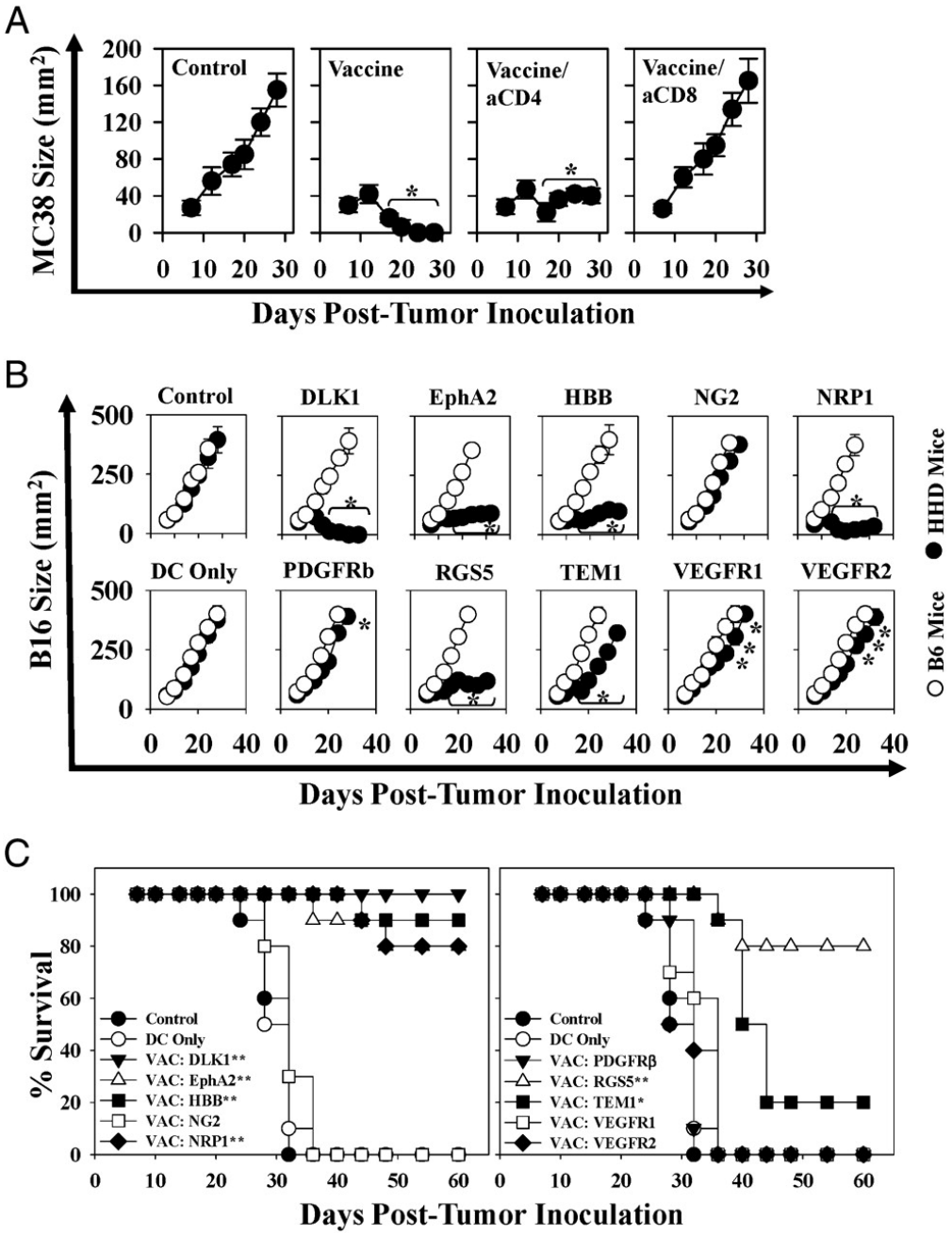

Figure 10. DC.IL12 vaccines containing TASA-derived peptides are therapeutic against MC38 colon carcinomas and B16 melanomas in HHD mice: requirement for $CD8^+$ T cells and HLA-$A2^+$ host (stromal) cells.

(**A**) HHD mice bearing established day 7 s.c. MC38 tumors (right flank) were left untreated, or they were vaccinated in the left flank with control DC.IL12 or DC.IL12 pulsed with an equimolar pool of the following TASA-derived peptides: $DLK1_{326–334}$, $EphA2_{883–891}$, $HBB_{31–39}$,

$NRP1_{869–877}$, $PDGFR\beta_{890–898}$, $RGS5_{5–13}$, and $TEM1_{691–700}$. Identical booster vaccines were provided on day 14 after tumor inoculation. As indicated, two vaccine cohorts were treated with depleting anti-CD4 or anti-CD8 mAbs as outlined in Materials and Methods. (**B**) Female HHD or C57BL/6 (B6) mice with established B16 tumors received vaccines consisting of control or peptide-pulsed DC.IL12 10 and 17 (after tumor inoculation). Tumor size (mean ± SD) was monitored every 3–4 d through day 34. Data are representative of those obtained in two independent experiments in each case. *$p < 0.05$ versus DC only on the indicated days. (**C**) HHD mice bearing s.c. B16 melanomas were treated as described in **B** and followed through day 60 after tumor inoculation. Data are reported in Kaplan–Meier plots depicting overall percentage of surviving animals over time. *$p < 0.02$ versus DC only; **$p < 0.002$ versus DC only (with refined p values for differences between treatment cohorts reported in **Appendix Table 2**). Data are cumulative for three independent experiments performed.

3.4.4 HHD mice cured of B16 tumors by TASA peptide-based therapeutic vaccines exhibit extended survival and durable Tc1 responses against tumor-associated pericytes and/or VEC and spreading in anti-TASA $CD8^+$ T cell repertoire

We followed mice treated in **Figure 10B** through 60 d after tumor inoculation and observed significant survival benefits if the animals had been treated with vaccines containing peptides derived from the TASA DLK-1, EphA2, HBB, NRP1, RGS5, or TEM1 (**Figure 10C**, **Appendix Table 2**). To analyze the status and specificity of Tc1 cells, HHD mice rendered free of B16 melanoma after therapeutic vaccination with DLK or RGS5 peptide-based vaccines were sacrificed 60 d after tumor inoculation. Freshly isolated spleen $CD8^+$ T cells were then analyzed for reactivity against HLA-$A2^+PDGFR\beta^+CD31^{neg}$pericytes, HLA-$A2^+PDGFR\beta^{neg}CD31^+$ VEC, or HLA-$A2^{neg}$ tumor cells flow-sorted from day 19 B16 tumors growing progressively in untreated HHD mice. As shown in **Figure 11**, splenic Tc1 cells isolated from mice cured after vaccination with DLK1 peptides recognized tumor-associated pericytes and VEC in an MHC class I-restricted manner but did not recognize pericytes or VEC isolated from the tumor-uninvolved kidneys of these same donor animals. These type 1 $CD8^+$ T cells strongly recognized the DLK1 peptides used in the protective vaccine formulation, but also (to a variable degree), a

number of additional TASA-derived peptides that were not included in the therapeutic vaccine. Similarly, B16-bearing HHD mice cured using a vaccine on the basis of the $RGS5_{5–13}$ peptide, demonstrated clear Tc1 recognition of tumor (but not tumor-uninvolved kidney) pericytes, as well as statistically significant response against HLA-$A2^+$ T2 cells pulsed with peptides derived from the TASA DLK1, EphA2, NG2, NRP1, PSMA, RGS5, or TEM1 (**Figure 11**).

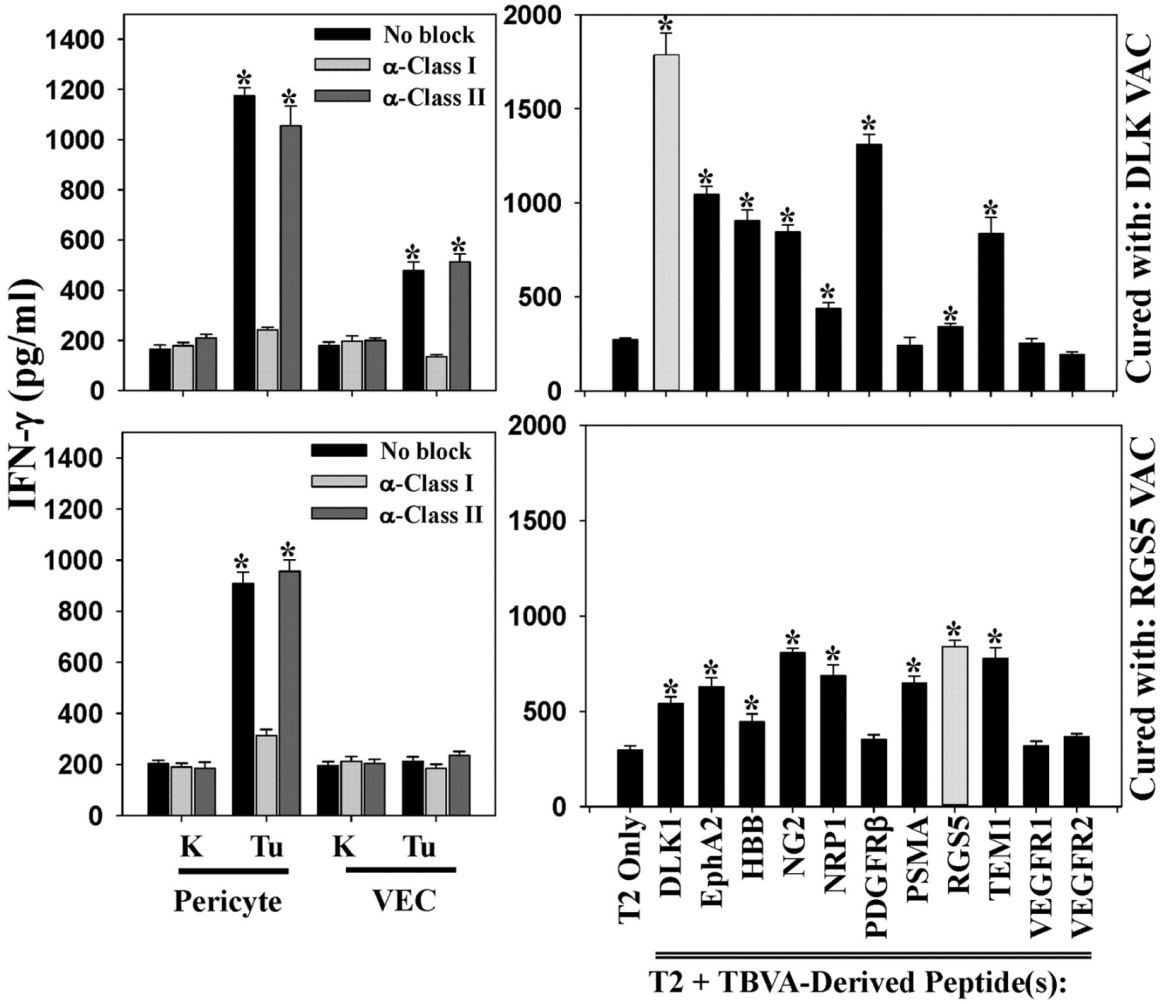

Figure 11. HHD mice cured of B16 melanoma by treatment with DC.IL12/peptide vaccination exhibit polyspecific anti-TASA Tc1 responses.

HHD mice bearing established day 7 B16 melanomas were therapeutically vaccinated with peptides derived from the TASA DLK1 or RGS5 as described in **Figure 10B**. Tumors regressed completely over the next 2 wk. Sixty days after tumor inoculation, splenic $CD8^+$ T cells were isolated and evaluated for IFN-γ production (by ELISA) in response to pericytes and VEC as well as HLA-$A2^+$ T2 cells (control or pulsed with the indicated peptides) as described in Materials and Methods. *$p < 0.05$ versus anti-class I mAb blockade (when evaluating responses

against pericytes, VEC, or B16 tumor cells) or T2 cells only (when evaluating anti-peptide responses). Data are representative of responses observed in three independent experiments.

3.4.5 HHD mice cured of B16 tumors by TASA peptide-based therapeutic vaccines either exhibit true "molecular cures" or a state of $CD8^+$ T cell-mediated tumor dormancy

Despite the high frequency of complete tumor regressors as a consequence of treating B16-bearing HHD mice with TASA peptide-based vaccines, it was conceivable that TASA-targeting T cells limit tumor expansion yielding occult disease rather than the complete eradication of cancer cells (*i.e.,* "molecular" cure). To assess this possibility, effectively treated HHD mice with no evidence of (macroscopic) disease were depleted of $CD8^+$ or $CD4^+$ T cells on days 60 and 67 or 180 and 187 by injection of specific Abs in vivo. As shown in **Figure 12**, depletion of $CD8^+$ T cells, but not $CD4^+$ T cells, resulted in the re-establishment of melanoma growth at sites of the primary tumor placement in seven of nine (*i.e.,* 78% for depletions on day 60 or 67) and three of eight (*i.e.,* 38% for depletions on day 180 or 187) cases, respectively. Interestingly, two of nine (22%) mice in the day 60 or 67 $CD8^+$ T cell-depleted group exhibited transient tumor expansion and then spontaneous regression over a period of weeks to months (**Figure 12**), presumably as TASA/tumor-specific $CD8^+$ T effector cells were recovered in these animals. We also noted that at the time of primary disease recurrence in $CD8^+$ T cell-depleted animals, melanomas did not present in distal cutaneous sites and that metastases were not detected in the lung, liver, or brain based on a histopathology examination of resected tissues (data not shown).

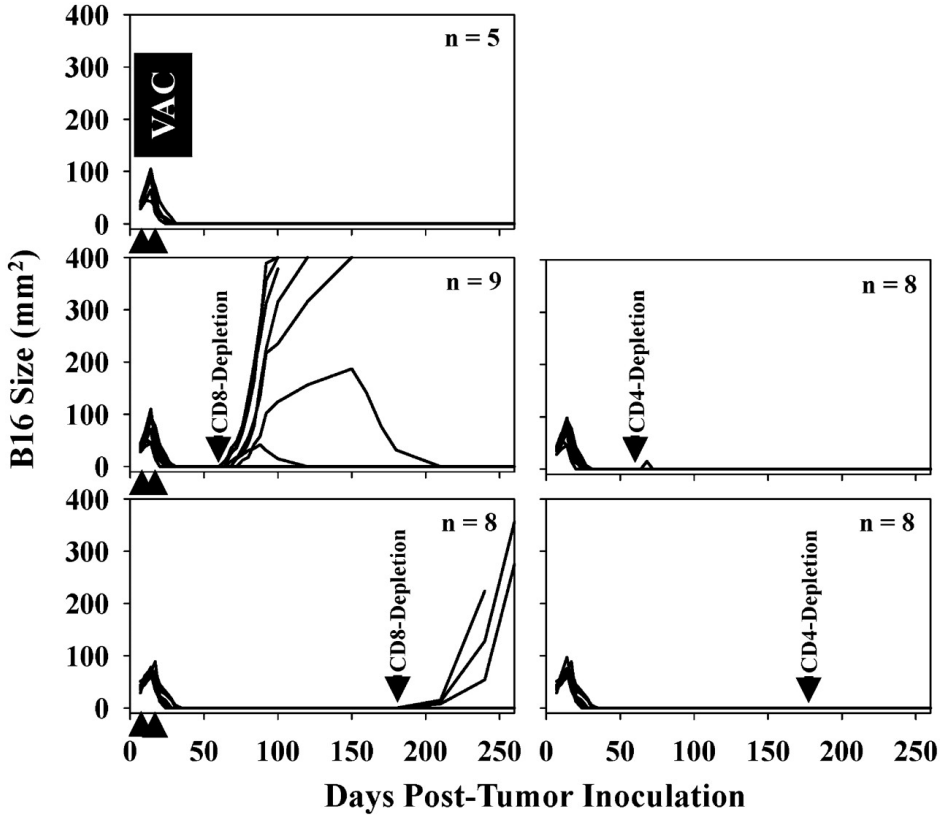

Figure 12. In vivo depletion of CD8$^+$, but not CD4+, T cells from a cohort of HHD mice effectively treated with TASA peptide-based vaccines results in recurrence of disease at the site of primary tumor inoculation.

HHD mice harboring established s.c. B16 melanomas received vaccines consisting of syngeneic DC.IL12 pulsed with a mixture of TASA peptides on days 7 and 14 (after tumor inoculation) as outlined in **Figure 10A**, resulting in tumor regression in 100% of treated animals. On days 60 and 67 or days 180 and 187 (after tumor inoculation), mice were depleted of CD4$^+$ or CD8$^+$ T cells as described in Materials and Methods. Control animals received isotype control Ab. Animals were then monitored for the reappearance and size of melanomas every 4–7 d. The number of animals evaluated per cohort is indicated within a given panel, with each line representing longitudinal data from a given animal. Data are cumulative from three experiments performed.

3.5 DISCUSSION

One major finding of the current chapter is that vaccines based on a subset of TASA-derived peptides elicit protective/therapeutic immunity against HLA-A2^{neg} (MC38 or B16)

transplantable tumors in HHD mice because of the apparent $CD8^+$ T cell targeting of HLA-$A2^+$ pericytes or VEC in the TME. Once protective anti-TASA immunity was established as a consequence of specific immunization, vaccinated animals exhibited durable protection against challenge with tumors of divergent histology (**Appendix Figure 6**). Similar peptide-based vaccines applied to CD8-depleted HHD mice or HLA-$A2^{neg}$recipient (C57BL/6) mice failed to yield treatment benefit, arguing for the critical involvement of $CD8^+$ T cells and the need for these effector cells to target HLA-$A2^+$stromal cells *in vivo* (**Figure 11** and **Appendix Figure 6**). A second major finding is that many apparent complete responders in our therapeutic vaccine models retain occult disease, because $CD8^+$, but not $CD4^+$, T cell depletion of "cured" animals resulted in the rapid recurrence of tumors selectively at the site of the original primary lesion in many cases. Although in most instances, recurrent tumors grew quickly and proved lethal, in some cases (*i.e.*, 2 of 10), tumors grew slowly and subsequently underwent spontaneous regression presumably after the Ab-depleted $CD8^+$ T cell repertoire had recovered. These data suggest that TASA peptide-based vaccines promote complete eradication of tumors or the establishment of a state of (occult) tumor dormancy over extended periods of time, which is regulated by vaccine-instigated $CD8^+$ T cells.

The exact nature of residual occult disease in treated animals that recur upon $CD8^+$ T cell depletion remains unknown. In our HHD model system, we failed to detect direct tumor cell recognition by therapeutic T cells, hence HLA-$A2^{neg}$ cancer cells would be afforded the possibility of maintaining microscopic nests that were limited in their expansion potential based on the anti-angiogenic activity of protective Tc1 effector cells as suggested in alternate models of immune-mediated tumor dormancy (211). Alternatively, or additionally, slowly replicating/quiescent tumor cells or tumor-initiating cell populations may persist in low numbers

in close proximity to blood vessels within the primary lesion site, undergoing a proliferative switch upon removal of existing anti-TASA $CD8^+$ T cells (212, 213). In such circumstances, combinational vaccines simultaneously targeting multiple TASA as well as Ag expressed by tumor cells and/or tumor-initiating cells might be expected to yield higher rates of complete cures (201, 214, 215).

Our data suggest that the strongest "clinical" correlates for vaccine efficacy may be the degree of therapeutic type 1 $CD8^+$ T cell infiltration into the TME and the degree to which Tc1 cells regulate the tumor blood supply. This is in keeping with current paradigms for successful immunotherapy outcome, where levels of specific TIL rather than circulating peripheral blood T cells may be predictive of better clinical prognosis (216). As we have previously suggested (68), treatment-associated vascular "normalization" in the TME may directly result from $CD8^+$ T cell-mediated death or functional disruption of VEC or pericytes *in vivo*. Such anti-vascular effects may provide a rich source of dead or dying tumor/stromal cells capable of supporting the corollary cross-priming of an evolving protective Tc1 repertoire (190). Indeed, we observed that TASA-based therapeutic vaccines that were capable of inducing tumor clearance resulted in the broadening of the protective memory Tc1 repertoire to include specificity against TASA unrelated to the original vaccine formulation. Our findings are consistent with the general paradigm of "epitope spreading" of the antitumor T cell repertoire as a mechanism underlying superior immunotherapeutic outcome (168, 191, 192).

Despite theoretical concerns that the anti-TASA $CD8^+$ T cell response could negatively impact normal tissue blood vessels or the normal process of neoangiogenesis/neovascularization, we failed to detect vaccine induced: 1) T cell responses against normal tissue pericytes or VEC; or 2) delay in the kinetics of skin closure after full thickness wounding (data not shown). Such

differential recognition of tumor over non-tumor blood vessel cells by Tc1 effector cells may well relate to higher levels of TASA expression (and by extension their derivative MHC-presented peptides) by tumor- versus normal tissue-associated pericytes and VEC (**Appendix Figure 4B**) (208), but this could also reflect tissue site-specific variation in blood vessel cell expression of 1) MHC class I APM components, 2) costimulatory/adhesion or coinhibitory molecules, or 3) "repulsion" molecules that inhibit $CD8^+$ T cell–target cell interactions (195-197, 217-219).

In conclusion, our data support the translational use of TASA-based vaccines and the integration of TASA targets in immune monitoring strategies applied to patients with solid forms of cancer. In particular, the ability to immunologically target tumor-associated pericytes and VEC via specific vaccination may pave the way for combinational therapy designs integrating anti-angiogenic agents (*i.e.,* TKI, VEGF/VEGFR antagonists) that have thus far yielded promising, but frequently transient, objective clinical responses in cancer patients (218-220). In these individuals, tumor blood vessels that become refractive to therapy are characterized by a high numbers of pericytes (220), potentially making these structures ideal targets for TASA vaccine-induced, anti-pericyte Tc1 cells.

4.0 DLK1: A NOVEL TARGET FOR IMMUNOTHERAPEUTIC REMODELING OF THE TUMOR BLOOD VASCULATURE

Nina Chi Sabins[1], Jennifer L. Taylor[2], Kellsye P. L. Fabian[1], Leonard J. Appleman[3,6], Jodi Maranchie[4,6], Donna Beer Stolz[5], and Walter J. Storkus[1,2,6]

From the Departments of [1]Immunology, [2]Dermatology, [3]Medicine, [4]Urology, and [5]Cell Biology, University of Pittsburgh School of Medicine, Pittsburgh, PA 15213, and the [6]University of Pittsburgh Cancer Institute, Pittsburgh, PA 15213.

These data have been reported in *Molecular Therapy* 2013 (In Press). All data in this chapter were obtained by Nina Chi Sabins. Donna Beer Stolz assisted in with the vascular permeability study. All authors contributed to the scientific discussion and constructive comments used in developing this manuscript.

4.1 ABSTRACT

Tumor blood vessels are frequently inefficient in their design and function, leading to high interstitial fluid pressure, hypoxia, and acidosis in the TME, rendering tumors refractory to the delivery of chemotherapeutic agents and immune effector cells. Here we identified the Notch antagonist delta-like 1 homolog (DLK1) as a vascular pericyte-associated antigen expressed in RCC, but not in normal kidney tissues in mice and humans. Vaccination of mice bearing established RCC against DLK1 led to immune-mediated elimination of $DLK1^+$ pericytes and to blood vessel normalization (*i.e.,* decreased vascular permeability and intra-tumoral hypoxia) in the TME, in association with tumor growth suppression. After therapeutic vaccination, tumors displayed increased prevalence of activated $VCAM1^+CD31^+$ vascular endothelial cells and CXCL10, a Type-1 T cell recruiting chemokine, in concert with increased levels of Type-1 $CD8^+$ TIL. Vaccination against DLK1 also yielded; i.) dramatic reductions in $Jarid1B^+$, $CD133^+$ and $CD44^+$ (hypoxia-responsive) stromal cell populations, ii.) enhanced tumor cell apoptosis and iii.) increased Notch signaling in the TME. Co-administration of a γ-secretase inhibitor that interferes with canonical Notch signaling resulted in the partial loss of therapeutic benefits associated with DLK1-based vaccination.

4.2 INTRODUCTION

The vasculature of solid tumors is structurally and functionally "abnormal", being composed of an irregular network of blood vessels characterized by aberrant coverage of endothelial tubes and a loosely-attached, largely immature population of mural cells (i.e. smooth muscle cells, pericytes) (73, 82). In contrast to mature pericyte-VEC interactions found in normal tissues that orchestrates blood vessel integrity/stability (221), in tumors, this relationship is deranged leading to a high-degree of vascular permeability, high interstitial fluid pressure, hypoxia and acidosis (79).

RCC is highly-vascularized and generally considered to represent an immunogenic form of cancer (222-224). Current treatment options mediate only transient efficacy in a minority of RCC patients, with frequent development of progressive disease that is refractory to conventional chemo-/radio-therapy (100, 102, 220, 225). Vaccines targeting tumor-associated antigens have also thus far demonstrated only modest curative value (118). The limited perfusion of tumor blood vessels likely contributes to the muted benefits of these treatment approaches by preventing the efficient delivery of chemotherapeutic agents and anti-tumor T cells into the TME (119, 120). As a consequence, the development of novel therapies that can "normalize" the tumor vasculature (by coordinately improving blood vessel perfusion, reducing tumor hypoxia, and allowing for improved and sustained delivery of anti-cancer agents into the TME) remains a high-priority (68, 95, 98, 120, 121).

To achieve the goal of tumor vascular normalization via immunization, we and others have recently advocated the use of vaccine formulations capable of promoting specific Type-1 $CD8^+$ T cell (aka Tc1) recognition of tumor-associated vascular cell antigens (119-121), including DLK1 (Chapters 2 and 3). DLK1 is a member of the EGF-like family of proteins,

which includes Notch receptors and their ligands (127, 131, 132) and serves as a functional inhibitor of Notch signaling. DLK1 has been reported to inhibit a broad range of Notch-dependent cell differentiation pathways (127). In the cancer setting, the functional impact of DLK1 modulation cannot be intuitively assumed, since Notch activation has been reported to either promote or suppress tumor development/progression based on the contextual influences of DLK1 on the myriad cell populations located within the evolving TME (127, 131, 132).

In this chapter, we investigated the therapeutic impact of active vaccination against DLK1 in a murine model of RCC (*i.e.*, RENCA tumor cells transplanted s.c. into syngenic BALB/c mice), where the DLK1 antigen is preferentially expressed by blood vessel-associated pericytes in the progressively-growing TME. We show that DLK1 peptide- or gene-based vaccines are both immunogenic and therapeutic against established RCC, with treatment benefits linked to $CD8^+$ T cell-mediated "normalization" of tumor-associated blood vessels (*i.e.*, reduction in blood vessel numbers and extent of arborization, loss of hypoxia and reduced vascular permeability) (98, 182). Responder tumors were highly-infiltrated by $CD8^+$ TIL that localized within the perivascular (pericyte-enriched) space. Residual pericytes lacked expression of DLK1 and were tightly-approximated to $CD31^+$ VEC. Consistent with the vaccine-induced, immune-mediated eradication of tumor-associated DLK1 protein expression, increased Notch signaling was evidenced within the therapeutic TME. These results are consistent with the ability of DLK1-based vaccines to promote therapeutic $CD8^+$ T cell-dependent vascular normalization in the RCC microenvironment, supporting the clinical translation of such approaches in the setting of RCC and other forms of solid cancer.

4.3 MATERIALS AND METHODS

4.3.1 Mice

Female 6-8 week old BALB/c mice (The Jackson Laboratory, Bar Harbor, ME) were maintained in a pathogen-free animal facility, with all animal work performed in accordance with an IACUC-approved protocol.

4.3.2 Tumor cells

The mouse RCC line RENCA derived from a spontaneous renal cortical adenocarcinoma in BALB/cCr mice (CRL-2947; American Type Culture Collection, Manassas, VA) (226) was cultured as previously reported (121).

4.3.3 Stromal cell isolation

Human RCC tumor and adjacent (patient-matched) normal kidney specimens were obtained with written-consent under an IRB-approved protocol. Murine RCC tumors and tumor-uninvolved kidneys were harvested 21 days after s.c. injection of 10^6 RENCA cells into syngenic BALB/c recipient animals. VEC and pericytes were isolated as previously mentioned in Chapters 2 and 3 with minor modifications (78). Briefly, tissues were enzymaticaly digested into a single cell suspensions and, for human specimens, labeled with anti- human CD146 FITC (Serotec), anti-human CD34 PE (DAKO), anti-human CD56 PE-Cy7 (Serotec), anti-human CD45 APC (BD-Biosciences) and for murine specimens, labeled with anti-mouse CD34-FITC

(eBioscience, San Diego, CA), anti-mouse CD146-PE (BD-Biosciences, San Diego, CA), and anti-mouse CD45-APC (BD-Biosciences) prior to flow sorting into pericyte ($CD146^{+}CD34^{neg}CD56^{neg}CD45^{neg}$) and VEC ($CD146^{+}CD34^{+}CD56^{ne}CD45^{neg}$) populations.

4.3.4 Real-time PCR

Messenger RNA was isolated from pericytes and VEC using the RNeasy® Plus Micro kit (Qiagen, Valencia, CA) according to manufacturer's instructions. cDNA was then generated using High Capacity RNA-to-cDNA kit (Applied Biosystems, Carlsbad, CA) and real-time PCR performed using Fast SYBR® Green Master Mix (Applied Biosystems) with primer pairs for human or mouse HPRT1 (Qiagen), human DLK1 (Applied Biosystems) or mouse DLK1 (forward primer: TGTGACCCCCAGTATGGATT, reverse primer: CCAGGGGCAGTTACACACTT). Reactions were performed in duplicate in a 96-well reaction plate on a StepOnePlus real-time PCR thermocycler (Applied Biosystems) using cycling conditions of 95°C for 20 min., then 35 cycles of 95°C for 3 min. and 60°C for 30 min.

4.3.5 In vitro generation of bone marrow-derived dendritic cells (DC) and DC.IL12

DC.IL12 were generated as previously described in Chapter 2 (208).

4.3.6 Synthetic peptides

The $H\text{-}2^{d}$ class I-presented $DLK1_{158\text{-}166}$ (CPPGFSGNF; presented by $H\text{-}2L^{d}$), $DLK1_{161\text{-}169}$ (GFSGNFCEI; presented by $H\text{-}2K^{d}$), $DLK1_{259\text{-}270}$ (TILGVLTSLVVL; containing overlapping

$DLK1_{259-267}$ and $DLK1_{262-270}$ sequences presented by H-$2K^d$) peptide were synthesized as previously described (120).

4.3.7 Recombinant lentiviral vector production

Genes encoding mDLK1 and the reverse sequence of mRGS5 (as a negative control) were cloned into the pLenti6/V5 D-TOPO vector downstream of the CMV promoter using the Lentiviral Directional TOPO® Expression Kit (Invitrogen, Grand Island, NY). To determine insert presence in the plasmid, expression of the V5 tag was detected by immunofluorescence using an anti-V5 FITC antibody (Invitrogen) and by western blot using an anti-V5 HRP antibody (Invitrogen). In the initial production of the lentiviruses, 293FT cells (Invitrogen) were transfected with plasmid DNA pLenti-DLK1 (or pLenti-NEG) using ViraPower™ Packaging Mix (Invitrogen) combined with Lipofectamine 2000 (Invitrogen) according to the manufacturer's instructions. After 48 hours, lentivirus was collected and concentrated using a Fast-Trap Virus Purification and Concentration kit (Millipore). Lentiviral (lvDLK1 and lvNEG) titers, reported in transduction units (TU), were determined by quantitating blasticidin (Invitrogen)-resistance in HT-1080 cells (kindly provided by Dr. Chuanyue Wu, University of Pittsburgh) according to the manufacturer's instructions. Expanded lentiviral production was performed by the University of Pittsburgh Cancer Institute Lentiviral Vector Core Facility. Lentivirus quality was assessed by infecting HT-1080 cells for 24h and monitoring cells for coordinate V5 protein expression (western blot) and cell-surface expression of DLK1 (flow cytometry using an anti-DLK1-PE conjugated antibody; Adipogen, San Diego, CA).

4.3.8 Animal therapy experiments

BALB/c mice received s.c. injection of 10^6 RENCA tumor cells (right flank) on day 0. Six days later, the animals were randomized into cohorts of 5 mice with comparable mean tumor sizes. On days 7 and 14 after tumor implantation, mice were treated with 100 μl s.c. injections (left flank) of PBS, 10^6 DC.IL12 or 10^6 DC.IL12 that had been pre-pulsed for 2h at 37°C with an equimolar (10 μM) mixture of the $DLK1_{158-166}$, $DLK1_{161-169}$ and $DLK1_{259-270}$ peptides. For lentivirus vaccination experiments, randomized BALB/c mice bearing established (day 10; right flank) s.c. RENCA tumors received a single left flank intradermal injection of lvDLK1 or negative control lvNEG at a dose of 4 x 10^4 or 2 x 10^5 TU in a total volume of 50 μl PBS. For all animal experiments, tumor size was assessed every 3 to 4 days and recorded in mm^2, as determined by the product of orthogonal measurements taken using vernier calipers. Data are reported as mean tumor area ± SD. To determine the impact of canonical NOTCH signaling on vaccine efficacy, tumor-bearing animals vaccinated with lvDLK1 or lvNEG were injected i.p. with the γ-secretase inhibitor DAPT (10 mg/kg/day in 50 μl DMSO (Sigma-Aldrich) on a 3 consecutive days (followed by 4 days without injections) per week schedule, for 2 weeks beginning on day 12 post-tumor inoculation) or vehicle control (DMSO).

4.3.9 Evaluation of specific $CD8^+$ T cell responses in vitro

Spleens were harvested from 3 mice per group 7 days after the second DC injection. Splenocytes were then stimulated *in vitro* for 5 days with syngeneic DC pulsed with an equimolar (10 μM) mix of the 3 DLK1 peptides applied in the vaccine. Responder $CD8^+$ T cells were then isolated using magnetic bead cell sorting (Miltenyi Biotec) and co-cultured with

syngeneic DC pulsed with individual DLK1 peptides for 72h, 37^{o}C and 5% CO_2, at which time cell-free supernatants were analyzed for mIFN-γ content using a cytokine-specific ELISA (BD-Biosciences).

4.3.10 Fluorescent imaging of tumors

Tumor tissue samples were prepared and sectioned as previously reported in Chapter 2 (120). Six-micron tissue sections were analyzed for expression of CD31 (BD-Biosciences), VCAM1 (R & D Systems, Minneapolis, MN), CXCL10 (R & D Systems), NG2 (Millipore, Billerica, MA), DLK1 (Santa Cruz), RGS5, Jarid1b (all from Abcam; Cambridge, MA), CD133 (BD-Biosciences), CD44 (Abcam) and Hes1 (Millipore) by immunofluorescence microscopy, with wide field images collected with fixed illumination conditions using a cooled CCD camera (Olympus Magnafire, Center Valley PA). Using Metamorph software (Molecular Devices, Downingtown PA), images were thresholded to delineate signal above background and individual structures measured as the integration of pixel number (total number of positive pixels in the structure above background) multiplied by the brightness of each pixel in grey scales. This product provides the integrated pixel intensity of positive structures and is reported as the mean integrated fluorescence intensity +/- SD. For the analysis of activated VEC in the TME, cellular identity was first defined using co-localization of specific markers (cells staining for both CD31 and VCAM-1) using image overlay and manual counting. We found this method was essential to ensure accuracy in cell identification in tissue with complex morphologies. To perform the quantification images were overlaid with Metamorph software and co-localized structures that could be defined as cells were counted. For analysis of cellular apoptosis, tissue sections were labeled using TUNEL kit (Roche; Indianapolis, IN) as per manufacturer's instructions, followed

by incubation with secondary anti-streptavidin Cy3 antibody (Jackson Immunoresearch, West Grove, PA). Some sections were analyzed by confocal microscopy to generate 30 μm 3-dimensional reconstructions of images. For the vascular permeability imaging, animals received retro-orbital intravenous injections of FITC-labeled tomato lectin (Sigma) and red 20 nm FluoSpheres® (Invitrogen), followed by cardiac perfusion of PBS and 4% paraformaldehyde. Tumors were then immediately resected and imaged by confocal microscopy to generate 17 μm 3-dimensional (3-D) reconstructions. White ruler insets: 50 microns (low magnification upper sub-panels); 10 microns (high magnification lower sub-panels).

4.3.11 Hemoglobin quantitation

The amount of hemoglobin contained in tissues was quantitated using the Drabkin method (227) and reported as μg Hb per mg wet weight of tissue.

4.3.12 Measurement of tumor hypoxia using pimonidazole

BALB/c mice bearing established (treated or untreated) day 21 s.c. RENCA tumors were injected intraperitoneally (i.p.) with 60 mg/kg pimonidazole hydrochloride (Hypoxyprobe™; HPI Inc., Burlington, MA) 30 min prior to euthanasia and tumor harvest and 6 μm tissue sections prepared and analyzed by immunohistochemistry as previously reported (121).

4.3.13 RNA purification and Real-Time PCR array

Total RNA was isolated from bulk single-cell suspensions of day 21 tumors harvested from lvNEG- or lvDLK1-treated mice using Trizol reagents (Invitrogen). Total RNA was further purified using the RNeasy Plus Mini Kit (Qiagen) including the gDNA Eliminator spin column. The purity and quantity of the total RNA was assessed using Nanodrop ND-1000 (CelBio SpA, Milan, Italy). Total RNA (1 μg) was reversed transcribed into cDNA using the RT2 First Strand Kit (Qiagen) and the cDNA added to RT2 SYBR Green ROX™ qPCR Mastermix (Qiagen) and used for quantitative PCR using the RT2 Profiler PCR Array (96-well) for Mouse Notch Signaling Pathway (Qiagen) all according to the manufacturer's instructions. Reactions were performed on a StepOnePlusTM Real-Time PCR thermocycler (Applied Biosystems) using the recommended cycling conditions. All mRNA expression levels were normalized to the expression of GAPDH.

4.3.14 Statistical analysis

Comparisons between groups were performed using a two-tailed Student's *t* test or one-way Analysis of Variance (ANOVA) with Tukey *post-hoc* analysis, as indicated. All data were analyzed using SigmaStat software, version 3.5 (Systat Software, Chicago, IL). Differences between groups with a p-value < 0.05 were considered significant.

4.4 RESULTS

4.4.1 RCC-associated pericytes differentially express the DLK1 antigen

In Chapters 2 and 3, we identified several melanoma-associated vascular antigens, including DLK1, which may represent promising therapeutic vaccine targets. Before assessing the therapeutic potential of DLK1 peptide- and gene-based vaccines in the setting of RCC, we first investigated the pattern of DLK1 expression in the TME and tumor-uninvolved kidneys of BALB/c mice harboring established syngeneic RENCA tumors. After enzymatic digestion of tissues, tumor- and kidney-derived pericytes and VEC were isolated via flow sorting from single-cell suspensions (**Figure 13A**) and their extracted mRNA (along with mRNA from the cultured RENCA cell line) was analyzed by real-time PCR for DLK1 (and housekeeping control HPRT1) transcript content (**Figure 13B**). We observed that pericytes sorted from RCC tumors were uniquely enriched for DLK1 transcripts (**Figure 13B**) when compared to normal kidney vascular cells or RENCA tumor cells, suggesting that DLK1 may represent a general tumor pericyte-associated antigen. Immunofluorescence microscopy performed on day 21 RENCA tumor sections confirmed that DLK1 protein was co-expressed by $NG2^+$ pericytes that were closely approximated to $CD31^+$ VEC *in situ* (**Figure 13C**), NG2 being a general pericyte marker in both normal and tumor tissues (228).

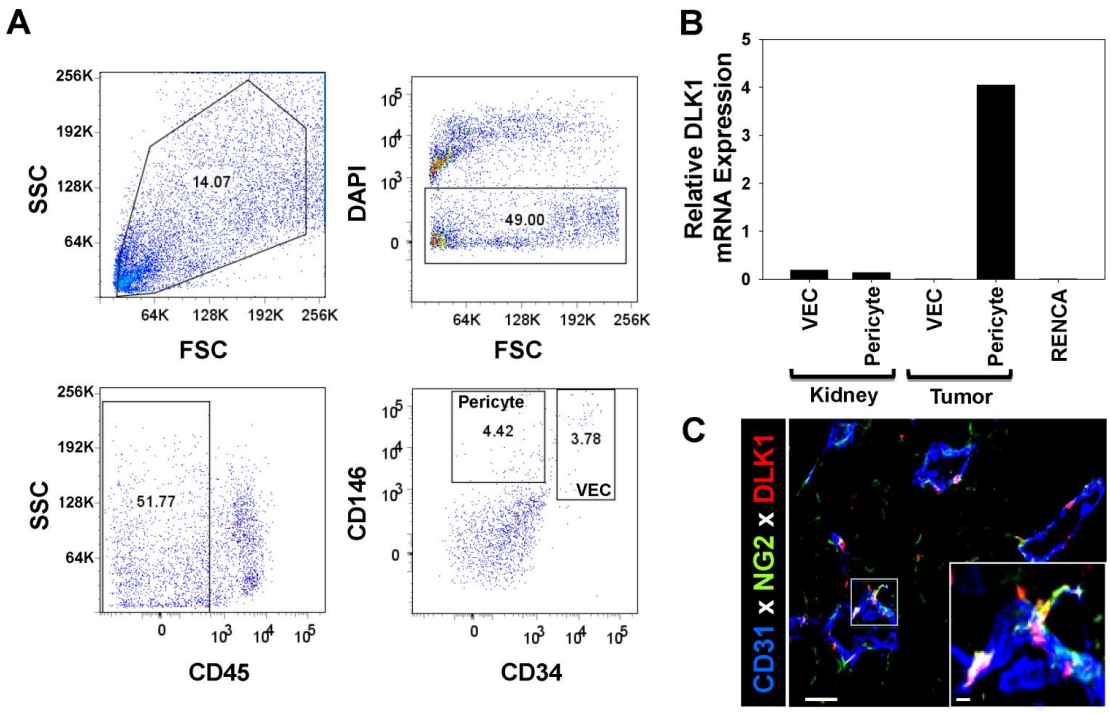

Figure 13. DLK1 is differentially expressed by RENCA tumor-associated pericytes.

RENCA (10^6 tumor cells) was injected s.c. into female BALB/c mice and allowed to progress for 21 days after which animals were euthanized and tumors and normal kidneys harvested. In **A**, tissues were processed into single-cell suspensions and sorted by flow cytometry based on forward versus side-scatter profiles, DAPI exclusion (to reject dead cells), a $CD45^{neg}$ phenotype (i.e. non-leukocytic), and then selectively into $CD146^{+}CD34^{neg}$ pericytes and $CD146^{+}CD34^{+}$ VEC populations based on published assignments of these cell lineage-restricted phenotypes (78, 229). In **B**, mRNA was then isolated from flow-sorted pericytes and VEC, and analyzed for DLK1 transcript expression by real-time PCR. Relative mRNA expression was normalized to housekeeping HPRT1 mRNA expression. In **C**, day 21 RENCA tumor tissue sections were analyzed for expression of CD31 (blue), NG2 (green), and DLK1 (red) by immunofluorescence microscopy. Metamorph quantitation (Materials and Methods) was performed on 10 high power field (HPF) of the fluorescent images, with 28.1 $\pm$ 4.4% of tumor-associated $NG2^{+}$ pericytes co-expressing the DLK1 marker. The analysis also revealed that the majority (i.e. 58.9 $\pm$ 7.6%) of $DLK1^{+}$ cells co-expressed the NG2 marker within the TME. All data are representative of 3 independent experiments performed.

4.4.2 Treatment of RENCA tumor-bearing mice with a DLK1 peptide-based vaccine is therapeutic and associated with specific Type-1 $CD8^+$ T cell (Tc1) activation and recruitment into the TME

As shown in Chapters 2 and 3, we demonstrated that vaccine formulations composed of DC.IL12 pulsed with MHC class I-presented peptides promote robust $CD4^+$ T helper cell-independent priming of antigen-specific $CD8^+$ T *cells in vivo*. Using this approach, we analyzed the impact of treating BALB/c mice bearing established s.c. RENCA tumors with a DLK1 peptide (a pooled equimolar mixture of the $DLK1_{158-166,}$ $DLK1_{161-169}$ and $DLK1_{259-270}$ peptides)-based vaccine. As depicted in **Figure 14A**, mice treated with the DLK1 peptide-based vaccine, but not a control vaccine (*i.e.*, DC.IL12, no peptide) or PBS, exhibited a significant reduction in the growth of RENCA tumors (**Figure 14A**; $p < 0.05$ (ANOVA) on days >13). On day 21 (i.e. 7 days after the booster immunization), $CD8^+$ splenocytes were isolated and analyzed for secretion of IFN-γ in response to stimulation with specific DLK1 peptides presented by syngeneic DC *in vitro*. We noted elevated levels of IFN-γ secretion from $CD8^+$ T cells isolated from mice treated with the DC.IL12 + DLK1 peptide vaccine (versus mice treated with DC.IL12 only or PBS) after stimulation with individual DLK1 peptides, indicating that the vaccine induced poly-specific, anti-DLK1 $CD8^+$ T cell responses *in vivo* (**Figure 14B**).

Since therapeutic Type-1 $CD8^+$ T cells preferentially express a VLA-4^+CXCR3^+ phenotype (111, 230), we next determined whether specific vaccination resulted in the altered expression of VLA-4 and CXCR3 ligands, VCAM-1 and CXCL10, respectively in the TME. A coordinate immunofluorescence microscopy analysis of the TME after DLK1 peptide-based vaccination versus control treatment revealed fewer $CD31^+$ tumor blood vessels (**Figure 14C**),

and these vessels contained VEC enriched in the activated VCAM1^{+} phenotype (**Figure 14D**). We also observed that these same tumors contained elevated levels of CXCL10/IP-10 chemokine protein expression versus control tumors (**Figure 14C)**, suggesting that the DLK1-based vaccination induces a pro-inflammatory TME that is competent to recruit Type-1 T effector cells.

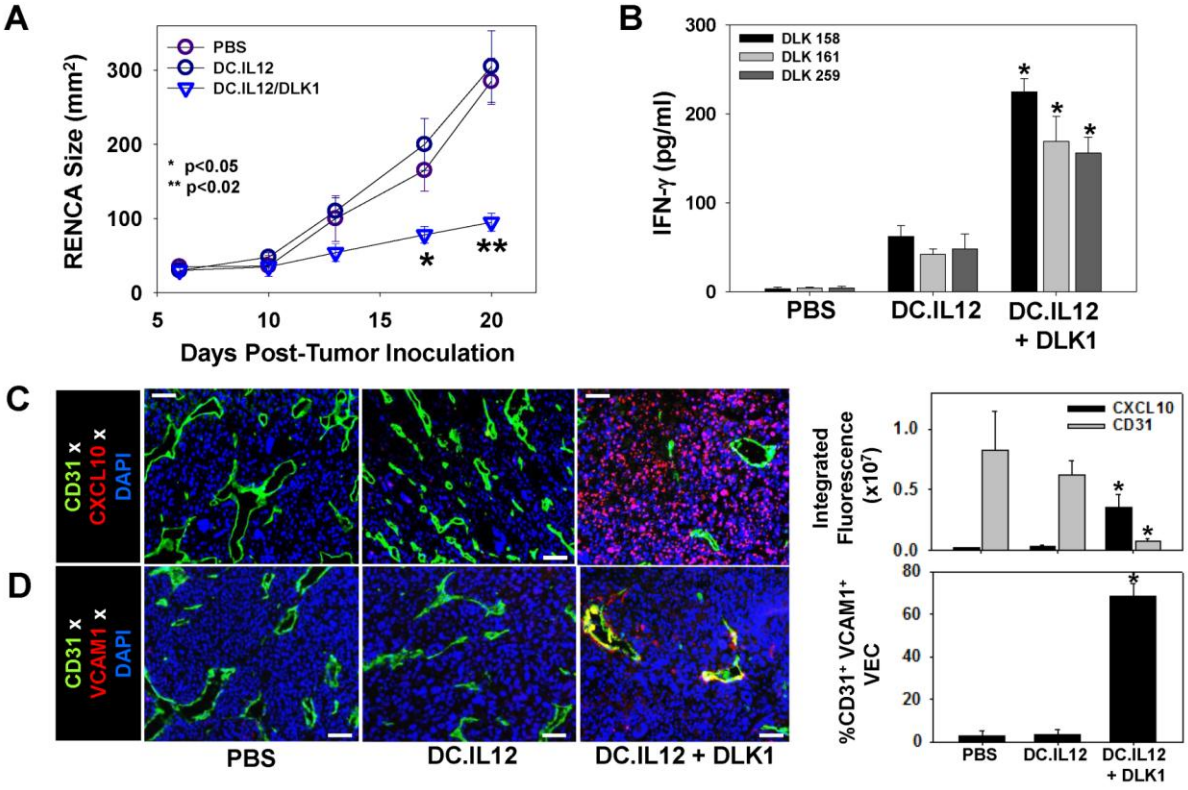

Figure 14. DC/DLK1 peptide-based vaccines are both immunogenic and therapeutic in the murine RENCA model of RCC.

BALB/c mice were inoculated with RENCA tumor cells s.c. on the right flank on day 0. (**A**) Mice were injected s.c. on their left flank on days 7 and 14 (post-tumor inoculation) PBS, 10^6 DC.IL12 or 10^6 DC.IL12 pre-pulsed DLK1 peptides. Tumor growth (mean ± SD) was then monitored over time. (**B**) On day 20 post-tumor inoculation, splenic CD8^{+} T cells were isolated from each cohort and co-cultured with syngenic DC pre-pulsed with individual DLK1 peptides for 24h, at which time, IFN-γ ELISA were performed on the harvested cell-free supernatants. In **C** and **D**, day 20 tumors were fixed, sectioned and analyzed by immunofluorescence microscopy; CD31 (green in panels **C, D**), CXCL10 (red in **C**), VCAM1 (red in panel **D**). The percentage of VCAM1 co-localization with CD31 is depicted as a yellow signal in panel **D** and was quantitated using Metamorph software as described in Materials and Methods. Histograms to the right of images reflect mean fluorescence intensity quantitation of the indicated markers (+/- SD) from 3

independent fields per slide as described in Materials and Methods. Data are representative of 3 independent experiments performed. *$p < 0.05$ versus control treatments (ANOVA).

4.4.3 Vaccination with a recombinant lentivirus encoding murine DLK1 cDNA is therapeutic in the RENCA model of RCC

Clinical trials implementing synthetic tumor peptide-based vaccines have needed to restrict patient accrual to those individuals expressing relevant HLA class I (peptide-presenting) allotypes. To develop a more universal immunization platform, we next engineered a genetic vaccine that would theoretically allow for virally-transduced host antigen-presenting cells to cross-prime a more comprehensive anti-DLK1 T effector cell repertoire. Given the reported superiority of lentiviral-based vaccines to promote prolonged antigen-specific $CD8^+$ T cell responses after a single administration *in vivo* (125), we first constructed a recombinant lentivirus encoding full-length murine DLK1 (lvDLK1) and a negative control virus (lvNEG; **Appendix Figure 7**).

To assess the therapeutic efficacy of specific genetic vaccination against the full-length DLK1 antigen, BALB/c mice bearing established day 7 RENCA tumors received a single intradermal (i.d.) injection of lvDLK1 or control lvNEG at a site distal to tumor (*i.e.*, contralateral). Animals treated with lvDLK1 exhibited significant reductions in tumor growth compared to animals treated with lvNEG (**Figure 15A**). As was the case for DLK1 peptide-based vaccines, immunofluorescence microscopy analysis of tumor sections supported decreased vascularity and loss of ($DLK1^+$) vascular pericytes (**Figure 15B**), and increased presence of the CXCR3 ligand chemokine, CXCL10 and $VCAM1^+CD31^+$ VEC, in the TME of mice treated with lvDLK1 versus lvNEG (**Figure 15C and D**). Enhanced expression of CXCL10 and VCAM1 in

the TME was associated with greater numbers of $CD8^+$ TIL in mice receiving lvDLK1-based vaccines (**Figure 15E**). These findings suggest that immune targeting of DLK1 via a single administration of lvDLK1 can effectively limit tumor growth and induce a pro-inflammatory TME promoting the improved recruitment of TIL.

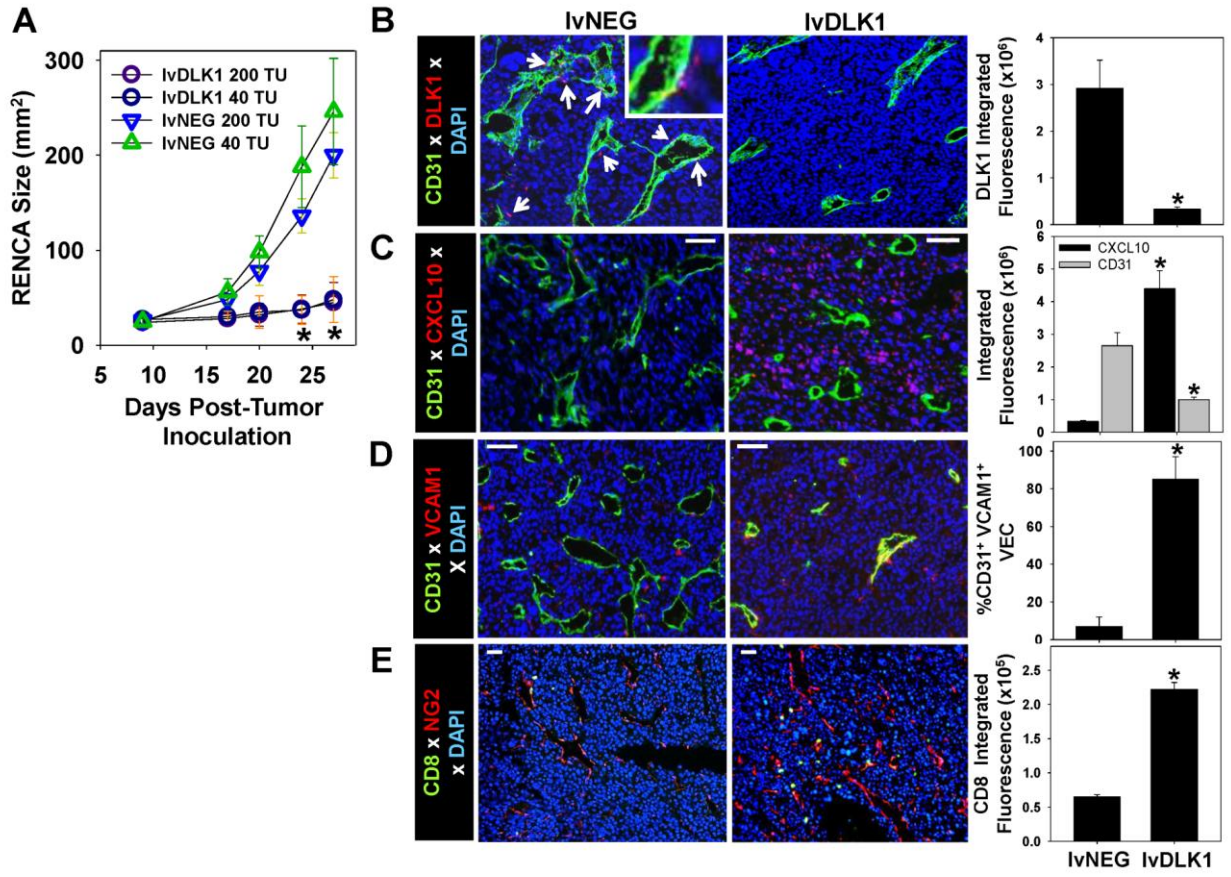

Figure 15. Recombinant lvDLK1-based vaccines are therapeutic and promote a Type-1-polarized TME.

BALB/c mice were inoculated s.c. with RENCA tumor cells in the right flank on day 0. (**A**) On day 10 mice were treated i.d. in the left flank with 40 or 200 transduction units (TU) of lvDLK1 or control virus, lvNEG. Tumor size was then monitored longitudinally. In panels **B-E**, on day 27, tumors were analyzed by immunofluorescence microscopy for expression of (**B-D**) CD31 (green) and (**B**) DLK1 (red) with white arrows indicating $DLK1^+$ cells, (**C**) CXCL10, (**D**) co-localization of VCAM1 with CD31, and (**E**) $CD8^+$ TIL (green) and NG2 (red). Histograms to the right of images reflect mean fluorescence intensity quantitation of the indicated markers (+/- SD) from 3 independent fields per slide as described in Materials and Methods. Data are representative of 3 independent experiments performed. *$p < 0.05$ versus control treatments (ANOVA).

4.4.4 Vaccination with lvDLK1 normalizes the RENCA vasculature

It has been suggested that the tumor-associated vasculature of mice deficient in immature pericytes appears "normal" with minimal arborization and reduced vascular permeability (68), supporting therapeutic strategies to selectively reduce or eradicate immature vascular pericytes within tumor sites. Given the ability of our lvDLK1-based genetic vaccine to reduce the content of $DLK1^+$ (immature) pericytes in the tumor stroma, we sought further evidence supporting therapeutic vascular remodeling as a consequence of treatment with this modality. We noted that RENCA tumors harvested from mice treated with lvDLK1 appeared "anemic" when compared to control tumors (**Figure 16A**), a subjective index that was subsequently confirmed based on an analysis of hemoglobin content in tumor lysates (**Figure 16B**). When we analyzed tumors for expression of NG2 using immunofluorescence microscopy, we observed that animals vaccinated with lvDLK1 exhibited tumors with significant reductions in numbers of $NG2^+$ pericytes in their TME versus tumors from animals vaccinated with lvNEG (**Figure 16C and D**). Residual tumor pericytes in lvDLK1-treated animals were tightly-approximated to $CD31^+$ VEC, unlike the randomly-distributed pattern of pericytes detected in the stroma of tumors isolated from control mice.

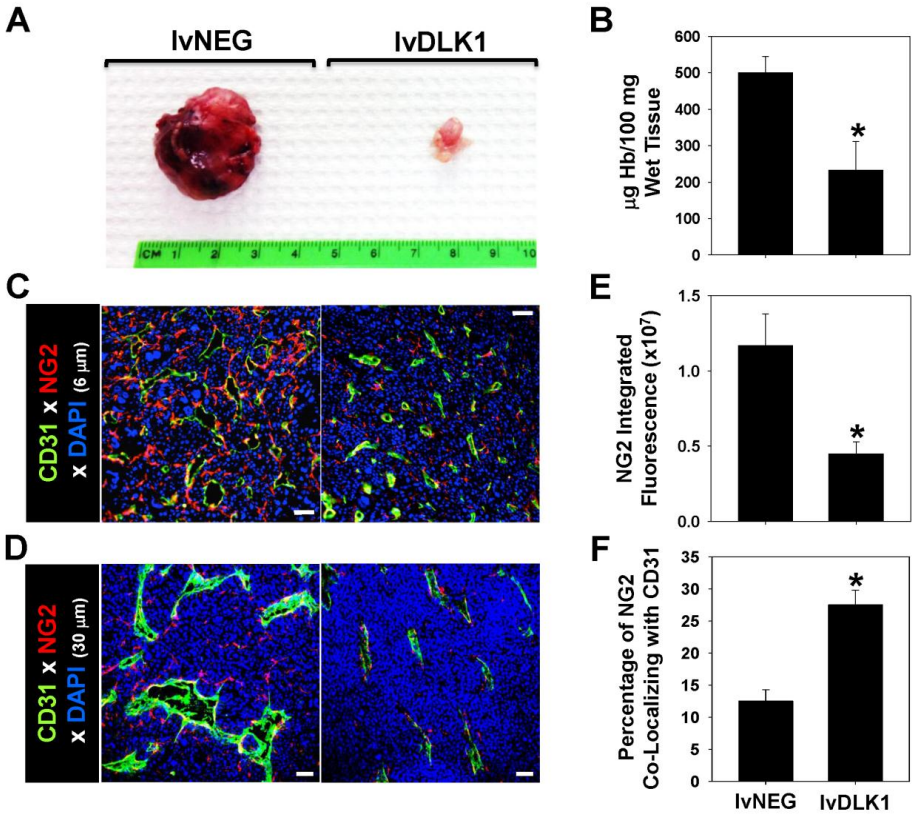

Figure 16. Recombinant lvDLK1-based vaccines promote normalization of the tumor vasculature.

Mice bearing day 10 RENCA tumors were treated with 200 TU of lvDLK1 or lvNEG as outlined in **Figure 15**. On day 27 post-tumor inoculation, tumors were evaluated macroscopically (**A**) and for hemoglobin content (**B**). In **C** and **D**, tumor sections were analyzed by immunofluorescence microscopy for expression of CD31 (green) and NG2 (red). In **C**, 6 µm sections were imaged by wide-field microscopy, while in **D**, 30 µm sections were imaged by confocal microscopy to generate 3-D reconstructions. For **C**, mean data ± SD of three independent fields per slide is reported for each group from 1 representative experiment of 3 performed.

To investigate changes in tumor vascular permeability, vaccinated animals received intravenous injections of two fluorescently-labeled probes, tomato lectin-FITC to bind/mark the vascular endothelium and small 20 nm (red) FluoSpheres® to determine vessel leakiness into tissue. When compared to controls, the tumor blood vessels in mice vaccinated with lvDLK1 displayed a simple tubular architecture devoid of extensive branching (**Figure 17A**). Furthermore, while

the perivascular stroma of tumors in control animals was littered with the red FluoSpheres®, these probes were virtually undetected in tumors harvested from lvDLK1 vaccinated mice, consistent with diminished vascular permeability in the TME of these latter animals (**Figure 17A**).

Given the apparent trimming of vascular branches in the RENCA TME, and reduction in vascular permeability after vaccination with lvDLK1 (but not lvNEG), we hypothesized that plasma nutrients required for sustaining tumor cell viability would be limited to regions adjacent to the remaining normalized blood vessel network. TUNEL analyses revealed that indeed, the level of cellular apoptosis in the TME of lvDLK1-treated mice was substantially increased when compared with tumors isolated from control treated animals (**Figure 17B**). Furthermore, virtually all apoptotic events (*i.e.*, "dead zones") in RENCA tumors isolated from lvDLK1-vaccinated mice were located in tissue regions approximately 60 microns away from residual $CD31^+$ blood vessels in planar tissue imaging analyses (**Figure 17B**). These data suggest that immunization against DLK1 allows for the immunotherapeutic "normalization" of tumor blood vessels *in vivo*.

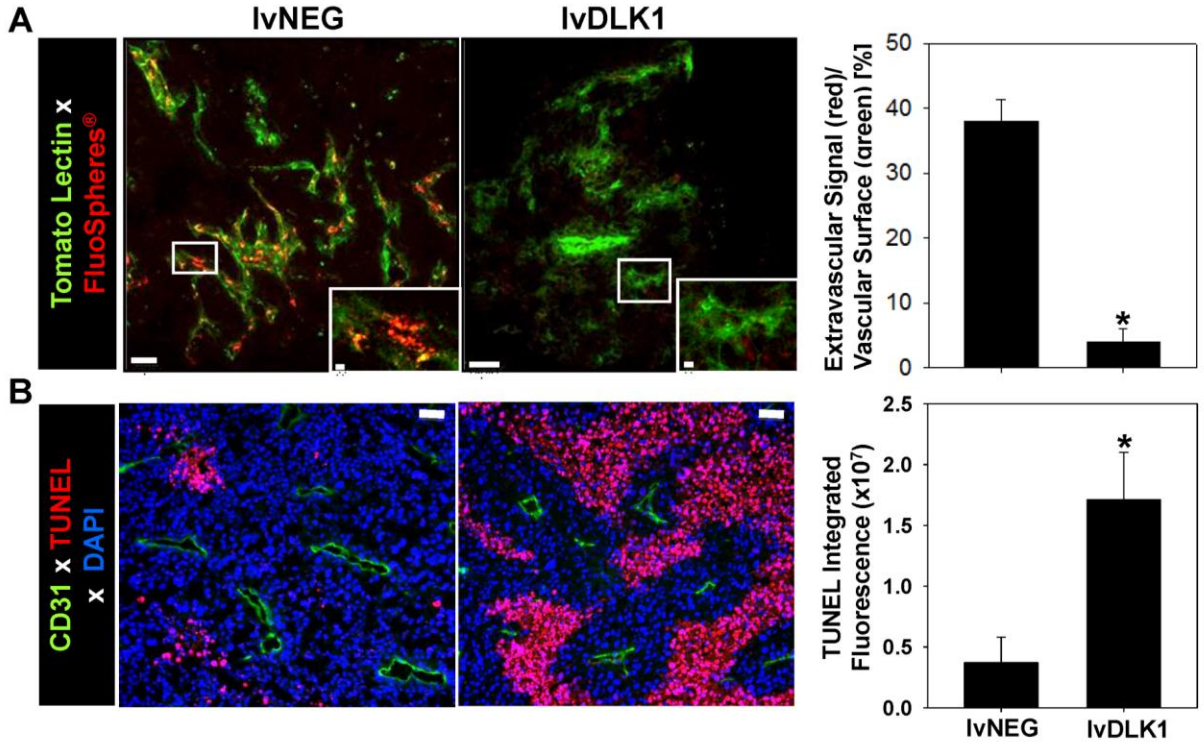

Figure 17. Recombinant lvDLK1-based vaccination reduces tumor vascular permeability resulting in the development of apoptotic "dead zones" in the TME distal to residual blood vessels.

In repeated experiments as outlined in **Figure 15**, (**A**) treated mice received intravenous injections of tomato lectin-FITC to label vascular endothelium (green) and 20 nm FluorSpheres® to assess vascular permeability (red) on day 24 post-tumor inoculation. Whole tumor tissue was then imaged immediately by confocal microscopy at a depth of 17 μm. *$p < 0.05$ for lvDLK1 versus lvNEG (t-test). (**B**) On the same day, tumors resected from unlabeled mice were analyzed for expression of CD31 (green) and apoptotic nuclear staining with TUNEL reagent (red). Histograms to the right of images reflect mean fluorescence intensity quantitation of the indicated markers (+/- SD) from 3 independent fields per slide as described in Materials and Methods. Data are representative of 3 independent experiments performed. *$p < 0.05$ for lvDLK1 versus lvNEG (t-test).

4.4.5 Therapeutic vaccination with lvDLK1 results in reduced hypoxia and a lower incidence of cell populations expressing hypoxia-responsive markers in the TME

Hypoxia frequently occurs in solid cancers as a consequence of inefficient perfusion of oxygen into tumors by "aberrant" blood vessels (231, 232), resulting in reduced recruitment and function of TIL, increased prevalence of immunosuppressive cells/modulators, dysregulated angiogenesis, and the accumulation of "stem-like" cell populations (i.e. cancer stem cells/tumor initiating cells, cells undergoing epithelial-to-mesenchymal transition) in the TME (233, 234). To investigate changes in hypoxia within tumors after vaccination with lvDLK1 versus lvNEG, we injected mice i.p. with pimonidazole (a hypoxia marker that undergoes reductive activation and then conjugates to thiol-containing proteins specifically in hypoxic cells, allowing for immunohistochemical detection of tissue regions exhibiting low [< 1.3%] O_2 tension) (235). Using this imaging technology, we found that tumors isolated from mice receiving lvDLK1 vaccines had a very low hypoxic index when compared to tumors culled from control animals (**Figure 18A**). Given this large reduction in TME hypoxia post-vaccination with lvDLK1, we next investigated treatment impact on expression of hypoxia-responsive gene products associated with immature vascular stromal cells (*i.e.*, RGS5) and/or stem-like cell populations (*i.e.*, Jarid1B aka histone demethylase lysine demethylase 5b; CD133, CD44) (236-238). Immunofluorescence microscopy analysis of day 27 tumor sections revealed that the expression of these markers was coordinately reduced in RENCA tumors after host vaccination with lvDLK1 (**Figure 18B-F**). When taken together, these data indicate that vaccination with lvDLK1 results in the recovery of normoxia in the TME in association with the conditional alteration in the phenotype (and presumably function) of a range of stromal cell subpopulations *in vivo*.

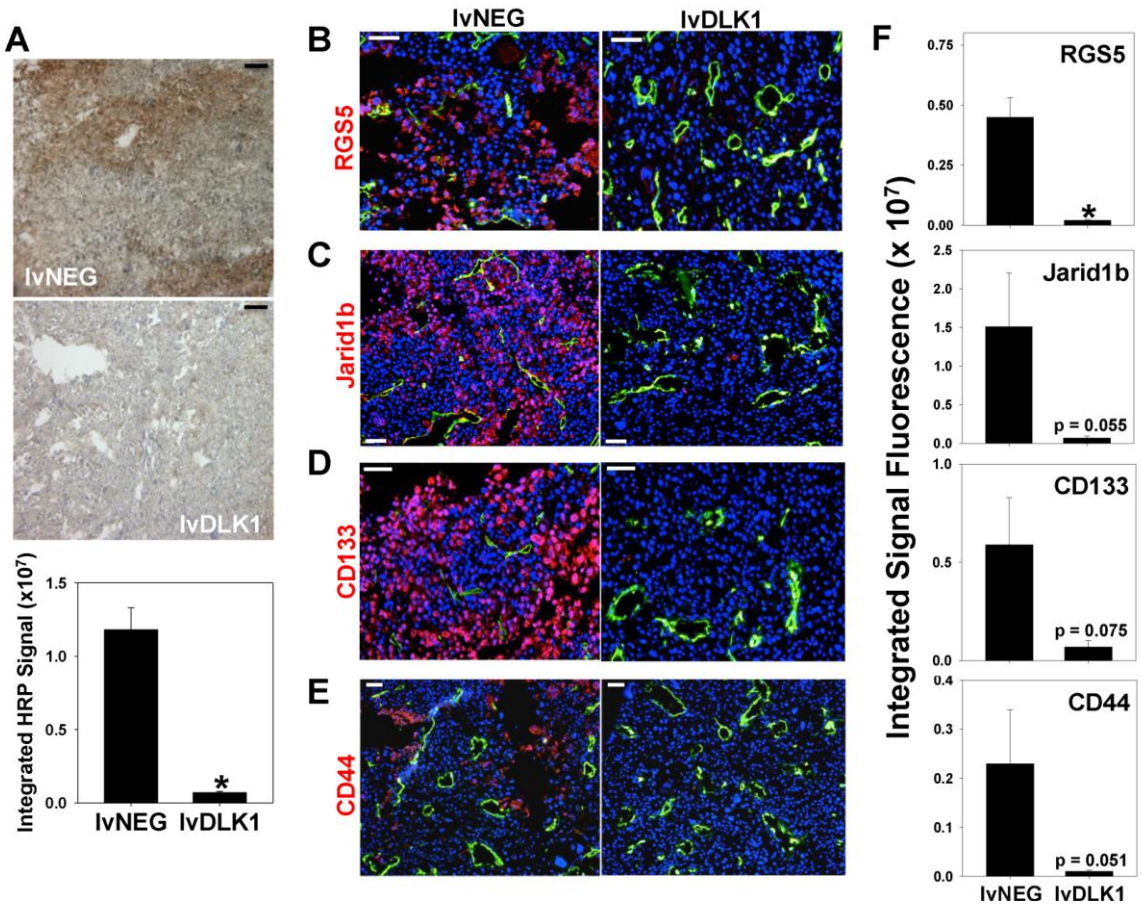

Figure 18. Recombinant lvDLK1-based vaccines promote normoxia in the TME in association with the loss of cells bearing stem cell-like phenotypes.

Mice bearing day 10 RENCA tumors were treated with 200 TU of lvDLK1 or lvNEG as outlined in **Figure 15**. (**A**) On day 21, mice were injected i.p. with the hypoxia probe pimonidazole, after which tumors were analyzed by HRP- immunohistochemistry. In **B-E**, day 21 tumors from that did not receive pimonidazole hydrochloride were analyzed by immunofluorescence microscopy for expression of CD31 and RGS5 (**B**), Jarid1b (**C**), CD133 (**D**) and CD44 (**E**). In **F**, histograms to the right of panel B-E images reflect mean fluorescence intensity quantitation of the indicated markers (+/- SD) from 3 independent fields per slide as described in Materials and Methods. Data are representative of 3 independent experiments performed. *$p < 0.05$ for lvDLK1 versus lvNEG (t-test).

4.4.6 Loss of DLK1 expression in the TME after therapeutic vaccination with lvDLK1 leads to increased locoregional activation of Notch.

Since lvDLK1-based vaccination leads to loss of DLK1 expression in the TME (**Figure 15**) and DLK1 represents a functional inhibitor of Notch signaling (127), we hypothesized that this therapeutic vaccine would promote enhanced canonical Notch signaling in therapeutic RENCA TME. As shown in **Figure 19A** and **B**, RENCA tumors isolated from lvDLK1-treated (but not control) mice contained cells strongly expressing cytoplasmic/nuclear Hes1 protein, a Notch transcriptional target required for the tumor-suppressor action of activated Notch (132, 134). $Hes1^+$ cells included both $CD31^+$ VEC and non-VEC stromal cell populations in the TME (**Figure 19A**). Corollary gene array analyses also supported the enhanced transcription of numerous Notch target genes (including the canonical Notch ligands (DLL1, DDL3, DLL4, Jag1/2) and the Notch1-4 receptors, among others), but not control β2-microglobulin, in lvDLK1- versus lvNEG-treated tumors (**Figure 19C**). To determine the importance of canonical Notch signaling on the anti-tumor efficacy of genetic vaccination against DLK1, we immunized BALB/c mice bearing established s.c. RENCA tumors with lvNEG or lvDLK1 as described in **Figure 15A**, with cohorts of lvDLK1-vaccinated animals injected i.p. with the γ-secretase inhibitor DAPT, which inhibits the generation of the Notch intracellular domain (NICD) required for downstream Notch signaling events (239), or vehicle control DMSO. As shown in **Figure 19D**, administration of DAPT partially suppressed the anti-tumor action of lvDLK1-based therapeutic vaccination.

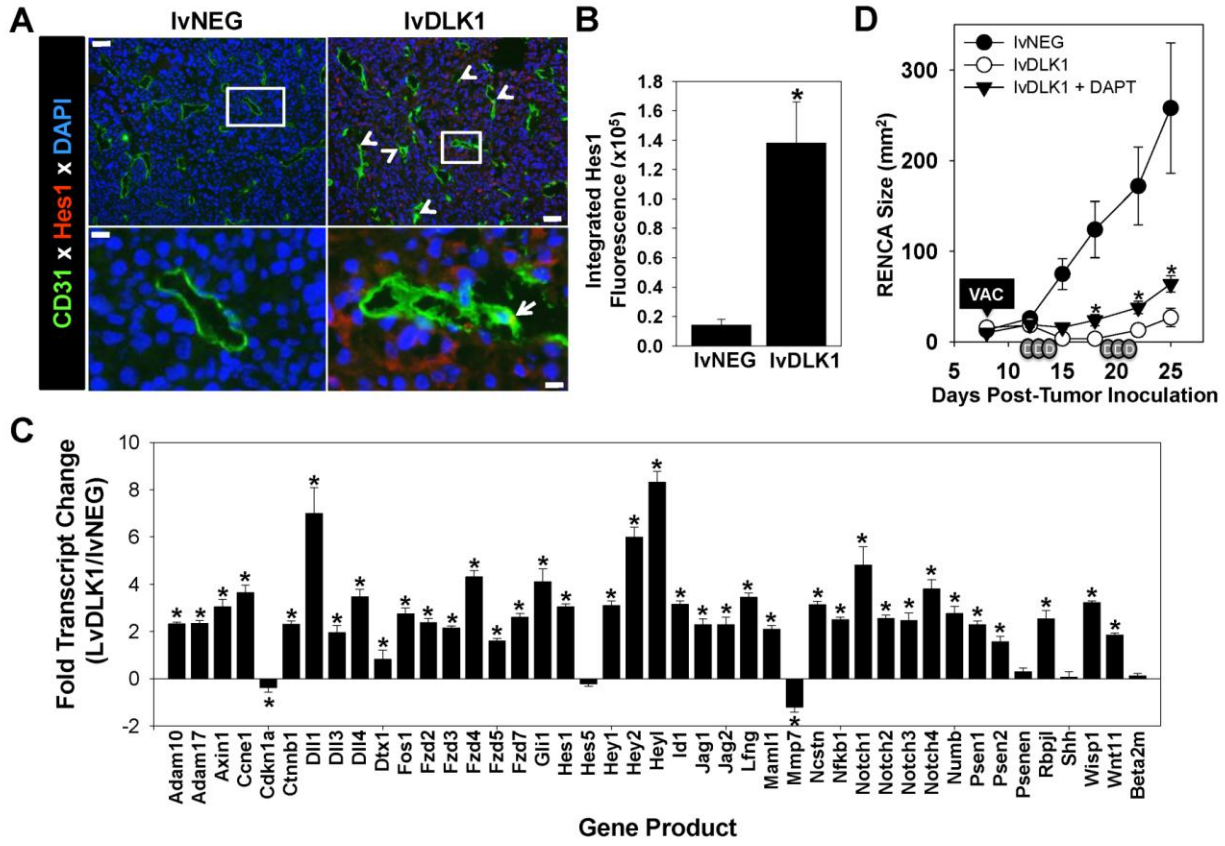

Figure 19. Treatment with lvDLK1 vaccines results in Notch activation in the TME which is partially responsible for the anti-tumor effectiveness of this treatment strategy.

(**A**) Tumor sections were isolated as described in **Figure 15** and evaluated by fluorescence microscopy using specific antibodies against CD31 (green) and Hes1 (red; from Millipore). DAPI counterstaining was used to image cell nuclei (blue). White arrows in image insets indicate $Hes1^{+}CD31^{+}$ VEC. (**B**) Mean fluorescence intensity quantitation of Hes1 protein expression (+/- SD) from 3 independent fields per slide is reported as described in Materials and Methods. Data are representative those obtained in 3 independent experiments performed. *$p < 0.05$ (t-Test). (**C**) mRNA transcripts of Notch target genes were analyzed using an Real time PCR gene array. The ratio of transcript levels for a given gene product among total tumor mRNA isolated from lvDLK1- versus lvNEG-treated mice is reported. Negative control transcript = β_2-microglobulin (beta 2-m). (**D**) Established day 8 s.c. RENCA tumors were treated with 200 TU of lvNEG or lvDLK1 (*i.e.*, VAC) as described in the **Figure 15A** legend and Materials and Methods. DAPT (depicted as small gray ovals labeled "D" on the x-axis) or vehicle control DMSO was then provided as indicated. Tumor size was then monitored longitudinally. *$p < 0.05$ for lvDLK1 + DAPT treatment versus lvDLK1 treatment; also $p < 0.05$ for the lvDLK1 + DAPT and lvDLK1 treatments versus lvNEG control treatment on days $\geq$ 15 post-tumor inoculation (ANOVA).

4.5 DISCUSSION

The major finding in this report is that DLK1 is a tumor pericyte-associated antigen that can be immunologically targeted via specific peptide- or gene-based vaccination *in vivo*, leading to the effective "normalization" of the vasculature in the TME and a drastic reduction in solid tumor growth *in vivo*. Effective therapeutic vaccination resulted in the activation of Type-1 (IFN-γ producing) DLK1-specific $CD8^+$ T cells in the periphery and the improved recruitment of $CD8^+$ T cells into/around residual blood vessels in the TME. Therapeutically-normalized blood vessels in tumors exhibit a simplified conduit design with tightly-approximated (abluminal) $NG2^+DLK1^{neg}RGS5^{neg}$ mature pericyte populations that appear improved in their structural integrity based on a reduction in vascular permeability. Tumors in DLK1-vaccinated mice became normoxic and displayed a dramatic increase in the rate of apoptotic death in regions of the tumor that were further away from residual blood vessels. These findings support a model paradigm in which specific immune effector T cells may serve as regulators of the "angiogenic switch" (68, 95, 120, 121, 231) by monitoring and controlling the status of $DLK1^+$ pericytes within the TME.

Vaccination against DLK1 also induced a pro-inflammatory TME based on the acquisition of activated $VCAM1^+$ VEC and concomitant production of the CXCR3 ligand chemokine CXCL10, responsible for recruiting Type 1 TIL. We hypothesize that an initial wave of DLK1-reactive Type-1 TIL results in perivascular secretion of IFN-γ and TNF-α in the TME, leading to locoregional upregulation of IFN-γ/TNF-α-responsive gene products such as VCAM-1 and CXCL10 (240, 241). Such alterations in the TME would then be expected to foster improved uptake of tumor debris (*i.e.*, apoptotic bodies) by recruited/activated antigen-

presenting cells and the corollary reiterative cross-priming of an expanded, protective T cell repertoire reactive against both tumor- and tumor vascular-associated antigens (120) that may be directed into the pro-inflammatory TME.

Interestingly, a recent report by Reis *et al.* (242) suggests that the conditional activation of the Wnt/β-catenin/Notch signaling pathway can lead to vascular normalization, as indicated by reduced vascular density and improved mural cell attachment, in intracranial murine glioma models. Our data support such a paradigm, with specific vaccination resulting in removal of DLK1 expression (and Notch antagonism (127, 243)) in the TME. Such immune pressure improved Notch signaling based on a dramatic increase in the intratumoral expression of Hes1 protein and the transcriptional activation of multiple Notch target genes. The transcriptional profiling also supports differentially increased expression of Frzd2, Frzd4, Frzd7 and β-catenin (Ctnnb1) in RENCA tumors harvested from lvDLK1-vaccinated mice supporting the co-activation of canonical Wnt/β-catenin signaling (244) in the therapeutic TME, consistent with the model proposed by Reis *et al*. (242). As such, our data suggest that vaccination against DLK1 (as an integral transmembrane protein or via its shed extracellular domain (245)) may derepress canonical Notch/Wnt/β-catenin signaling in endothelial cells (and other stromal cell populations) within the TME, thereby promoting vascular quiescence/normalization (127, 242, 246). Vaccination against DLK1 may also improve Type-1 functionality of tumor-associated macrophages and DC (*i.e.*, enhanced IL-12p70 and CXCL10 production) and T cells (247). Indeed, we observed that the functional antagonism of Notch signaling *in vivo* (based on administration of the γ-secretase inhibitor DAPT) partially ablated the anti-tumor benefits associated with lvDLK1-based therapeutic vaccination, suggesting a supporting role for canonical Notch signaling in treatment outcome. Future studies will investigate the potential role

of Wnt/β-catenin signaling in therapeutic benefit associated with DLK1-based vaccines by applying specific inhibitors of these pathways in our therapeutic model.

The TME of progressively-growing, control tumors was enriched in cells expressing markers known to contain HRE in their promoter regions, such as CD44, CD133 and Jarid1B (236-238), that have been previously linked to cell populations with "stem-like" characteristics (233, 234). Notably, the "normalized" TME after therapeutic vaccination with lvDLK1 was normoxic and largely devoid of cells expressing these hypoxia-responsive antigens. Although the most simplistic reason for this change reflects the transcriptional silencing of these gene products in the TME of lvDK1-vaccinated animals, it is also conceivable that the therapeutic TME is poor in recruiting cells bearing these phenotypic markers, and/or that the vaccine evoked corollary cross-priming of cytotoxic $CD8^+$ T cell responses capable of eradicating $CD44^+$, $CD133^+$ and $Jarid1B^+$ target cells in effectively-treated tumors. With regard to the latter scenario, we currently plan to longitudinally evaluate the reactivity of the evolving therapeutic $CD8^+$ T cell repertoire against peptide epitopes derived from the CD44, CD133 and Jarid1B (as well as alternate "stem cell"-associated/hypoxia-responsive markers such as ALDH1, Oct4 and Nanog) (237) antigens in RENCA-bearing mice treated with DLK1 peptide/gene-based vaccines.

The anti-angiogenic action mediated by the DLK1 vaccine-induced $CD8^+$ T cell repertoire would be anticipated to differ, and likely complement, that of alternative pharmacological anti-angiogenic treatment modalities such as anti-VEGF antibodies (*i.e.*, bevacizumab) and small molecule TKI (*i.e.*, sunitinib) (99, 220, 248). In most cases, tumors treated with these agents rapidly become drug-refractory due to their adoption of compensatory growth/progression pathways. As such, DLK1-based vaccines could represent a logical second-line approach in the many cases of developed resistance to bevacizumab, sunitinib or similar

anti-angiogenic drugs. DLK1-based vaccines may also represent effective co-first line therapeutic agents, since the specific activation, recruitment and function of anti-DLK1 T effector cells in the TME would be anticipated to be improved by the co-administration of anti-angiogenic TKI that reduce suppressor cell populations (most notably in RCC patients) and activate a pro-inflammatory TME *in vivo* (109-111). Based on these expectations, we plan to evaluate the comparative therapeutic efficacy of combined sunitinib + lvDLK1 vaccination treatment in our existing subcutaneous RENCA model, as well as, in an orthotopic RCC model using RENCA.luc (RENCA cells transduced with luciferase cDNA) to allow for vital bioluminescence monitoring of tumor growth and metastasis. Although we have not observed signs of off-target autoimmune pathology as a consequence of DLK1-targeted vaccination (*i.e.,* inhibition of cutaneous wound healing (120), tissue vasculitis; data not shown) to date, these new models will provide us with additional opportunities to investigate potential combination treatment-associated toxicities in future.

Consistent with our findings in the RENCA model, pericytes from freshly-isolated human RCC (but not patient-matched normal adjacent kidney tissue) also differentially (over)express the DLK1 antigen *in situ* (**Appendix Figure 8**). When coupled with the knowledge that anti-DLK1 $CD8^+$ T cell responses can be developed from human cancer patients after *in vitro* sensitization, as shown in Chapter 2 (208), we believe that DLK1-based vaccines (as single agents or in combination approaches) represent attractive candidates for clinical translation in the setting of RCC and alternate well-vascularized forms of solid cancer.

5.0 GENERAL DISCUSSION

Given the muted clinical efficacy that has been observed thus far for conventional therapeutics applied against solid tumor targets, including RCC, there has been increasing interest in developing and applying agents that mitigate the pro-cancer supportive influence of stromal cell populations in the TME [including VEC, pericytes and (myo)fibroblasts (119, 249)]. In the second chapter, I reported that therapeutic intratumoral treatment with DC engineered to express IL-12 induces the crosspriming of protective $CD8^+$ T cells reactive against tumor-associated pericytes and VEC, as well as, antigens that are differentially expressed by these cell populations in the B16 melanoma TME (*i.e.,* DLK1, HBB, PDGFRβ, RGS5, EphA2, and TEM1) but expressed at very low levels, if at all, on pericytes and VEC isolated from normal tissues. Additionally, I found via real-time PCR that DLK1, RGS5, PDGFRβ, and TEM1 expression was enriched in the tumor pericytes isolated from the RENCA RCC TME, but these genes were minimally expressed in pericytes from normal kidney and VEC from tumor and normal kidney (**Appendix Figure 9**), thereby limiting concerns for any off-target effects in treated individuals. Indeed, vascular antigen vaccine-induced $CD8^+$ T cells failed to react against VEC and pericytes isolated from the tumor-uninvolved kidneys of treated mice and no apparent inflammation or vasculitis in normal tissue. We also did not observe any delay in the kinetics of the cutaneous wound-healing processes, changes in blood chemistry, or alterations in gross tissue pathology in healthy mice pre-vaccinated against TASA.

There exists a number of therapeutic means by which to target the tumor-associated blood vasculature that can lead to at least transient tumor regression (68, 96, 111, 119, 122). In the third chapter of my thesis, I described an anti-vasculature vaccine implementing DC.IL12 loaded with MHC class I-restricted TASA peptides, and found that not only did this vaccine elicit anti-tumor immunity, it promoted reduced vascularity and increased $CD8^+$ TIL in the TME, implying that the treatment had invoked vascular remodeling or "normalization" *in vivo*. The "normalization" of the tumor vasculature in response to treatment has shown correlative clinical benefit in successful cancer therapies (68, 181-183) and may be the direct result of the $CD8^+$ T cell-mediated death of pericytes and/or VEC within the TME. Indeed, we have shown through various studies that this vaccine formuation induces MHC class I/$CD8^+$ T cell-dependent recognition of tumor vascular cells and TASA peptides. As a result, tumor-associated stromal cells become targets of activated effector Tc1 cells resulting in a downstream vascular remodeling event. These vascular changes may then lead to accumulation of dead/dying tumor cells, as well as other stromal cell populations within the TME, providing non-pericyte/VEC antigens for cross-priming of an evolving protective and highly-diversified Tc1 repertoire (168, 190-192) capable of destroying the myriad targets within the heterogeneous TME.

Based on these findings, I examined the efficacy of a targeted vaccine against tumor pericytes. As shown in Chapters 2 and 3, and in **Appendix Figure 9**, RGS5 is overexpressed in tumor pericytes and was an immunologically relevant target in both the B16 melanoma and MC38 colon carcinoma models. It has been reported that RGS5 is transiently expressed throughout development, with one of the earliest studies showing RGS5 expression restricted to pericytes in mouse embryos (84). RGS5 was also found to be highly upregulated in PDGFRβ^+ pericytes isolated from murine tumors (83). Indeed, I showed RGS5 to be expressed in pericytes

isolated from both human and mouse RCC tumors, but not in normal kidney pericytes or VEC (**Appendix Figure 10**).

It has been shown that genetic deletion of RGS5 led to a normalized vasculature in insulinomas, similar to what is observed in disease free pancreas (68). Given the observed therapeutic benefit seen in HHD mice when given DC.IL12 with HLA-A2-restricted RGS5 peptides in both the B16 melanoma and MC38 colon carcinoma models, I investigated the effects of a similar vaccine in the mouse RENCA tumor model with BALB/c mice. In chapters 2 and 3, synthetic RGS5 peptides were selected for the study based on a high algorithm predicted binding score to the HLA-A2.1 class I molecule. In the RENCA model RGS5 epitopes were selected based on a predicted high binding affinity to the BALB/c MHC class I molecule, H-2^d: $RGS5_{161\text{-}176}$ (LPRFVRSEF), $RGS5_{11\text{-}20}$ (SCLERAKEI), and $RGS5_{150\text{-}159}$ (SFDLAQKRI). Animals with established RENCA tumors were injected twice with DC.IL12 loaded with pooled equimolar amounts of the RGS5 peptides. However, treated animals showed no changes in tumor growth compared to control groups receiving PBS or DC.IL12 without peptide (**Appendix Figure 11**). This lack of response was confounding, given the profound effect observed in the HHD model using HLA-A2 presented RGS5 peptides. We postulated that the predicted H-2^d-presented epitopes chosen may not have been immunogenic or recognizable to the endogenous T cell repertoire of the BALB/c model. It has been shown that cutaneous vaccination with lentivirus results in specific transduction of skin DC, leading to activation of antigen-specific T cells (125), therefore we tested the therapeutic efficacy of a genetic vaccine using a lentivirus encoding full-length *human* RGS5 (lvRGS5) that was currently available. Human RGS5 shares 88% homology with mouse RGS5 with shared epitopes, as shown in Chapters 2 and 3, therefore we assumed the human homolog could be processed and presented similarly in the mouse. I first

confirmed that the lentivirus was functional by transducing bone marrow derived dendritic cells and looked for RGS5 mRNA expression by reverse transcriptase PCR (**Appendix Figure 12A**). I treated RENCA tumor-bearing mice with a single intradermal injection of lvRGS5 or PBS and found that animals treated with the lentivirus had significantly delayed tumor growth compared to PBS-treated animals (**Appendix Figure 12B**). When I looked at expression of Type-1 pro-inflammatory genes in bulk tumor lysate by reverse transcriptase PCR, I found and overall increase of proinflammatory chemokine/cytokine transcript levels (CXCL9, CXCL10, CXCL11, IL-12p40, and IFN-γ) in lentivirus-treated animals compared to PBS controls (**Appendix Figure 12C**). Interestingly, splenic T cells isolated from animals treated with varying concentrations of lentivirus (lv-LO, lv-MED, lv-HI), which despite exhibiting a seemingly dose-dependent anti-tumor response (**Appendix Figure 13A)** showed no RGS5-specific response (as measured by CFSE dilution and IFN-γ production of $CD4^+$ and $CD8^+$ T cells) compared to PBS-treated animals (**Appendix Figure 13B-E**). This raises the question of whether the anti-tumor effect and increase in pro-inflammatory gene expression observed was due to immune targeting of RGS5 of simply a general response against the lentivirus itself. At the time these experiments were performed, no blank lentivirus (*i.e.*, lentivirus that did not encode a gene) was available as a negative control. However, these experiments were repeated using a lentivirus that encoded full-length ovalbumin (lvOVA) as a negative control. To determine whether the lvOVA was functional, I transduced bone marrow DC with the lentivirus (DC.ova) and co-cultured them with OT-I T cells. OT-I T cells proliferated, as indicated by CFSE dilution, and produced high amounts of IFN-γ when co-cultured with DC.ova compared to DC that were not transduced (DC.null) or when cultured alone (**Appendix Figure 14A** and **B**), confirming that lvOVA was a functional lentivirus that could transduce DC to express the antigen. When I tested lvRGS5,

using lvOVA as a negative control, I found that lvRGS5 did not confer any therapeutic benefit compared to lvOVA (**Appendix Figure 14C**). While it is possible that RGS5 is not as immunogenic of a target in the BALB/c model as it is in the HHD model, explaining why neither peptide nor gene vaccine was effective in inhibition of RENCA tumor growth, there may still be alternative RGS5 epitopes that would be more immunologically relevant that were not produced with the lentivirus encoding the human homolog of RGS5. A lentivirus encoding mouse RGS5 is currently under development to further investigate whether RGS5 could be a therapeutic target for vaccination in the RENCA model.

In my subsequent studies reported in the fourth chapter, the focus of anti-vascular therapy was narrowed down to another antigen that was enriched in tumor pericytes: DLK1. As shown in Chapters 2 and 3, DLK1 was an immunologically relevant target for TASA-based vaccines. We found that, as was the case in the B16 melanoma and MC38 colon carcinoma models with HHD mice, DLK1 was also overexpressed in the tumor-associated pericytes RENCA RCC tumors grown in BALB/c mice but not from same animal-matched (tumor-uninvolved) kidney tissue. To recapitulate the studies performed in Chapters 2 and 3, I effectively treated established RENCA tumor-bearing animals with a cellular vaccine consisting of DC.IL12 loaded with MHC class I (H-2^d)-restricted DLK1 peptides. Since clinical trials implementing synthetic tumor peptide-based vaccines are restricted to those patients expressing relevant MHC class I allotypes, I also developed a lentivirus-based genetic vaccine that could theoretically allow for virally-transduced host antigen-presenting cells to cross-prime a more comprehensive anti-DLK1 T cell repertoire in any treated individual. I showed that therapeutic vaccination (cellular or genetic) results in the activation of Type-1 (IFN-γ producing) DLK1-specific $CD8^+$ T cells in the

periphery (spleen) and the improved recruitment of these $CD8^+$ T cell populations into/around residual blood vessels in the TME.

In the third chapter, I reported that a reduction in vascularity was observed in therapeutically vaccinated animals, implying that immunological targeting of the tumor stroma led to vascular "normalization." I investigated this phenomenon further in studies reported in the fourth chapter and discovered that upon treatment with lvDLK1, blood vessels in RENCA tumors exhibited a simple conduit design with tightly-approximated mature pericytes with improved structural integrity based on a reduction in vascular leakiness/permeability and hypoxia. I also found that vaccination against DLK1 induced a pro-inflammatory TME with increased $VCAM1^+$ VEC and concomitant production of CXCL10 chemokine. These "normalizing" conditions render the TME to be more permissive to Type 1 T cell recruitment and function.

It has been shown that cutaneous injection with lentivirus leads to transduction and activation of skin-derived dendritic cells (bearing a $DEC205^+$, $CD8^{-/lo}$ phenotype) (125). These skin DC become activated in mice injected i.d. with lentivirus encoding ovalbumin leading to DC transport of the OVA antigen to draining lymph nodes leading to stimulation of specific $CD8^+$ T cells capable of regulating the growth of OVA-expressing melanoma. While my studies have focused on increased $CD8^+$ TIL upon lentivirus treatment, it is also possible that apoptosis of lentivirally-transduced cells (both APC and non-APC, *i.e.*, fibroblasts, *etc.*) could lead to extracellular antigen uptake by DC, and the subsequent induction of Ag-specific $CD4^+$ T cells. If such activated $CD4^+$ T cells were Type-1 in functionality, they would be expected to release IFN-γ into their surroundings, promoting the proinflammatory skewing of the TME as well as provide "help" in the development and recruitment of effector $CD8^+$ TIL.

While these findings address the immune-mediating effects of an anti-DLK1 vaccine, as mentioned in the introduction of Chapter 4, DLK1 also plays an important role as a regulator of Notch signaling. It has been shown that activation of the Wnt/β-catenin/Notch signaling pathway can lead to vascular normalization (242). Indeed, our data support such a paradigm, with immune-mediated removal of DLK1 expression resulting in the activation of Notch, and possibly Wnt signaling (as indicated by increased expression of Frzd2, Frzd4 and Frzd7 transcription in RENCA tumors harvested from lvDLK1-vaccinated mice), (127) (244) in the TME. As such, inhibition of DLK1 expression may actually reinforce Notch/Wnt signaling it its negative regulation of angiogenesis (127, 250). A more comprehensive prospective investigation of the impact of anti-DLK1 vaccine on the Wnt/β-catenin/Notch signaling pathway in the RENCA TME is clearly warranted. This question may be at least partially addressed based on Notch signaling interference by administration of inhibitors of γ-secretase (aka ADAM10), an enzyme that releases the Notch intracellular domain from its membrane anchor, allowing for the activation of Notch-dependent gene transcriptional programs (251). While global knockouts of Notch1 alone or Notch1/4 together are embryonic lethal with evidence of severe vascular defects (252), mice with Floxed alleles flanking Notch signaling molecules may be crossed with Cre recombinase mice to generate conditional knockouts (253). Specifically, mice with flox alleles of *Adam10* bred with *Tie2-Cre* mice produce mice deficient in Notch signaling in endothelial cells that would allow one to observe whether the anti-tumor impact of DLK1-based vaccines depends on Notch signaling in the vasculature compartment of the TME.

The Notch pathway has also been shown to regulate and shape the immune response. Dendritic cells express both Notch and Notch ligands (254), but depending on which ligands bind to their Notch receptors, DC may become either proinflammatory or immunosuppressive.

Jagged and Delta-like ligands activate the canonical Notch signaling pathway in DC; however, DC matured via Jagged1 and LPS secrete high levels of IL-2 and IL-10, resulting in the expansion of regulatory T cells. Notch activation is also involved in a differential secretion of cytokines and chemokines by DC subsets (247). Notch signaling has also been implicated in macrophage differentiation and polarization. Xu *et al.* showed Notch regulated expression of IRF8 and downstream activation of M1 macrophage-promoting genes in response to LPS (66). Interestingly, the binding of Notch ligand, Delta-1, inhibits the differentiation of monocytes into macrophages, but permits their differentiation into dendritic cells (255), thus supporting the functional importance of the context in which the Notch pathway is activated. In our tumor model, we assume a sterile environment, in which TLR4 ligands are absent, and therefore any activation of Notch signaling by DC would be expected to be largely proinflammatory in nature. Additionally, it has recently been shown that Notch signaling plays an important role in $CD8^+$ T cell activation (256). Here the authors showed that antagonism of Notch led to reduced expansion and function of tumor antigen-specific $CD8^+$ T cells. Given the inhibitory role of DLK1 in Notch signaling, it is possible that vaccine-induced immune-mediated removal of DLK1 would also lead to the proinflammatory activation of DC as well as, the increased activation and proliferation of endogenous tumor-specific $CD8^+$ T cells, resulting in reduced tumor growth in vivo. In addition to removal of Notch antagonism via vaccination, treatment with recombinant agonists may further augment T cell activation and function to inhibit tumor growth. In a recent publication by Huang *et al*., the authors showed that tumor immune escape was caused, at least in part, by VEGF-mediated reduction in Notch signaling of T cell precursors (65). Selective stimulation of DLL1-Notch signaling with DLL1-Fc fusion protein rescues T cell function and reduces tumor progression. It would be of interest to observe any additive effects

of such a treatment along with an anti-DLK1 vaccine towards promoting a more robust anti-tumor T cell response.

In my studies, it was also interesting to observe that the therapeutically "normalized" TME post-vaccination with lvDLK1 exhibited a decrease in cell populations expressing stem cell-associated markers. This treatment-associated difference could reflect the ability of vaccine-induced T cells to: i.) alter the supportive TME in a manner that limits the recruitment, accumulation or expansion of such stem cell-like populations in the TME; ii.) decrease hypoxia in the TME, leading to transcriptional silencing of hypoxia-responsive stem cell-associated gene products (236-238); iii.) promote the corollary cross-priming (120, 208) of specific immune responses against alternate tumor-associated stromal antigens, including stem cell antigens, leading to the inhibition/eradication of cells expressing these markers *in vivo*. It has been reported that pericytes exhibit mesenchymal stem cell characteristics in their ability to differentiate into mature cells of various tissues (78). Presumably, by immunologically targeting and removal of $DLK1^+$ tumor pericytes, we may in fact be eliminating these MSC-like cells from the TME. Additionally, given the role of DLK1 in various stem cell differentiation pathways via its repression of Notch signaling, it is also possible that by eliminating DLK1, and thus activating Notch signaling in vaccinated animals, stem-like cell populations are permitted to undergo terminal differentiation (leading to a loss of stem-cell phenotype). Lastly, it is conceivable that cells bearing stem cell-associated markers may be directly targeted by anti-DLK1 Tc1, since cells expressing DLK1 may co-express stem cell-associated markers such as CD133, c-kit, and SOX2 (257, 258). These mechanisms of action are clearly not mutually-exclusive and a combination of these processes may be involved in the biologic outcomes that I have reported in my publications and the current thesis document.

Although there is a significant delay in tumor progression of animals treated with lvDLK1, ultimately tumors progress in these mice. I have shown that DLK1 antigen cannot be detected in tumor-bearing mice treated with a single lvDLK1 injection; however, in progressor tumors, it is possible that DLK1 expression could be resumed based on a re-establishment of hypoxia or to the suppression of anti-DLK1 T effector cells. In such a scenario, a prime-boost vaccination strategy could be implemented to fortify and sustain T cell memory against the DLK1 antigen. In a preliminary study, I showed no therapeutic benefit of treating animals twice with lvDLK1 versus a single injection (data not shown). To eliminate the possibility of neutralizing antibodies against the lentivirus, I also conducted a study in which animals were primed with the DC.IL12 loaded with DLK1 peptides, followed by the lvDLK1 boost. However, this study also failed to show a therapeutic advantage over the single lvDLK1 treatment (data not shown). While this may be due to a sub-optimal treatment schedule, it may also be due to compensatory transcriptional mechanisms occurring after DLK1 removal from the TME. It has been shown that DLK2, an alternate (non-canonical) Notch ligand, that is highly-homologous to DLK1, also acts as a Notch signaling antagonist (130) and is upregulated in cells upon suppression of DLK1 expression. It is possible that upon vaccine-mediated removal of DLK1, expression of DLK2 in the TME may be augmented as a compensatory mechanism to counter-regulate Notch signaling in support of renewed tumor progression. Indeed, preliminary studies in our group support increased DLK2 expression in RENCA tumors only after successful vaccination against DLK1. This would clearly support future development of vaccines capable of promoting the coordinate $CD8^+$ T cell targeting of both tumor-associated $DLK1^+$ and $DLK2^+$ cells, leading to sustained, reinforced Notch signaling in the therapeutic TME

Targeting the Notch signaling pathway in the cancer setting is not a novel concept, as *NOTCH* was first identified as an oncogene in T-ALL (259). Notch has been suggested to contribute to carcinogenesis in a variety of ways, including inhibiting cell differentiation, inhibiting apoptosis, promoting tumor proliferation (239), promoting the process of EMT (260-262) and sustaining cancer stem/initiating cell populations (239, 263). In addition to its role in tumor cell maintenance, there is also strong evidence for Notch signaling involvement in tumor-stroma interactions and in promoting angiogenesis (264). Indeed, given that Notch signaling has been found to be constitutively active in many cancers (239) multiple clinical trials are currently testing the safety and efficacy of inhibitors, such as γ-secretase inhibitors (GSI), in the setting of solid tumors (265-268). Conversely, an emerging body of evidence suggests that Notch signaling is critically involved in tumor suppression. Hence, the deletion or inactivation of Notch may lead to increased incidence of squamous cell carcinomas (269). An inverse correlation has also been observed between Notch and HER2 signaling, in which breast cancer cell lines with increased HER2 expression exhibit reduced levels of Notch transcriptional activity (270). This functional duality in Notch signaling appears to depend on the activation/repression of specific genes along the signaling pathway as well as the cell type in which these signals are being modulated (239, 269). Thus, the context-dependent nature of Notch signaling in cancer will likely further complicate attempts to treat patients with therapies that generically target and inhibit/inactivate the Notch signaling pathway.

In conclusion, I have shown that immune targeting of the solid tumor stroma, specifically tumor pericytes, as an effective means to inhibit tumor progression. Activation of the host immune response against specific tumor stromal antigens can be achieved via multiple routes, including cellular vaccination with engineered dendritic cells or genetic vaccination with

lentivirus. Immune targeting of DLK1, a tumor pericyte antigen involved in the repression of Notch signaling and stem cell differentiation, is a promising therapeutic strategy in the setting of RCC, as it leads to a vascular normalization event that promotes and/or syngergizes with anti-tumor effects. While much remains to be explored in regards to anti-tumor immunotherapy, I believe that the results and conclusions presented in this thesis document will greatly enhance the foundation for developing more effective treatments for many vascularized forms of solid cancer, including RCC.

6.0 APPENDIX

Target	RT-PCR primers	Product (bp)
CD31	Forward 5'-3': AGCCCACCAGAGACATGGAA Reverse 5'-3': CTGGCTCTGTTGGAGGCTGT	337
DLK1	Forward 5'-3': CTGCACACCTGGGTTCTCTG Reverse 5'-3': GCATGGGTTAGGGGTACAGC	202
EphA2	Forward 5'-3': GGGGATGCCAACAGCTATAA Reverse 5'-3': CTCCTGCCAGTACCAGAAGC	232
gp100	Forward 5'-3': CATCAATGGGAGCCAGGTGT Reverse 5'-3': TGAAGGTTGAACTGGCGTGA	296
HBB	Forward 5'-3': TCAGAAACAGACATCATGGTGC Reverse 5'-3': TAGACAATAGCAGAAAAGGGGC	480
NG2	Forward 5'-3': ACAGACGCCTTTGTTCTGCT Reverse 5'-3': TCGGAAGAAATGTCCAGGAG	399
NRP1	Forward 5'-3': TCCAAGTGGACCTGGGAGAT Reverse 5'-3': TTCACAGCCCAGTAGCTCCA	299
NRP2	Forward 5'-3': CCGGAAGAGACCTGTGGTTG Reverse 5'-3': CCGATCGTCCCTTCCCTATC	394
PDGFRβ	Forward 5'-3': TGCTCCTGGAGAGGCTTCTG Reverse 5'-3': GGAGGAAGTGTTGACTTCATTC	301
PSMA	Forward 5'-3': CCTGCGGTGAAGTCCTATCC Reverse 5'-3': GTTTCCAGCAAAGCCAGGTC	300
RGS5	Forward 5'-3': AAGTTGGGAATTCTCCTCCAG Reverse 5'-3': TTCCTCACTGAATTCAGACTTC	203
TEM1	Forward 5'-3': TTCACCAACTGGGCCCAGC Reverse 5'-3': GTTGACACACATCTGCTGGC	645
VEGFR1	Forward 5'-3': CCAACTACCTCAAGAGCAAAC Reverse 5'-3': CCAGGTCCCGATGAATGCAC	318
VEGFR2	Forward 5'-3': ACAGACAGTGGGATGGTCC Reverse 5'-3': AAACAGGAGGTGAGCGCAG	271
β-actin	Forward 5'-3': GGCATCGTGATGGACTCCG Reverse 5'-3': GCTGGAAGGTGGACAGCGA	615

Appendix Table 1. RT-PCR primers used in this study.

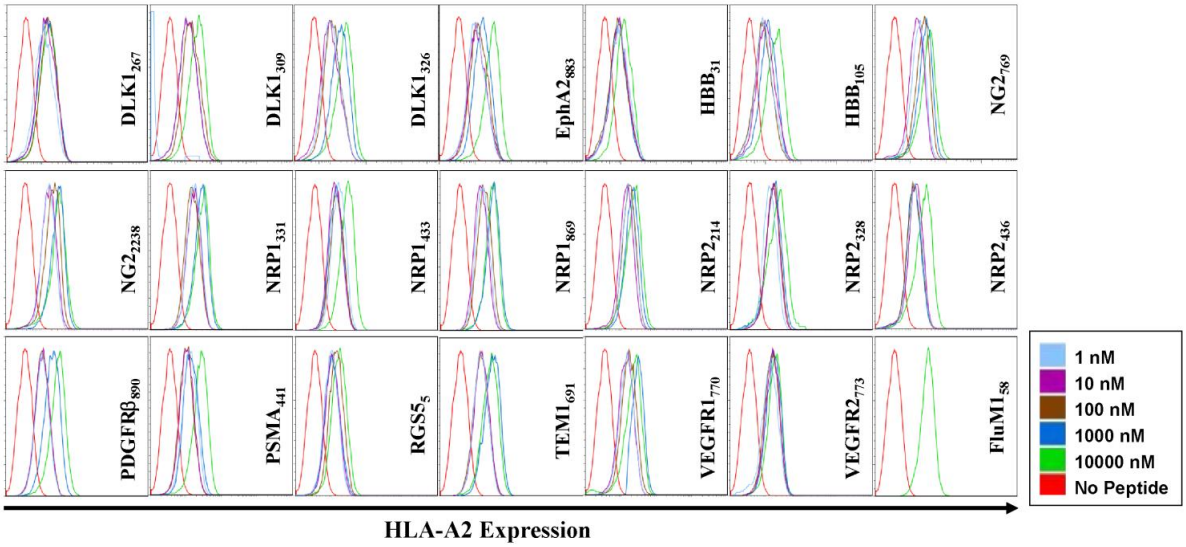

Appendix Figure 1. Synthetic peptides are competent to bind and stabilize HLA-A2 complexes by T2 cells.

TASA-derived peptides bind to HLA-A2 to a variable degree based on the T2 class I stabilization assay. Peptide stabilization of HLA-A2 complexes on the T2 cell line by synthetic peptides was assessed as previously described [50]. FluM158-66 (GILGFVFTL) was used as a positive HLA-A2 binding control peptide [27]. Overlays of fluorescence histograms are provided for each peptide over a 1-10000 nM dose range, as indicated. Evidence for productive stabilization of HLA-A2 complexes is supported by a shift in staining intensity to the right vs. the no peptide control. Negative control (HLA-A3/A11-binding) HIV-nef73-82 peptide [27] failed to promote enhanced HLA-A2 stabilization on T2 cells (data not shown). Data are from 1 representative experiment of 3 independent assays performed.

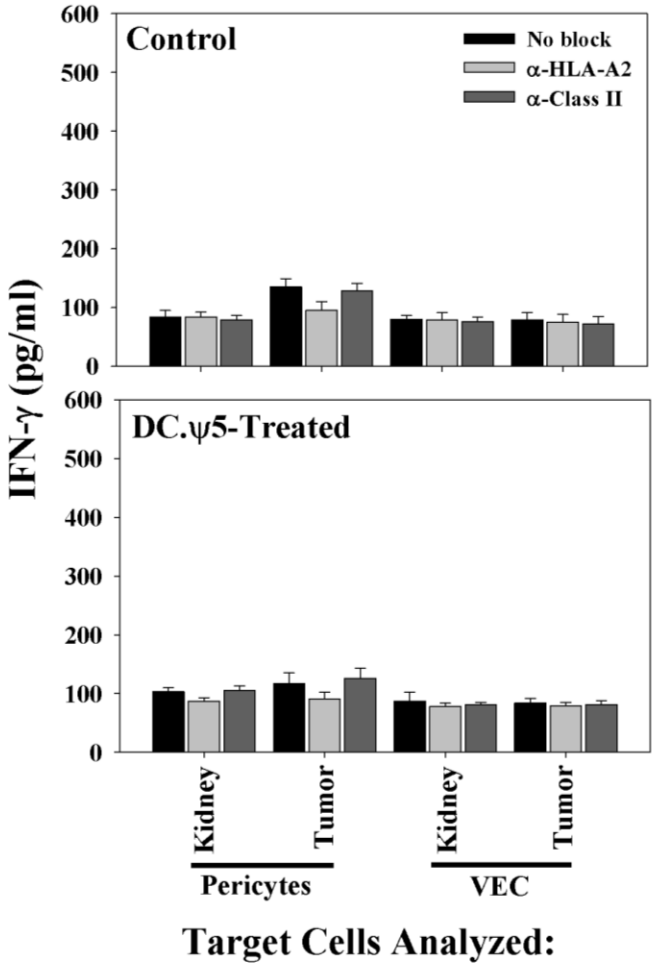

Appendix Figure 2. Splenic CD8$^+$ T cells isolated from the untreated and DC.ψ5-treated animals failed to recognize HLA-A2$^+$ pericytes and VEC flow sorted from single-cell digests of B16 tumors (versus DC.IL12 treatment).

CD8$^+$ T cells isolated from B16-bearing HHD mice left untreated or treated with DC. ψ5 fail to recognize tumor-associated pericytes/VEC. CD8+ T cells were MACS-isolated from the spleens of tumor-bearing animals that were left untreated (Control) or that were treated with i.t. delivered DC.ψ5, as outlined in **Figure 4B**. These T cells were then cultured with flow-sorted tumor- or kidney-derived pericytes or VEC +/- blocking anti-HLA-A2 (BB7.2) or class II (L243) mAbs as described in Materials and Methods. Cell-free supernatant was harvested after 24h incubation at 37°C and analyzed using a specific IFN-γ ELISA. Representative data is presented from 1 of 2 independent experiments performed.

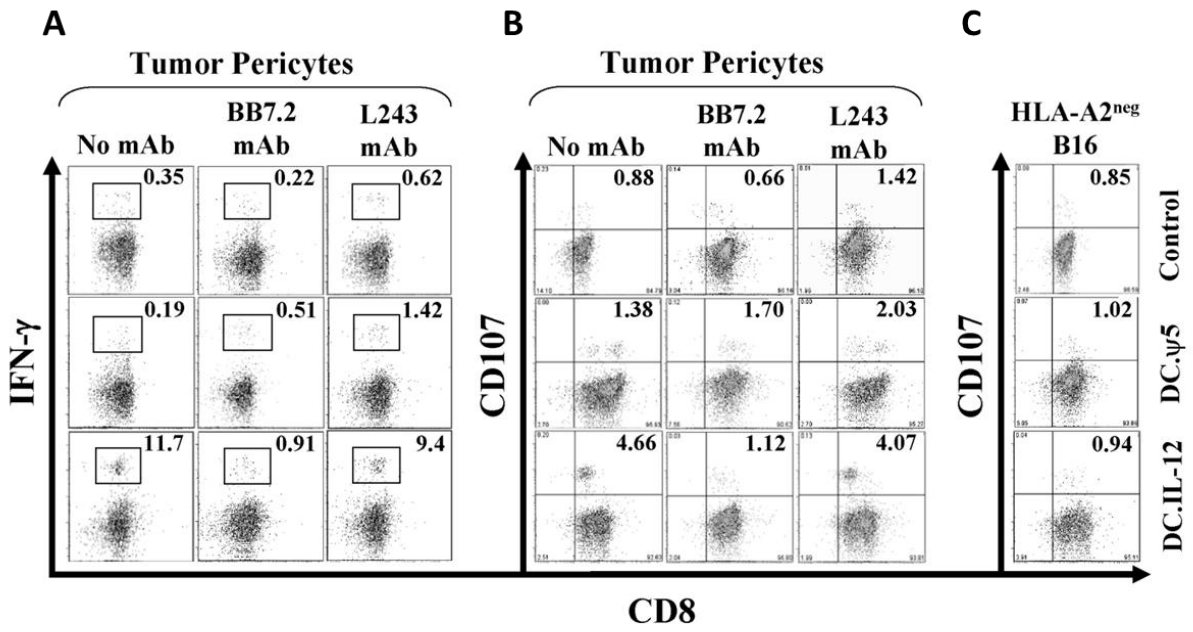

Appendix Figure 3. CD8$^+$ TIL isolated from untreated or DC.ψ5-treated melanoma had decreased recognition of tumor-associated pericytes (versus DC.IL12 treatment).

CD8$^+$ TIL isolated from B16-bearing HHD mice treated with DC.IL12 recognize tumor-associated pericytes in an HLA-A2-restricted manner, and fail to recognize HLA-A2neg B16 tumor cells. TIL were isolated from the day 17 melanomas of mice (treated as indicated) and analyzed for reactivity against flow-sorted tumor pericytes as described in **Figure 5** for intracellular IFN-γ or cell surface expression of translocated CD107 using flow cytometry. To assess MHC-restriction in T cell recognition of tumor pericytes, 10 μg of anti-HLA-A2 mAb BB7.2 or anti-pan class II mAb L243 were added to cultures during the 4-5h co-incubation period prior to flow cytometry-based analysis. Inset numbers reflect the percentage of CD8$^+$ T cells exhibiting positive response to tumor pericytes or B16 melanoma cells. Data derive from 1 representative experiment of 2 independent experiments performed.

TBVA	AA Positions	Peptide Sequence	Tc1 Response to Peptide Vaccine (HHD)[a]	Anti-tumor efficacy in MC38 protection model[b]	Anti-tumor efficacy in B16 therapy model (survival: p-value)[c]
DLK1	267-275	RLTPGVHEL	+	+	.0013
	309-317	ILGVLTSLV	+		
	326-334	FLNKCETWV	+		
EphA2	883-891	TLADFDPRV	+	+	.0012
HBB	31-39	RLLVVYPWT	+	+	.0012
	105-114	RLLGNVLVCV	+		
NG2	770-778	TLSNLSFPV	-	+	NS
	2238-2246	LILPLLFYL	+		
NRP1	331-339	GLLRFVTAV	+	+	.0013
	433-441	GMLGMVSGL	+		
	869-877	VLLGAVCGV	+		
NRP2	214-222	DIWDGIPHV	+	-	NT
	328-336	YLQVDLRFL	-		
	436-444	NMLGMLSGL	-		
PDGFRβ	890-898	ILLWEIFTL	+	+	NS
PSMA	441-450	LLQERGVAYI	+	-	NT
RGS5	5-13	LAALPHSCL	+	+	.0012
TEM1	691-700	LLVPTCVFLV	+	+	.0102
VEGFR1	770-778	TLFWLLLTL	+	+/-	NS
VEGFR2	773-781	VIAMFFWLL	+	+/-	NS

Appendix Table 2. In vivo immunogenicity and anti-tumor efficacy of TASA-based vaccines in HHD models.

Data are summarized from **Figures 3 and 5**. a+, $p < 0.05$ versus DC only. bVaccines consisted of DC.IL12 pulsed with a pool of 1 or more peptides derived from the indicated TASA. +/-, $p < 0.05$ versus DC only for 2 consecutive time points; +, $p < 0.05$ versus DC only for > 2 consecutive time points; - not significant at any time point analyzed. cp-value versus mice treated with DC only vaccine (from **Figure 5C**). NS, not significant; NT, not tested.

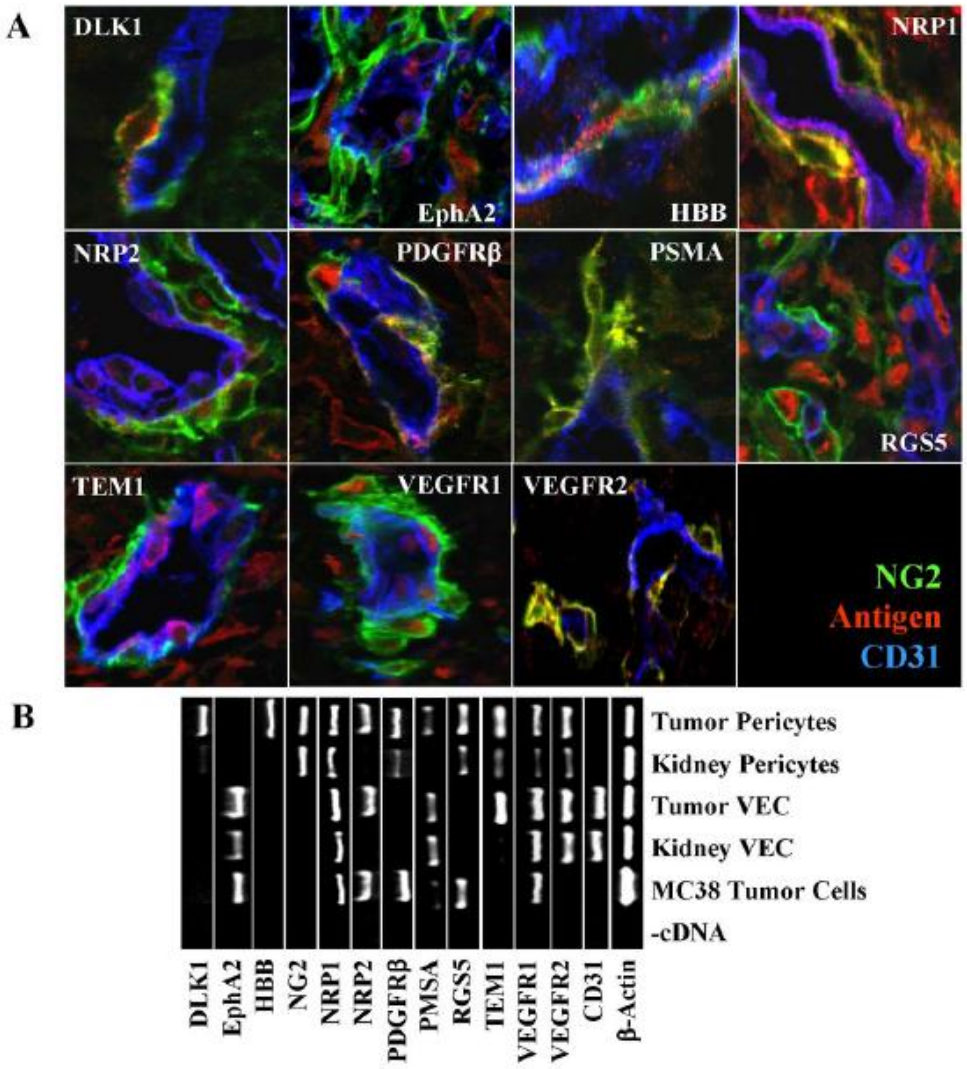

Appendix Figure 4. Expression of TASA in the established MC38 TME.

(A) MC38 colon carcinoma cells were injected s.c. in the right flank of female HHD mice and allowed to establish/progress for 14 days. Animals were then euthanized, with tumors resected, fixed, sectioned and analyzed for expression of the indicated antigens using specific Abs and fluorescence microscopy as outlined in Materials and Methods. Specific pAb against NG2 (green), the indicated antigen of interest (red), and CD3 1 (blue) were used to distinguish preferential antigen expression in tumor blood vessel-associated pericytes, VEC, alternate stromal cells and/or tumor cells. Images are reflective of those obtained in 3 independent experiments performed. **(B)** MC38 colon carcinoma cell lines, as well as, flow-sorted pericytes and VEC (isolated from HHD mice bearing untreated day 14 MC38 tumors) isolated from tumors and tumor-uninvolved kidneys were analyzed for expression of the indicated mRNAs using RT-PCR as described in Materials and Methods.

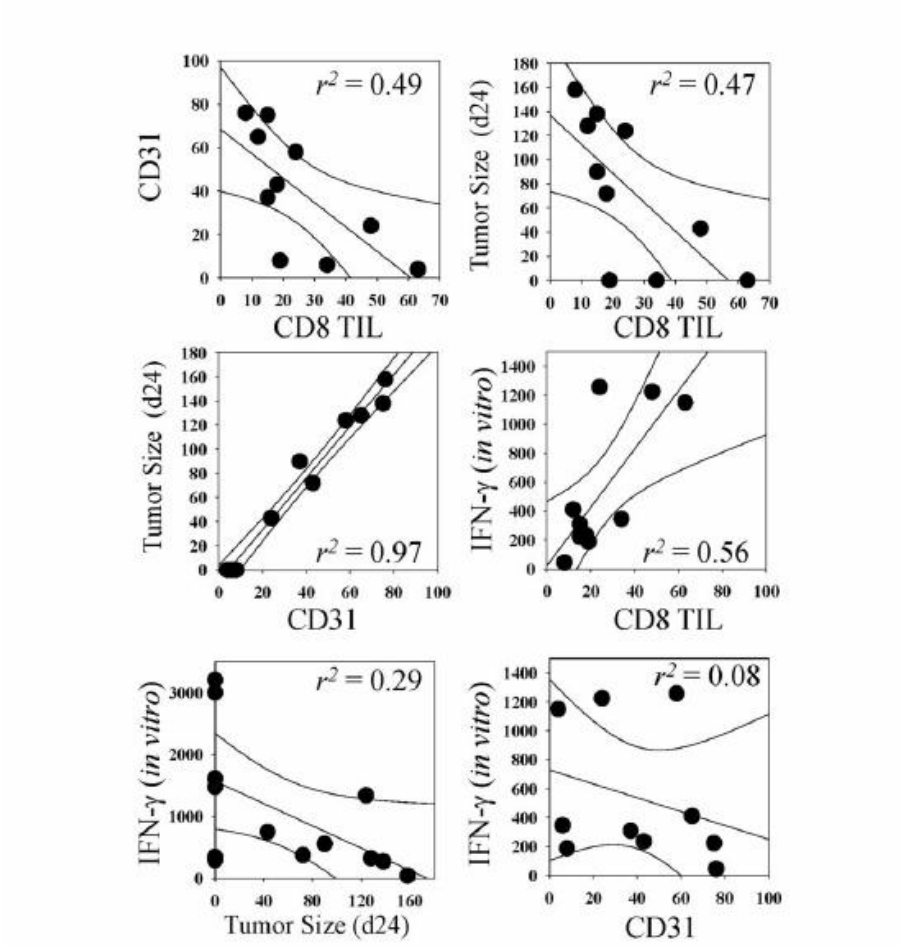

Appendix Figure 5. Correlation of biologic parameters assessed in the MC38 tumor model system.

Data gathered from **Figures 3** and **4** were analyzed for the correlation of indicated markers in a pair-wise manner. Individual data included: i.) $CD8^+$ TIL (day 7 post tumor-inoculation (in mean numbers per HPF), ii.) $CD31^+$ vessels in these same lesions (reported a mean number/10 HPF), iii.) Tumor size (in mm^2) on day 24 post-tumor inoculation, and iv.) specific production of IFN-γ from splenic $CD8^+$ T cells harvested from control and vaccinated mice on day 14 post-tumor inoculation. Each dot represents a control (DC only) or vaccine cohort evaluated (n = 10). For panels including *in vitro* T cell response data, each symbol reflects cumulative response against a given TASA (i.e. for DLK1, this represents the summation of responses against each of 3 peptides, while for RGS5, this reflects response against the single peptide evaluated in these studies) . Note that in all instances, except for the IFN-γ x Tumor Size comparison (n = 13), the cohorts vaccinated using DLK1-, NRP1- or PDGFRβ - derived peptides are not included in the indicated analysis, as these mice failed to develop lesions capable of being resected for analyses. Linear regression lines are inserted in each panel , with the associated r^2 values reported in each in stance. Lines indicating 95% confidence intervals are also provided in each panel.

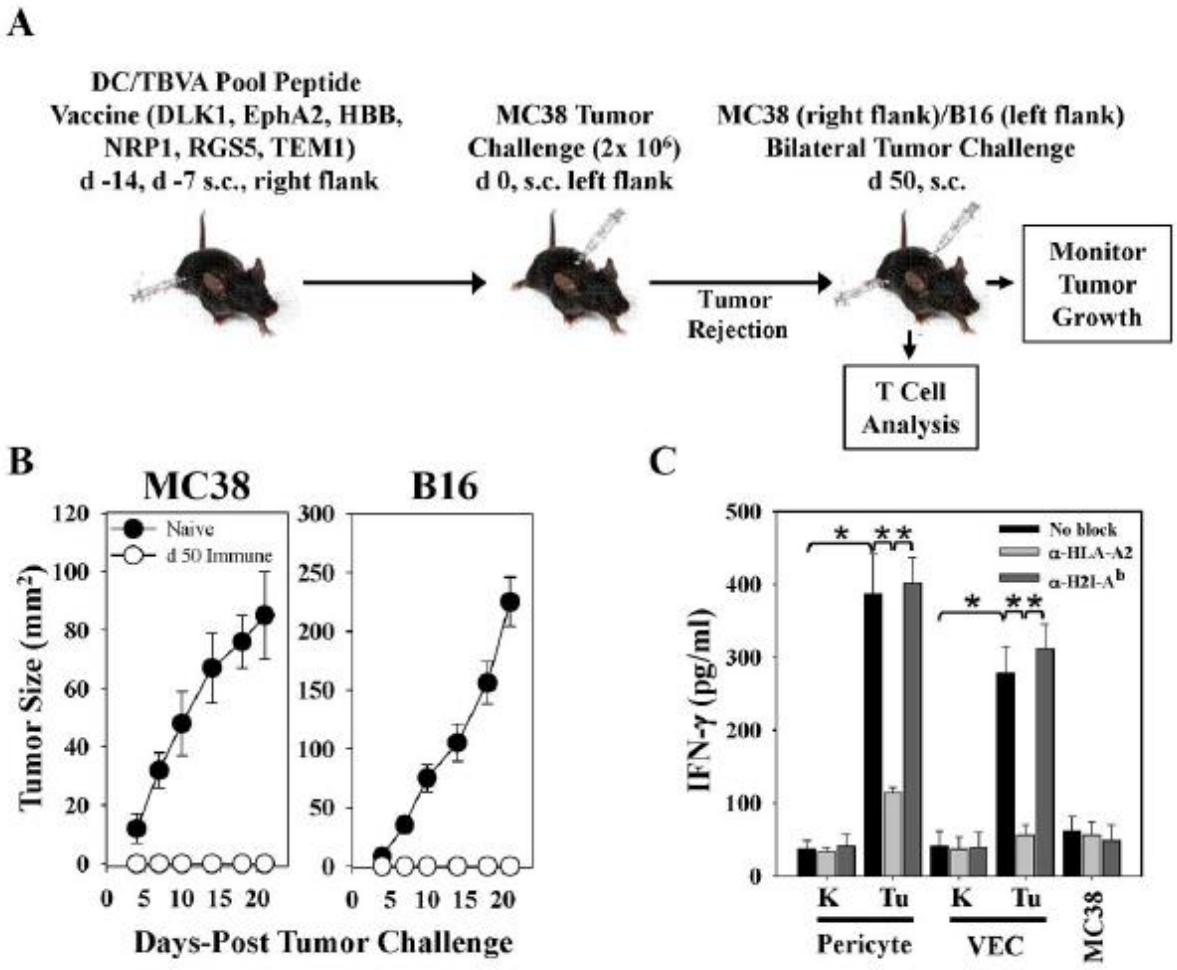

Appendix Figure 6. Mice protected against initial MC38 tumor challenge as a consequence of TASA-based prophylactic vaccination display durable immunity against a subsequent challenge with both MC38 sarcoma and B16 melanoma cells.

(A) HHD mice received prophylactic vaccination as described in Figure 3B with DC.IL12 pulsed with an equimolar pool of TASA peptides (per Figure 5A). All animals rejected this initial MC38 tumor challenge. Fifty days after the initial challenge, animals were challenged with 2 x 10^6 MC38 sarcoma (s.c., right flank) and 10^5 BI6 melanoma (s.c., left flank) cells. (B) The size of each tumor was monitored every 3-4 days thereafter in these day 50 immune animals or in naïve, control mice. (C) $CD8^+$ T cells isolated from day 50 immune animals were analyzed for reactivity against flow-sorted $PDGFR\beta^+CD31^{neg}$ pericytes or $PDGFR\beta^{neg}CD31^+$ vascular endothelial cells (VEC) flow-sorted from the tumor or tumor-uninvolved kidneys of MC38-bearing HHD mice. Cultured $HLA\text{-}A2^{neg}$ MC38 tumor cells were also analyzed as target cells. T cells and target cells were co-cultured for 24h prior to analysis of the cell-free supernatant using IFN-γ ELISA as outlined in Materials and Methods. The MHC-restricted nature of specific T cell recognition was assessed by inclusion of no mAb, or 10 μg/well of anti-HLA-A2 (BB7.2; ATCC, Manassas, VA) or anti-$H2\text{-}IA^b$ mAb (AF6-120.1; Biolegend, San Diego, CA). K = Kidney; Tu = Tumor; *$p < 0.05$ for tumor versus kidney, and for anti-HLA-A2 versus No block or anti-$H2\text{-}IA^b$.

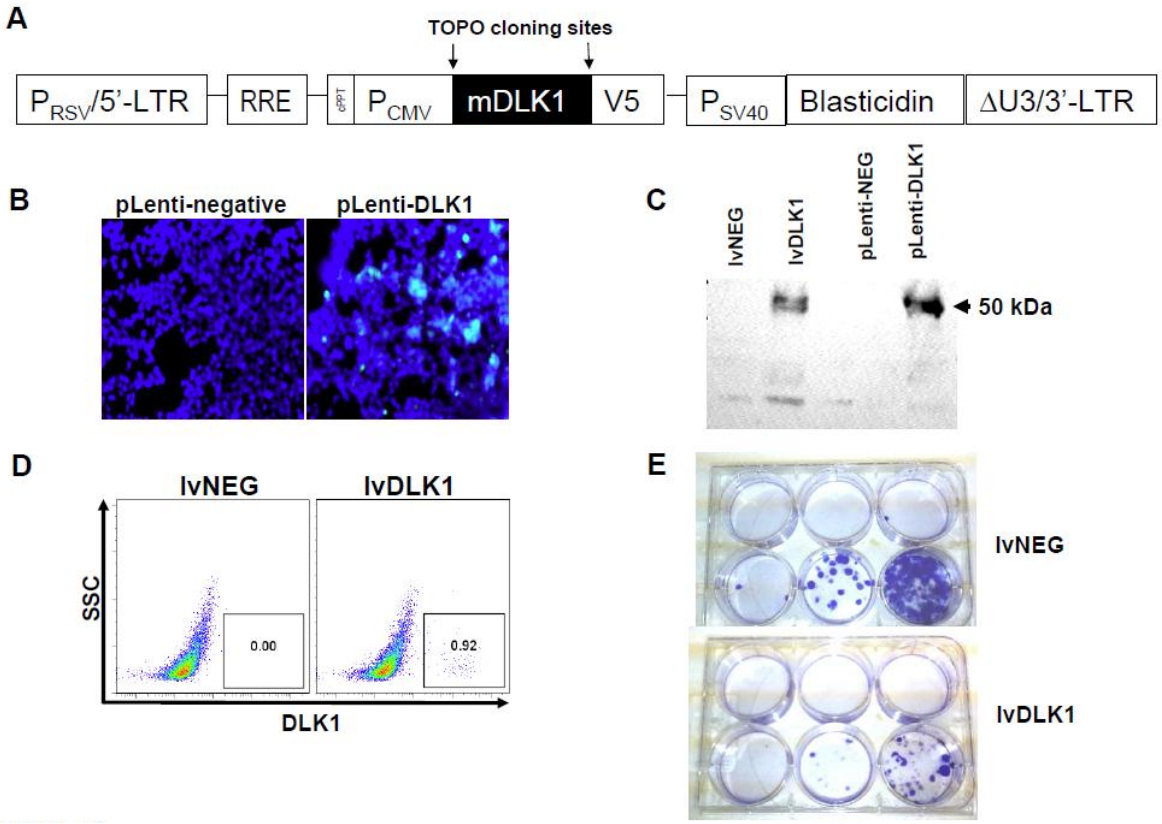

Appendix Figure 7. Production of recombinant lvDLK1 and control lvNEG lentiviruses.

(A) A schematic diagram is provided for lvDLK1. pRSV/5′LTR, RSV LTR and HIV LTR chimeric promoter; RRE, Rev response element sequences; CMVp, CMV promoter used to drive transgene expression; whole mouse DLK1 gene with V5 reporter tag; SV40p-Blasticidin, SV40 virus promoter used to drive selection marker blasticidin gene expression; ΔU3/HIV 3′LTR, promoter deleted in U3 region so that the lvv become self-inactivated; TOPO cloning sites also indicated. 293T cells were transfected with plasmid DNA pLenti-DLK1 (or pLenti-NEG) and analyzed for V5 protein expression by immunofluorescence and western blot as shown in **B** and **C**. HT-1080 cells were infected with lentivirus and analyzed for V5 protein expression by western blot and DLK1 protein expression by flow cytometry as shown in **C** and **D**, respectively. (**E**) Production of a live functional virus (lvNEG) is confirmed by the formation of blasticidin-resistant colonies of lentivirus-infected HT-1080 cells stained with crystal violet.

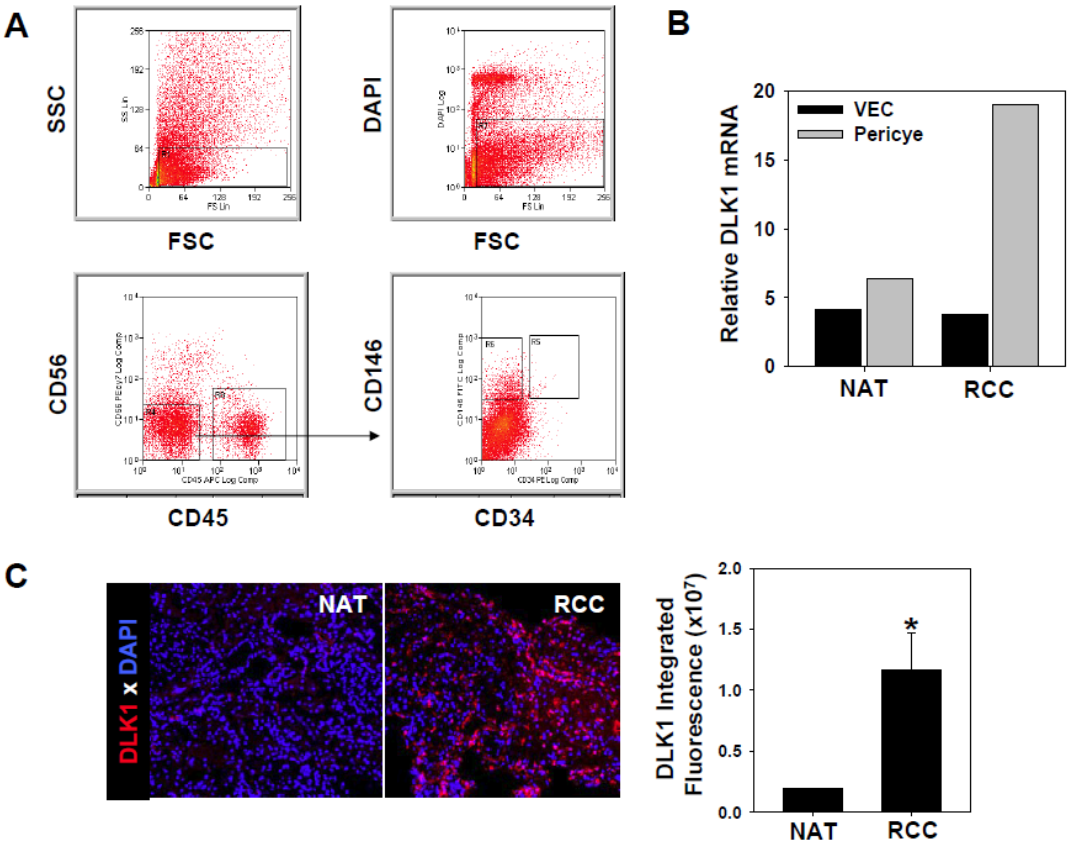

Appendix Figure 8. DLK1 is differentially expressed by human RCC-associated pericytes.
(A) Freshly-harvested RCC tumor and patient-matched normal adjacent kidney tissues (NAT) were mechanically and enzymatically digested into single-cell suspension and sorted by flow cytometry based on forward scatter and side scatter, DAPI exclusion (to exclude dead cells), a CD56negCD45neg phenotype, and then selectively into $CD146^{+}CD34^{neg}$ pericytes and $CD146^{+}CD34^{+}$ VEC populations. **(B)** mRNA was isolated from sorted pericytes and VEC from NAT and RCC tumor and analyzed for DLK1 expression by real-time PCR. Relative mRNA expression was normalized to housekeeping HPRT1 transcript expression. **(C)** RCC tumor and NAT sections were analyzed for expression of DLK1 (red) by immunofluorescence microscopy. Mean fluorescence intensity +/- SD was quantitated from 3 independent fields per slide as described in Materials and Methods. Data are representative those obtained in 3 independent experiments performed. *$p < 0.05$ (t-Test).

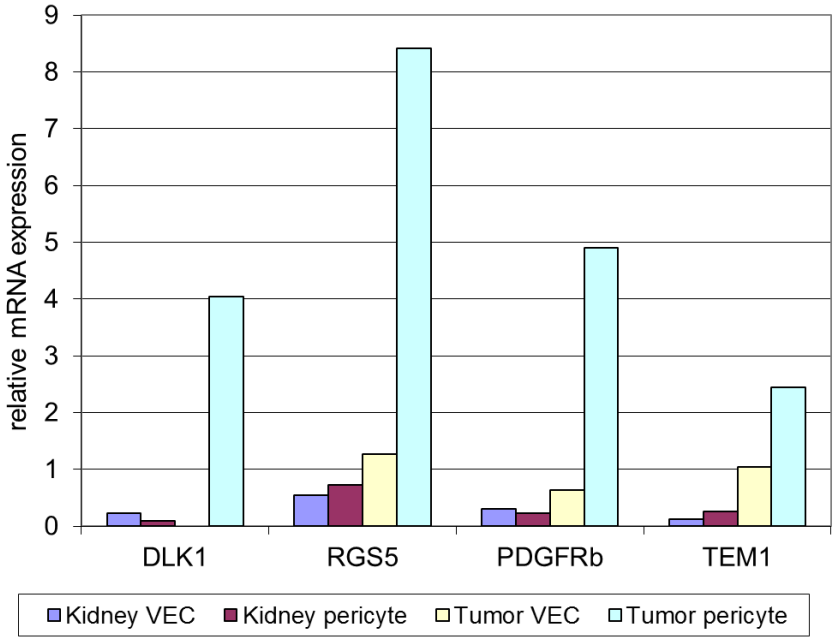

Appendix Figure 9. Expression of subset of TASA in RENCA tumor pericytes.

RENCA tumor cells were injected s.c. in the right flank of female BALB/c mice and allowed to establish/progress for 21 days. Freshly-harvested tumor and normal kidneys were mechanically and enzymatically digested into single-cell suspension and sorted by flow cytometry. mRNA was isolated from sorted pericytes and VEC analyzed for DLK1, RGS5, PDGFRβ, and TEM1 expression by real-time PCR. Relative mRNA expression was normalized to housekeeping HPRT1 transcript expression.

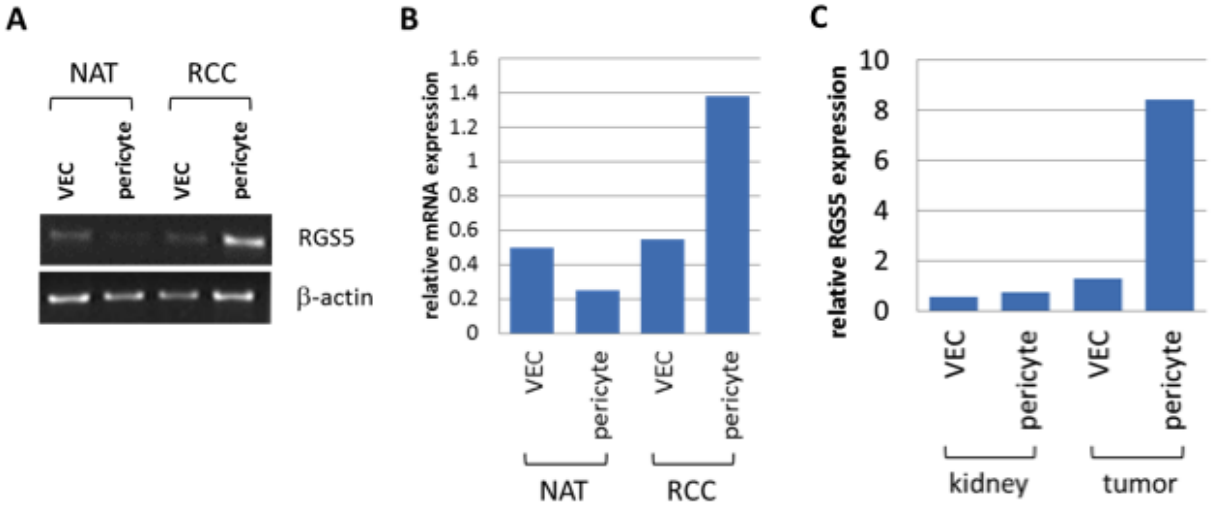

Appendix Figure 10. RGS5 expression in RENCA tumor pericytes.

(A) Pericytes and VEC from human RCC tumors and NAT were sorted by flow cytometry as mentioned in Appendix Figure 8. mRNA was isolated from sorted pericytes and VEC and analyzed for RGS5 expression by reverse transcriptase PCR as mentioned in Materials and

Methods in Chapter 2. **(B)** Relative RGS5 transcript levels were quantified based on densitometry values normalized to β-actin control. **(C)** Pericytes and VEC were sorted from mouse RENCA tumors and tumor-uninvolved kidneys as shown in Figure 13. mRNA was then isolated from flow-sorted pericytes and VEC, and analyzed for RGS5 transcript expression by real-time PCR. Relative mRNA expression was normalized to housekeeping HPRT1 mRNA expression.

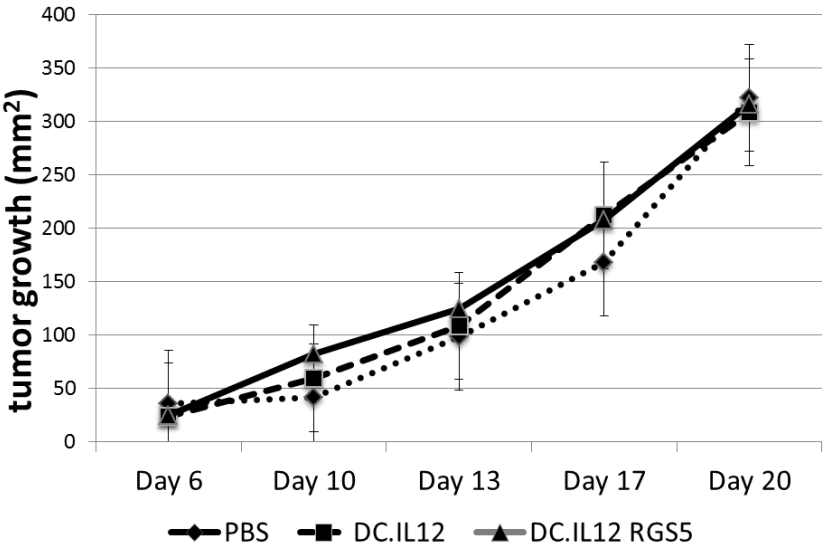

Appendix Figure 11. DC/RGS5 peptide-based vaccine does not impact tumor growth in the murine RENCA model of RCC.

BALB/c mice were inoculated with RENCA tumor cells s.c. on the right flank on day 0. After randomizing for similar mean tumor size per treatment cohort (n = 5), mice were injected s.c. on their left flank on days 7 and 14 (post-tumor inoculation) PBS, 10^6 DC.IL12 or 10^6 DC.IL12 pre-pulsed with equimolar mix (10 μM each) of the 3 synthetic RGS5 peptides. Tumor growth (mean ± SD) was then monitored over time.

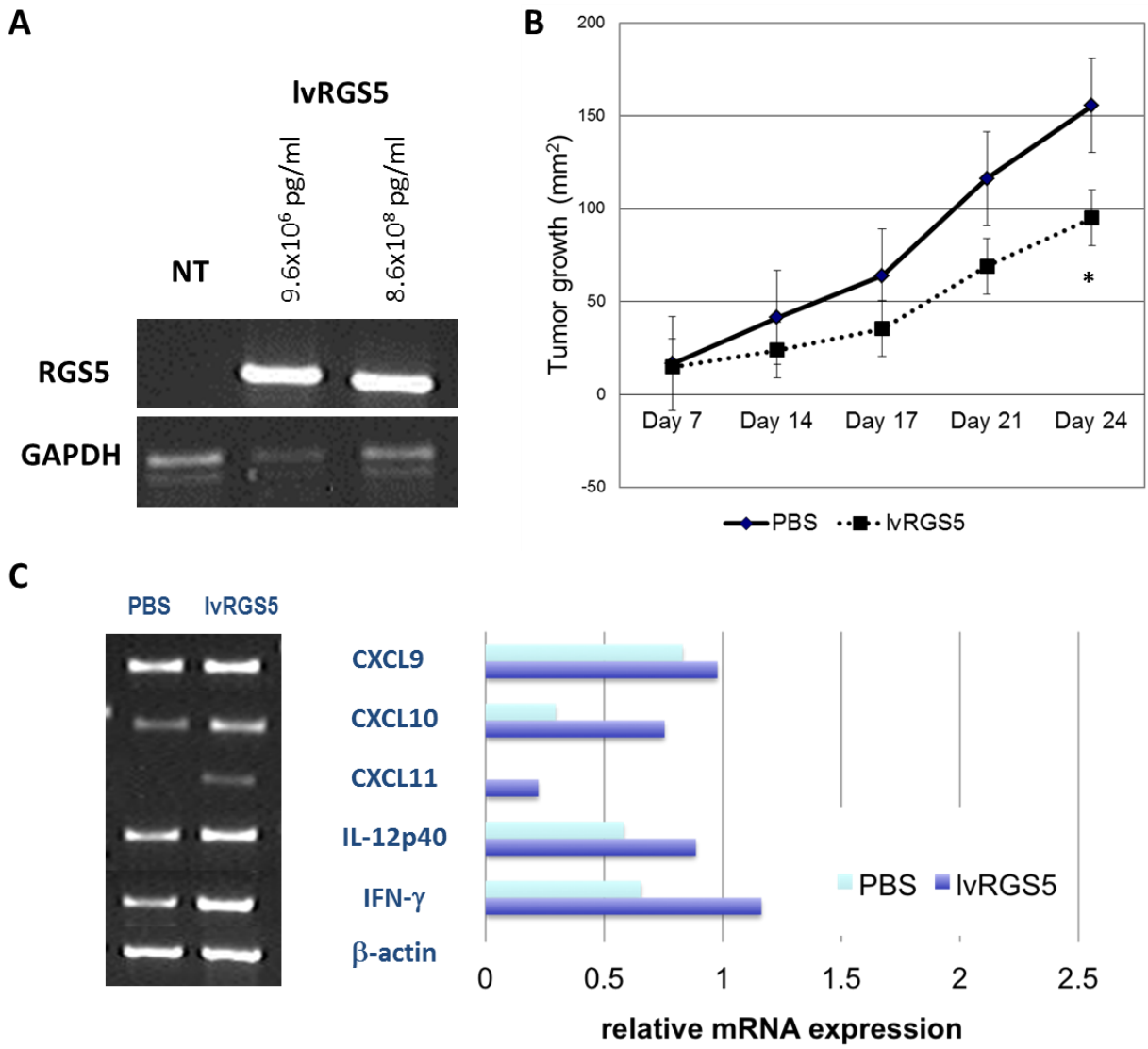

Appendix Figure 12. Live lentivirus encoding human RGS5 delayed tumor growth in murine RENCA tumor model with increased expression of Type 1 proinflammatory genes in the TME.

(**A**) Bone marrow dendritic cells from female BALB/c mice were transduced with lvRGS5 at $9.6x10^6$ and $8.6x10^8$ pg/ml as previously reported (29) and analyzed for human RGS5 mRNA expression by reverse transcriptase PCR with GAPDH as control. In (**B**) BALB/c mice were inoculated s.c. with RENCA tumor cells in the right flank on day 0. After cohort (n = 4) randomization for similar mean tumor size on day 7 post-tumor inoculation, mice were treated s.c. in the left flank with $2.4x10^6$ pg/mouse lvRGS5 or PBS control. Tumor size was then monitored longitudinally. * $p < 0.05$ versus PBS control (student t-test). (**C**) Day 24 tumors were isolated from lvRGS5-treated and PBS-treated control mice as outlined in B, with total mRNA extracted for reverse transcriptase PCR using specific primer pairs for mouse CXCL9, CXCL10, CXCL11, IL-12p40, IFN-γ, and β-actin. For these analyses, relative gene expression values based on densitometry were normalized to β-actin.

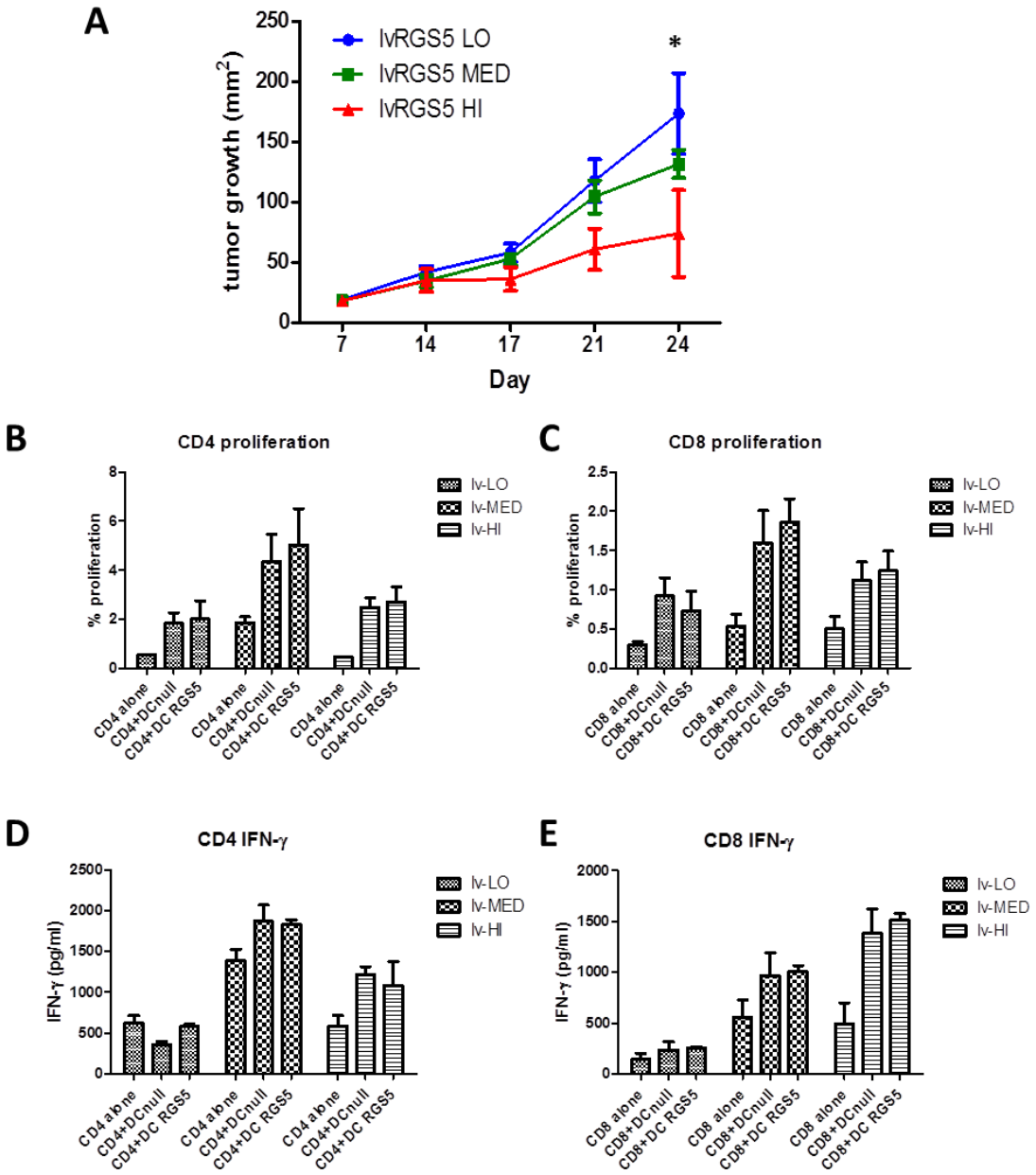

Appendix Figure 13. Vaccination of RENCA tumor-bearing mice with lvRGS5 does not induce RGS5-specific T cell responses.

BALB/c mice were inoculated s.c. with RENCA tumor cells in the right flank on day 0. (**A**) After cohort (n = 5) randomization for similar mean tumor size on day 10 post-tumor inoculation, mice were treated s.c. in the left flank with $1.44x10^6$, $1.44x10^7$, and $1.44x10^8$pg/mouse (lv-LO, lv-MED, and lv-HI, respectively) of lvRGS5. Tumor growth was monitored longitudinally. *$p < 0.05$ versus lower dilutions of lvRGS5 (ANOVA). (**B - E**) On day 21 post-tumor inoculation, splenic $CD4^+$ and $CD8^+$ T cells were isolated from each cohort, labeled with CFSE, and co-cultured with syngenic DC transduced with lvRGS5. In **B** and **C**, percent proliferation of the $CD4^+$ and $CD8^+$ T cells, respectively, was measured by CFSE dilution using flow cytometry. In **D** and **E**, IFN-γ ELISA was performed on cell-free supernatants collected from the $CD4^+$ and $CD8^+$ co-cultures, respectively.

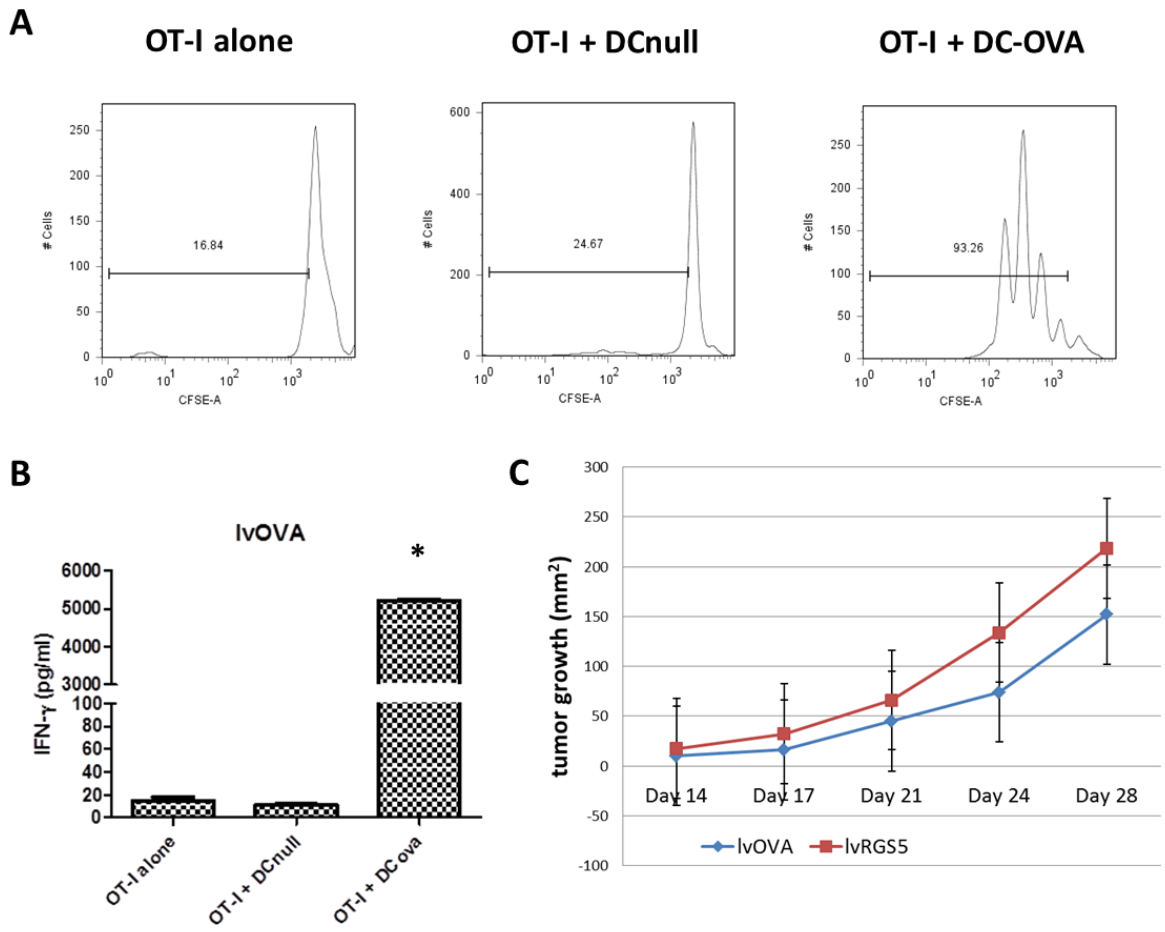

Appendix Figure 14. Vaccination of RENCA tumor-bearing mice with lvRGS5 does not confer additional therapeutic benefit compared to vaccination with lentivirus encoding irrelevant antigen ovalbumin.

In **A** and **B**, bone marrow DC from female C57/B6 mice were transduced with lentivirus encoding full-length ovalbumin (lvOVA) as previously reported (29) at $1x10^9$ pg/ml and co-cultured with freshly isolated OT-I T cells. T cell responses were measured by (**A**) CFSE dilution via flow cytometry and (**B**) IFN-γ levels from harvested cell-free supernatants via ELISA. In **C**, BALB/c mice were inoculated s.c. with RENCA tumor cells in the right flank on day 0. After cohort (n = 4) randomization for similar mean tumor size on day 14 post-tumor inoculation, mice were treated s.c. in the left flank with $2.4x10^6$ pg/mouse lvRGS5 or lvOVA. Tumor growth was monitored longitudinally.

7.0 BIBLIOGRAPHY

1. Finn, O. J. 2012. Immuno-oncology: understanding the function and dysfunction of the immune system in cancer. *Annals of oncology : official journal of the European Society for Medical Oncology / ESMO* 23 Suppl 8: viii6-9.
2. van der Bruggen, P., C. Traversari, P. Chomez, C. Lurquin, E. De Plaen, B. Van den Eynde, A. Knuth, and T. Boon. 1991. A gene encoding an antigen recognized by cytolytic T lymphocytes on a human melanoma. *Science* 254: 1643-1647.
3. Novellino, L., C. Castelli, and G. Parmiani. 2005. A listing of human tumor antigens recognized by T cells: March 2004 update. *Cancer Immunol Immunother* 54: 187-207.
4. Ritchie, A. W., and J. B. deKernion. 1987. The natural history and clinical features of renal carcinoma. *Semin Nephrol* 7: 131-139.
5. Rohrmann, K., M. Staehler, N. Haseke, A. Bachmann, C. G. Stief, and M. Siebels. 2005. Immunotherapy in metastatic renal cell carcinoma. *World J Urol* 23: 196-201.
6. Radhakrishnan, S., K. R. Wiehagen, V. Pulko, V. Van Keulen, W. A. Faubion, K. L. Knutson, and L. R. Pease. 2007. Induction of a Th1 response from Th2-polarized T cells by activated dendritic cells: dependence on TCR:peptide-MHC interaction, ICAM-1, IL-12, and IFN-gamma. *J Immunol* 178: 3583-3592.
7. Krawczyk, C. M., H. Shen, and E. J. Pearce. 2007. Functional plasticity in memory T helper cell responses. *J Immunol* 178: 4080-4088.
8. Giermasz, A. S., J. A. Urban, Y. Nakamura, P. Watchmaker, R. L. Cumberland, W. Gooding, and P. Kalinski. 2009. Type-1 polarized dendritic cells primed for high IL-12 production show enhanced activity as cancer vaccines. *Cancer Immunol Immunother* 58: 1329-1336.
9. Arroyo, J. C., F. Gabilondo, L. Llorente, M. A. Meraz-Rios, and C. Sanchez-Torres. 2004. Immune response induced in vitro by CD16- and CD16+ monocyte-derived dendritic cells in patients with metastatic renal cell carcinoma treated with dendritic cell vaccines. *J Clin Immunol* 24: 86-96.
10. Wesa, A., P. Kalinski, J. M. Kirkwood, T. Tatsumi, and W. J. Storkus. 2007. Polarized type-1 dendritic cells (DC1) producing high levels of IL-12 family members rescue patient TH1-type antimelanoma CD4+ T cell responses in vitro. *J Immunother* 30: 75-82.
11. Lipscomb, M. W., L. Chen, J. L. Taylor, C. Goldbach, S. C. Watkins, P. Kalinski, L. H. Butterfield, A. K. Wesa, and W. J. Storkus. 2009. Ectopic T-bet expression licenses dendritic cells for IL-12-independent priming of type 1 T cells in vitro. *J Immunol* 183: 7250-7258.
12. Uemura, H., K. Fujimoto, M. Tanaka, M. Yoshikawa, Y. Hirao, S. Uejima, K. Yoshikawa, and K. Itoh. 2006. A phase I trial of vaccination of CA9-derived peptides for

HLA-A24-positive patients with cytokine-refractory metastatic renal cell carcinoma. *Clin Cancer Res* 12: 1768-1775.

13. Iiyama, T., K. Udaka, S. Takeda, T. Takeuchi, Y. C. Adachi, Y. Ohtsuki, A. Tsuboi, S. Nakatsuka, O. A. Elisseeva, Y. Oji, M. Kawakami, H. Nakajima, S. Nishida, T. Shirakata, Y. Oka, T. Shuin, and H. Sugiyama. 2007. WT1 (Wilms' tumor 1) peptide immunotherapy for renal cell carcinoma. *Microbiol Immunol* 51: 519-530.
14. Rahma, O. E., E. Ashtar, R. Ibrahim, A. Toubaji, B. Gause, V. E. Herrin, W. M. Linehan, S. M. Steinberg, F. Grollman, G. Grimes, S. A. Bernstein, J. A. Berzofsky, and S. N. Khleif. A pilot clinical trial testing mutant von Hippel-Lindau peptide as a novel immune therapy in metastatic renal cell carcinoma. *J Transl Med* 8: 8.
15. Miller, G. A., J. E. Pontes, R. P. Huben, and M. H. Goldrosen. 1985. Humoral immune response of patients receiving specific active immunotherapy for renal cell carcinoma. *Cancer Res* 45: 4478-4482.
16. Tani, K., Y. Nakazaki, H. Hase, K. Takahashi, M. Azuma, J. Ohata, R. Kitamura, F. Komine, M. Oiwa, A. Masunaga, T. Maekawa, N. Satoh, D. Adachi, Y. Soda, U. Machida, M. Endo, T. Yamazaki, K. Watari, A. Tojo, N. Yamashita, S. Tomikawa, M. Eriguchi, H. Hamada, Y. Wakumoto, K. Hanazawa, and K. Okumura. 2000. Progress reports on immune gene therapy for stage IV renal cell cancer using lethally irradiated granulocyte-macrophage colony-stimulating factor-transduced autologous renal cancer cells. *Cancer chemotherapy and pharmacology* 46 Suppl: S73-76.
17. Maini, A., N. Nishisaka, Y. Kinoshita, R. F. Jones, C. Y. Wang, and G. P. Haas. 2003. Combination of radiation and vaccination with autologous tumor cells expressing IL-2, IFN-gamma and GM-CSF for treatment of murine renal carcinoma. *In vivo* 17: 119-123.
18. Avigan, D. E., B. Vasir, D. J. George, W. K. Oh, M. B. Atkins, D. F. McDermott, P. W. Kantoff, R. A. Figlin, M. J. Vasconcelles, Y. Xu, D. Kufe, and R. M. Bukowski. 2007. Phase I/II study of vaccination with electrofused allogeneic dendritic cells/autologous tumor-derived cells in patients with stage IV renal cell carcinoma. *Journal of immunotherapy* 30: 749-761.
19. Heiser, A., M. A. Maurice, D. R. Yancey, D. M. Coleman, P. Dahm, and J. Vieweg. 2001. Human dendritic cells transfected with renal tumor RNA stimulate polyclonal T-cell responses against antigens expressed by primary and metastatic tumors. *Cancer Res* 61: 3388-3393.
20. Geiger, C., S. Regn, A. Weinzierl, E. Noessner, and D. J. Schendel. 2005. A generic RNA-pulsed dendritic cell vaccine strategy for renal cell carcinoma. *Journal of translational medicine* 3: 29.
21. Su, Z., J. Dannull, A. Heiser, D. Yancey, S. Pruitt, J. Madden, D. Coleman, D. Niedzwiecki, E. Gilboa, and J. Vieweg. 2003. Immunological and clinical responses in metastatic renal cancer patients vaccinated with tumor RNA-transfected dendritic cells. *Cancer Res* 63: 2127-2133.
22. Bleumer, I., D. M. Tiemessen, J. C. Oosterwijk-Wakka, M. C. Voller, K. De Weijer, P. F. Mulders, and E. Oosterwijk. 2007. Preliminary analysis of patients with progressive renal cell carcinoma vaccinated with CA9-peptide-pulsed mature dendritic cells. *Journal of immunotherapy* 30: 116-122.
23. Wierecky, J., M. Mueller, and P. Brossart. 2006. Dendritic cell-based cancer immunotherapy targeting MUC-1. *Cancer Immunol Immunother* 55: 63-67.

24. Walter, S., T. Weinschenk, A. Stenzl, R. Zdrojowy, A. Pluzanska, C. Szczylik, M. Staehler, W. Brugger, P. Y. Dietrich, R. Mendrzyk, N. Hilf, O. Schoor, J. Fritsche, A. Mahr, D. Maurer, V. Vass, C. Trautwein, P. Lewandrowski, C. Flohr, H. Pohla, J. J. Stanczak, V. Bronte, S. Mandruzzato, T. Biedermann, G. Pawelec, E. Derhovanessian, H. Yamagishi, T. Miki, F. Hongo, N. Takaha, K. Hirakawa, H. Tanaka, S. Stevanovic, J. Frisch, A. Mayer-Mokler, A. Kirner, H. G. Rammensee, C. Reinhardt, and H. Singh-Jasuja. 2012. Multipeptide immune response to cancer vaccine IMA901 after single-dose cyclophosphamide associates with longer patient survival. *Nature medicine* 18.
25. Bonini, C., S. P. Lee, S. R. Riddell, and P. D. Greenberg. 2001. Targeting antigen in mature dendritic cells for simultaneous stimulation of CD4+ and CD8+ T cells. *J Immunol* 166: 5250-5257.
26. Hodge, J. W., M. Chakraborty, C. Kudo-Saito, C. T. Garnett, and J. Schlom. 2005. Multiple costimulatory modalities enhance CTL avidity. *J Immunol* 174: 5994-6004.
27. Kass, E., J. Schlom, J. Thompson, F. Guadagni, P. Graziano, and J. W. Greiner. 1999. Induction of protective host immunity to carcinoembryonic antigen (CEA), a self-antigen in CEA transgenic mice, by immunizing with a recombinant vaccinia-CEA virus. *Cancer Res* 59: 676-683.
28. Yang, S., K. Y. Tsang, and J. Schlom. 2005. Induction of higher-avidity human CTLs by vector-mediated enhanced costimulation of antigen-presenting cells. *Clin Cancer Res* 11: 5603-5615.
29. He, Y., J. Zhang, Z. Mi, P. Robbins, and L. D. Falo, Jr. 2005. Immunization with lentiviral vector-transduced dendritic cells induces strong and long-lasting T cell responses and therapeutic immunity. *J Immunol* 174: 3808-3817.
30. Auman, J. T. 2010. Gene therapy: Have the risks associated with viral vectors been solved? *Current opinion in molecular therapeutics* 12: 637-638.
31. Amato, R. J., W. Shingler, S. Naylor, J. Jac, J. Willis, S. Saxena, J. Hernandez-McClain, and R. Harrop. 2008. Vaccination of renal cell cancer patients with modified vaccinia ankara delivering tumor antigen 5T4 (TroVax) administered with interleukin 2: a phase II trial. *Clin Cancer Res* 14: 7504-7510.
32. Amato, R. J., W. Shingler, M. Goonewardena, J. de Belin, S. Naylor, J. Jac, J. Willis, S. Saxena, J. Hernandez-McClain, and R. Harrop. 2009. Vaccination of renal cell cancer patients with modified vaccinia Ankara delivering the tumor antigen 5T4 (TroVax) alone or administered in combination with interferon-alpha (IFN-alpha): a phase 2 trial. *Journal of immunotherapy* 32: 765-772.
33. Amato, R. J., R. E. Hawkins, H. L. Kaufman, J. A. Thompson, P. Tomczak, C. Szczylik, M. McDonald, S. Eastty, W. H. Shingler, J. de Belin, M. Goonewardena, S. Naylor, and R. Harrop. 2010. Vaccination of metastatic renal cancer patients with MVA-5T4: a randomized, double-blind, placebo-controlled phase III study. *Clin Cancer Res* 16: 5539-5547.
34. Oudard, S., O. Rixe, B. Beuselinck, C. Linassier, E. Banu, J. P. Machiels, M. Baudard, F. Ringeisen, T. Velu, M. A. Lefrere-Belda, J. M. Limacher, W. H. Fridman, M. Azizi, B. Acres, and E. Tartour. 2011. A phase II study of the cancer vaccine TG4010 alone and in combination with cytokines in patients with metastatic renal clear-cell carcinoma: clinical and immunological findings. *Cancer Immunol Immunother* 60: 261-271.
35. Rittig, S. M., M. Haentschel, K. J. Weimer, A. Heine, M. R. Muller, W. Brugger, M. S. Horger, O. Maksimovic, A. Stenzl, I. Hoerr, H. G. Rammensee, T. A. Holderried, L.

Kanz, S. Pascolo, and P. Brossart. 2011. Intradermal vaccinations with RNA coding for TAA generate CD8+ and CD4+ immune responses and induce clinical benefit in vaccinated patients. *Mol Ther* 19: 990-999.

36. Saenger, Y. M., and J. D. Wolchok. 2008. The heterogeneity of the kinetics of response to ipilimumab in metastatic melanoma: patient cases. *Cancer Immun* 8: 1.
37. Schlom, J., P. M. Arlen, and J. L. Gulley. 2007. Cancer vaccines: moving beyond current paradigms. *Clin Cancer Res* 13: 3776-3782.
38. Zhou, J., D. Weng, F. Zhou, K. Pan, H. Song, Q. Wang, H. Wang, Y. Li, L. Huang, H. Zhang, W. Huang, and J. Xia. 2009. Patient-derived renal cell carcinoma cells fused with allogeneic dendritic cells elicit anti-tumor activity: in vitro results and clinical responses. *Cancer Immunol Immunother* 58: 1587-1597.
39. Jocham, D., A. Richter, L. Hoffmann, K. Iwig, D. Fahlenkamp, G. Zakrzewski, E. Schmitt, T. Dannenberg, W. Lehmacher, J. von Wietersheim, and C. Doehn. 2004. Adjuvant autologous renal tumour cell vaccine and risk of tumour progression in patients with renal-cell carcinoma after radical nephrectomy: phase III, randomised controlled trial. *Lancet* 363: 594-599.
40. Berntsen, A., R. Trepiakas, L. Wenandy, P. F. Geertsen, P. thor Straten, M. H. Andersen, A. E. Pedersen, M. H. Claesson, T. Lorentzen, J. S. Johansen, and I. M. Svane. 2008. Therapeutic dendritic cell vaccination of patients with metastatic renal cell carcinoma: a clinical phase 1/2 trial. *J Immunother* 31: 771-780.
41. Schwaab, T., A. Schwarzer, B. Wolf, T. S. Crocenzi, J. D. Seigne, N. A. Crosby, B. F. Cole, J. L. Fisher, J. C. Uhlenhake, D. Mellinger, C. Foster, Z. M. Szczepiorkowski, S. M. Webber, A. R. Schned, R. D. Harris, R. J. Barth, Jr., J. A. Heaney, R. J. Noelle, and M. S. Ernstoff. 2009. Clinical and immunologic effects of intranodal autologous tumor lysate-dendritic cell vaccine with Aldesleukin (Interleukin 2) and IFN-{alpha}2a therapy in metastatic renal cell carcinoma patients. *Clin Cancer Res* 15: 4986-4992.
42. Keilholz, U., J. Weber, J. H. Finke, D. I. Gabrilovich, W. M. Kast, M. L. Disis, J. M. Kirkwood, C. Scheibenbogen, J. Schlom, V. C. Maino, H. K. Lyerly, P. P. Lee, W. Storkus, F. Marincola, A. Worobec, and M. B. Atkins. 2002. Immunologic monitoring of cancer vaccine therapy: results of a workshop sponsored by the Society for Biological Therapy. *J Immunother* 25: 97-138.
43. Lyerly, H. K. 2003. Quantitating cellular immune responses to cancer vaccines. *Semin Oncol* 30: 9-16.
44. Nagorsen, D., C. Scheibenbogen, E. Thiel, and U. Keilholz. 2004. Immunological monitoring of cancer vaccine therapy. *Expert Opin Biol Ther* 4: 1677-1684.
45. Joyce, J. A., and J. W. Pollard. 2009. Microenvironmental regulation of metastasis. *Nat Rev Cancer* 9: 239-252.
46. Robson, N. C., S. Hoves, E. Maraskovsky, and M. Schnurr. 2010. Presentation of tumour antigens by dendritic cells and challenges faced. *Current opinion in immunology* 22: 137-144.
47. Savina, A., and S. Amigorena. 2007. Phagocytosis and antigen presentation in dendritic cells. *Immunological reviews* 219: 143-156.
48. Turcotte, S., and S. A. Rosenberg. 2011. Immunotherapy for metastatic solid cancers. *Advances in surgery* 45: 341-360.

49. Kolbeck, P. C., F. F. Kaveggia, S. L. Johansson, M. T. Grune, and R. J. Taylor. 1992. The relationships among tumor-infiltrating lymphocytes, histopathologic findings, and long-term clinical follow-up in renal cell carcinoma. *Mod Pathol* 5: 420-425.
50. Hernberg, M. 1999. Lymphocyte subsets as prognostic markers for cancer patients receiving immunomodulative therapy. *Med Oncol* 16: 145-153.
51. Nakano, O., M. Sato, Y. Naito, K. Suzuki, S. Orikasa, M. Aizawa, Y. Suzuki, I. Shintaku, H. Nagura, and H. Ohtani. 2001. Proliferative activity of intratumoral CD8(+) T-lymphocytes as a prognostic factor in human renal cell carcinoma: clinicopathologic demonstration of antitumor immunity. *Cancer Res* 61: 5132-5136.
52. Kondo, T., H. Nakazawa, F. Ito, Y. Hashimoto, Y. Osaka, K. Futatsuyama, H. Toma, and K. Tanabe. 2006. Favorable prognosis of renal cell carcinoma with increased expression of chemokines associated with a Th1-type immune response. *Cancer Sci* 97: 780-786.
53. Troy, A. J., K. L. Summers, P. J. Davidson, C. H. Atkinson, and D. N. Hart. 1998. Minimal recruitment and activation of dendritic cells within renal cell carcinoma. *Clin Cancer Res* 4: 585-593.
54. Uzzo, R. G., P. Rayman, V. Kolenko, P. E. Clark, T. Bloom, A. M. Ward, L. Molto, C. Tannenbaum, L. J. Worford, R. Bukowski, R. Tubbs, E. D. Hsi, N. H. Bander, A. C. Novick, and J. H. Finke. 1999. Mechanisms of apoptosis in T cells from patients with renal cell carcinoma. *Clin Cancer Res* 5: 1219-1229.
55. Kiertscher, S. M., J. Luo, S. M. Dubinett, and M. D. Roth. 2000. Tumors promote altered maturation and early apoptosis of monocyte-derived dendritic cells. *J Immunol* 164: 1269-1276.
56. Rayman, P., A. K. Wesa, A. L. Richmond, T. Das, K. Biswas, G. Raval, W. J. Storkus, C. Tannenbaum, A. Novick, R. Bukowski, and J. Finke. 2004. Effect of renal cell carcinomas on the development of type 1 T-cell responses. *Clin Cancer Res* 10: 6360S-6366S.
57. Tatsumi, T., C. J. Herrem, W. C. Olson, J. H. Finke, R. M. Bukowski, M. S. Kinch, E. Ranieri, and W. J. Storkus. 2003. Disease stage variation in CD4+ and CD8+ T-cell reactivity to the receptor tyrosine kinase EphA2 in patients with renal cell carcinoma. *Cancer Res* 63: 4481-4489.
58. Tatsumi, T., L. S. Kierstead, E. Ranieri, L. Gesualdo, F. P. Schena, J. H. Finke, R. M. Bukowski, J. Mueller-Berghaus, J. M. Kirkwood, W. W. Kwok, and W. J. Storkus. 2002. Disease-associated bias in T helper type 1 (Th1)/Th2 CD4(+) T cell responses against MAGE-6 in HLA-DRB10401(+) patients with renal cell carcinoma or melanoma. *J Exp Med* 196: 619-628.
59. Onishi, T., Y. Ohishi, K. Imagawa, Y. Ohmoto, and K. Murata. 1999. An assessment of the immunological environment based on intratumoral cytokine production in renal cell carcinoma. *BJU Int* 83: 488-492.
60. Griffiths, R. W., E. Elkord, D. E. Gilham, V. Ramani, N. Clarke, P. L. Stern, and R. E. Hawkins. 2007. Frequency of regulatory T cells in renal cell carcinoma patients and investigation of correlation with survival. *Cancer Immunol Immunother* 56: 1743-1753.
61. Saff, R. R., E. S. Spanjaard, A. M. Hohlbaum, and A. Marshak-Rothstein. 2004. Activation-induced cell death limits effector function of CD4 tumor-specific T cells. *J Immunol* 172: 6598-6606.
62. Lu, B., and O. J. Finn. 2008. T-cell death and cancer immune tolerance. *Cell Death Differ* 15: 70-79.

63. Welford, S. M., and A. J. Giaccia. 2011. Hypoxia and senescence: the impact of oxygenation on tumor suppression. *Molecular cancer research : MCR* 9: 538-544.
64. Yu, H., M. Kortylewski, and D. Pardoll. 2007. Crosstalk between cancer and immune cells: role of STAT3 in the tumour microenvironment. *Nat Rev Immunol* 7: 41-51.
65. Huang, Y., L. Lin, A. Shanker, A. Malhotra, L. Yang, M. M. Dikov, and D. P. Carbone. 2011. Resuscitating cancer immunosurveillance: selective stimulation of DLL1-Notch signaling in T cells rescues T-cell function and inhibits tumor growth. *Cancer Res* 71: 6122-6131.
66. Xu, H., J. Zhu, S. Smith, J. Foldi, B. Zhao, A. Y. Chung, H. Outtz, J. Kitajewski, C. Shi, S. Weber, P. Saftig, Y. Li, K. Ozato, C. P. Blobel, L. B. Ivashkiv, and X. Hu. 2012. Notch-RBP-J signaling regulates the transcription factor IRF8 to promote inflammatory macrophage polarization. *Nature immunology* 13: 642-650.
67. Wang, Y. C., F. He, F. Feng, X. W. Liu, G. Y. Dong, H. Y. Qin, X. B. Hu, M. H. Zheng, L. Liang, L. Feng, Y. M. Liang, and H. Han. 2010. Notch signaling determines the M1 versus M2 polarization of macrophages in antitumor immune responses. *Cancer Res* 70: 4840-4849.
68. Hamzah, J., M. Jugold, F. Kiessling, P. Rigby, M. Manzur, H. H. Marti, T. Rabie, S. Kaden, H. J. Grone, G. J. Hammerling, B. Arnold, and R. Ganss. 2008. Vascular normalization in Rgs5-deficient tumours promotes immune destruction. *Nature* 453: 410-414.
69. Chung, A. S., J. Lee, and N. Ferrara. 2010. Targeting the tumour vasculature: insights from physiological angiogenesis. *Nat Rev Cancer* 10: 505-514.
70. Ferrara, N., H. P. Gerber, and J. LeCouter. 2003. The biology of VEGF and its receptors. *Nature medicine* 9: 669-676.
71. Gerhardt, H., M. Golding, M. Fruttiger, C. Ruhrberg, A. Lundkvist, A. Abramsson, M. Jeltsch, C. Mitchell, K. Alitalo, D. Shima, and C. Betsholtz. 2003. VEGF guides angiogenic sprouting utilizing endothelial tip cell filopodia. *The Journal of cell biology* 161: 1163-1177.
72. Hellstrom, M., L. K. Phng, J. J. Hofmann, E. Wallgard, L. Coultas, P. Lindblom, J. Alva, A. K. Nilsson, L. Karlsson, N. Gaiano, K. Yoon, J. Rossant, M. L. Iruela-Arispe, M. Kalen, H. Gerhardt, and C. Betsholtz. 2007. Dll4 signalling through Notch1 regulates formation of tip cells during angiogenesis. *Nature* 445: 776-780.
73. Gerhardt, H., and H. Semb. 2008. Pericytes: gatekeepers in tumour cell metastasis? *J Mol Med* 86: 135-144.
74. Betsholtz, C., P. Lindblom, and H. Gerhardt. 2005. Role of pericytes in vascular morphogenesis. *Exs*: 115-125.
75. Bergers, G., S. Song, N. Meyer-Morse, E. Bergsland, and D. Hanahan. 2003. Benefits of targeting both pericytes and endothelial cells in the tumor vasculature with kinase inhibitors. *J Clin Invest* 111: 1287-1295.
76. Xian, X., J. Hakansson, A. Stahlberg, P. Lindblom, C. Betsholtz, H. Gerhardt, and H. Semb. 2006. Pericytes limit tumor cell metastasis. *J Clin Invest* 116: 642-651.
77. Farrington-Rock, C., N. J. Crofts, M. J. Doherty, B. A. Ashton, C. Griffin-Jones, and A. E. Canfield. 2004. Chondrogenic and adipogenic potential of microvascular pericytes. *Circulation* 110: 2226-2232.
78. Crisan, M., S. Yap, L. Casteilla, C. W. Chen, M. Corselli, T. S. Park, G. Andriolo, B. Sun, B. Zheng, L. Zhang, C. Norotte, P. N. Teng, J. Traas, R. Schugar, B. M. Deasy, S.

Badylak, H. J. Buhring, J. P. Giacobino, L. Lazzari, J. Huard, and B. Peault. 2008. A perivascular origin for mesenchymal stem cells in multiple human organs. *Cell Stem Cell* 3: 301-313.

79. Fukumura, D., D. G. Duda, L. L. Munn, and R. K. Jain. 2010. Tumor microvasculature and microenvironment: novel insights through intravital imaging in pre-clinical models. *Microcirculation* 17: 206-225.
80. Lin, P., J. A. Buxton, A. Acheson, C. Radziejewski, P. C. Maisonpierre, G. D. Yancopoulos, K. M. Channon, L. P. Hale, M. W. Dewhirst, S. E. George, and K. G. Peters. 1998. Antiangiogenic gene therapy targeting the endothelium-specific receptor tyrosine kinase Tie2. *Proc Natl Acad Sci U S A* 95: 8829-8834.
81. Lu, C., T. Bonome, Y. Li, A. A. Kamat, L. Y. Han, R. Schmandt, R. L. Coleman, D. M. Gershenson, R. B. Jaffe, M. J. Birrer, and A. K. Sood. 2007. Gene alterations identified by expression profiling in tumor-associated endothelial cells from invasive ovarian carcinoma. *Cancer Res* 67: 1757-1768.
82. Morikawa, S., P. Baluk, T. Kaidoh, A. Haskell, R. K. Jain, and D. M. McDonald. 2002. Abnormalities in pericytes on blood vessels and endothelial sprouts in tumors. *Am J Pathol* 160: 985-1000.
83. Berger, M., G. Bergers, B. Arnold, G. J. Hammerling, and R. Ganss. 2005. Regulator of G-protein signaling-5 induction in pericytes coincides with active vessel remodeling during neovascularization. *Blood* 105: 1094-1101.
84. Bondjers, C., M. Kalen, M. Hellstrom, S. J. Scheidl, A. Abramsson, O. Renner, P. Lindahl, H. Cho, J. Kehrl, and C. Betsholtz. 2003. Transcription profiling of platelet-derived growth factor-B-deficient mouse embryos identifies RGS5 as a novel marker for pericytes and vascular smooth muscle cells. *Am J Pathol* 162: 721-729.
85. Sen, C. K. 2009. Wound healing essentials: let there be oxygen. *Wound repair and regeneration : official publication of the Wound Healing Society [and] the European Tissue Repair Society* 17: 1-18.
86. Bao, B., A. S. Azmi, S. Ali, A. Ahmad, Y. Li, S. Banerjee, D. Kong, and F. H. Sarkar. 2012. The biological kinship of hypoxia with CSC and EMT and their relationship with deregulated expression of miRNAs and tumor aggressiveness. *Biochim Biophys Acta* 1826: 272-296.
87. Denko, N. C. 2008. Hypoxia, HIF1 and glucose metabolism in the solid tumour. *Nat Rev Cancer* 8: 705-713.
88. Pugh, C. W., and P. J. Ratcliffe. 2003. Regulation of angiogenesis by hypoxia: role of the HIF system. *Nature medicine* 9: 677-684.
89. Hermann, P. C., S. Bhaskar, M. Cioffi, and C. Heeschen. 2010. Cancer stem cells in solid tumors. *Seminars in cancer biology* 20: 77-84.
90. Panchision, D. M. 2009. The role of oxygen in regulating neural stem cells in development and disease. *Journal of cellular physiology* 220: 562-568.
91. Wang, Z., Y. Li, A. Ahmad, A. S. Azmi, D. Kong, S. Banerjee, and F. H. Sarkar. 2010. Targeting miRNAs involved in cancer stem cell and EMT regulation: An emerging concept in overcoming drug resistance. *Drug resistance updates : reviews and commentaries in antimicrobial and anticancer chemotherapy* 13: 109-118.
92. Wang, Z., Y. Li, D. Kong, and F. H. Sarkar. 2010. The role of Notch signaling pathway in epithelial-mesenchymal transition (EMT) during development and tumor aggressiveness. *Current drug targets* 11: 745-751.

93. Folkman, J. 2002. Role of angiogenesis in tumor growth and metastasis. *Semin Oncol* 29: 15-18.
94. Heath, V. L., and R. Bicknell. 2009. Anticancer strategies involving the vasculature. *Nat Rev Clin Oncol* 6: 395-404.
95. Jain, R. K. 2005. Normalization of tumor vasculature: an emerging concept in antiangiogenic therapy. *Science* 307: 58-62.
96. Ma, J., and D. J. Waxman. 2008. Combination of antiangiogenesis with chemotherapy for more effective cancer treatment. *Molecular cancer therapeutics* 7: 3670-3684.
97. Greenberg, J. I., and D. A. Cheresh. 2009. VEGF as an inhibitor of tumor vessel maturation: implications for cancer therapy. *Expert opinion on biological therapy* 9: 1347-1356.
98. Huang, Y., J. Yuan, E. Righi, W. S. Kamoun, M. Ancukiewicz, J. Nezivar, M. Santosuosso, J. D. Martin, M. R. Martin, F. Vianello, P. Leblanc, L. L. Munn, P. Huang, D. G. Duda, D. Fukumura, R. K. Jain, and M. C. Poznansky. 2012. Vascular normalizing doses of antiangiogenic treatment reprogram the immunosuppressive tumor microenvironment and enhance immunotherapy. *Proc Natl Acad Sci U S A* 109: 17561-17566.
99. Faivre, S., G. Demetri, W. Sargent, and E. Raymond. 2007. Molecular basis for sunitinib efficacy and future clinical development. *Nat Rev Drug Discov* 6: 734-745.
100. Motzer, R. J., T. E. Hutson, P. Tomczak, M. D. Michaelson, R. M. Bukowski, S. Oudard, S. Negrier, C. Szczylik, R. Pili, G. A. Bjarnason, X. Garcia-del-Muro, J. A. Sosman, E. Solska, G. Wilding, J. A. Thompson, S. T. Kim, I. Chen, X. Huang, and R. A. Figlin. 2009. Overall survival and updated results for sunitinib compared with interferon alfa in patients with metastatic renal cell carcinoma. *J Clin Oncol* 27: 3584-3590.
101. Gore, M. E., C. Szczylik, C. Porta, S. Bracarda, G. A. Bjarnason, S. Oudard, S. Hariharan, S. H. Lee, J. Haanen, D. Castellano, E. Vrdoljak, P. Schoffski, P. Mainwaring, A. Nieto, J. Yuan, and R. Bukowski. 2009. Safety and efficacy of sunitinib for metastatic renal-cell carcinoma: an expanded-access trial. *Lancet Oncol* 10: 757-763.
102. Escudier, B., J. Roigas, S. Gillessen, U. Harmenberg, S. Srinivas, S. F. Mulder, G. Fountzilas, C. Peschel, P. Flodgren, E. C. Maneval, I. Chen, and N. J. Vogelzang. 2009. Phase II study of sunitinib administered in a continuous once-daily dosing regimen in patients with cytokine-refractory metastatic renal cell carcinoma. *J Clin Oncol* 27: 4068-4075.
103. Huang, D., Y. Ding, Y. Li, W. M. Luo, Z. F. Zhang, J. Snider, K. Vandenbeldt, C. N. Qian, and B. T. Teh. 2010. Sunitinib acts primarily on tumor endothelium rather than tumor cells to inhibit the growth of renal cell carcinoma. *Cancer Res* 70: 1053-1062.
104. Czabanka, M., M. Vinci, F. Heppner, A. Ullrich, and P. Vajkoczy. 2009. Effects of sunitinib on tumor hemodynamics and delivery of chemotherapy. *Int J Cancer* 124: 1293-1300.
105. Zhou, Q., P. Guo, and J. M. Gallo. 2008. Impact of angiogenesis inhibition by sunitinib on tumor distribution of temozolomide. *Clin Cancer Res* 14: 1540-1549.
106. Ganss, R., E. Ryschich, E. Klar, B. Arnold, and G. J. Hammerling. 2002. Combination of T-cell therapy and trigger of inflammation induces remodeling of the vasculature and tumor eradication. *Cancer Res* 62: 1462-1470.
107. Feldman, E. D., D. M. Weinreich, N. M. Carroll, M. L. Burness, A. L. Feldman, E. Turner, H. Xu, and H. R. Alexander, Jr. 2006. Interferon gamma-inducible protein 10

selectively inhibits proliferation and induces apoptosis in endothelial cells. *Ann Surg Oncol* 13: 125-133.

108. van Cruijsen, H., A. A. van der Veldt, L. Vroling, D. Oosterhoff, H. J. Broxterman, R. J. Scheper, G. Giaccone, J. B. Haanen, A. J. van den Eertwegh, E. Boven, K. Hoekman, and T. D. de Gruijl. 2008. Sunitinib-induced myeloid lineage redistribution in renal cell cancer patients: CD1c+ dendritic cell frequency predicts progression-free survival. *Clin Cancer Res* 14: 5884-5892.
109. Finke, J. H., B. Rini, J. Ireland, P. Rayman, A. Richmond, A. Golshayan, L. Wood, P. Elson, J. Garcia, R. Dreicer, and R. Bukowski. 2008. Sunitinib reverses type-1 immune suppression and decreases T-regulatory cells in renal cell carcinoma patients. *Clin Cancer Res* 14: 6674-6682.
110. Ozao-Choy, J., G. Ma, J. Kao, G. X. Wang, M. Meseck, M. Sung, M. Schwartz, C. M. Divino, P. Y. Pan, and S. H. Chen. 2009. The novel role of tyrosine kinase inhibitor in the reversal of immune suppression and modulation of tumor microenvironment for immune-based cancer therapies. *Cancer Res* 69: 2514-2522.
111. Bose, A., J. L. Taylor, S. Alber, S. C. Watkins, J. A. Garcia, B. I. Rini, J. S. Ko, P. A. Cohen, J. H. Finke, and W. J. Storkus. 2011. Sunitinib facilitates the activation and recruitment of therapeutic anti-tumor immunity in concert with specific vaccination. *Int J Cancer* 129: 2158-2170.
112. Khong, H. T., and N. P. Restifo. 2002. Natural selection of tumor variants in the generation of "tumor escape" phenotypes. *Nature immunology* 3: 999-1005.
113. Ebos, J. M., C. R. Lee, W. Cruz-Munoz, G. A. Bjarnason, J. G. Christensen, and R. S. Kerbel. 2009. Accelerated metastasis after short-term treatment with a potent inhibitor of tumor angiogenesis. *Cancer cell* 15: 232-239.
114. Paez-Ribes, M., E. Allen, J. Hudock, T. Takeda, H. Okuyama, F. Vinals, M. Inoue, G. Bergers, D. Hanahan, and O. Casanovas. 2009. Antiangiogenic therapy elicits malignant progression of tumors to increased local invasion and distant metastasis. *Cancer cell* 15: 220-231.
115. Okaji, Y., N. H. Tsuno, J. Kitayama, S. Saito, T. Takahashi, K. Kawai, K. Yazawa, M. Asakage, N. Hori, T. Watanabe, Y. Shibata, K. Takahashi, and H. Nagawa. 2004. Vaccination with autologous endothelium inhibits angiogenesis and metastasis of colon cancer through autoimmunity. *Cancer Sci* 95: 85-90.
116. Yoshiura, K., T. Nishishita, T. Nakaoka, N. Yamashita, and N. Yamashita. 2009. Inhibition of B16 melanoma growth and metastasis in C57BL mice by vaccination with a syngeneic endothelial cell line. *Journal of experimental & clinical cancer research : CR* 28: 13.
117. Matejuk, A., Q. Leng, S. T. Chou, and A. J. Mixson. 2011. Vaccines targeting the neovasculature of tumors. *Vascular cell* 3: 7.
118. Vujanovic, L., and L. H. Butterfield. 2007. Melanoma cancer vaccines and anti-tumor T cell responses. *J Cell Biochem* 102: 301-310.
119. Ahmed, F., J. C. Steele, J. M. Herbert, N. M. Steven, and R. Bicknell. 2008. Tumor stroma as a target in cancer. *Curr Cancer Drug Targets* 8: 447-453.
120. Zhao, X., A. Bose, H. Komita, J. L. Taylor, N. Chi, D. B. Lowe, H. Okada, Y. Cao, D. Mukhopadhyay, P. A. Cohen, and W. J. Storkus. 2012. Vaccines targeting tumor blood vessel antigens promote CD8(+) T cell-dependent tumor eradication or dormancy in HLA-A2 transgenic mice. *J Immunol* 188: 1782-1788.

121. Komita, H., X. Zhao, J. L. Taylor, L. J. Sparvero, A. A. Amoscato, S. Alber, S. C. Watkins, A. D. Pardee, A. K. Wesa, and W. J. Storkus. 2008. CD8+ T-cell responses against hemoglobin-beta prevent solid tumor growth. *Cancer Res* 68: 8076-8084.
122. Chinnasamy, D., Z. Yu, M. R. Theoret, Y. Zhao, R. K. Shrimali, R. A. Morgan, S. A. Feldman, N. P. Restifo, and S. A. Rosenberg. 2010. Gene therapy using genetically modified lymphocytes targeting VEGFR-2 inhibits the growth of vascularized syngenic tumors in mice. *J Clin Invest* 120: 3953-3968.
123. Rocha, F. G., K. C. Chaves, R. Chammas, J. P. Peron, L. V. Rizzo, N. Schor, and M. H. Bellini. 2010. Endostatin gene therapy enhances the efficacy of IL-2 in suppressing metastatic renal cell carcinoma in mice. *Cancer Immunol Immunother* 59: 1357-1365.
124. Kundig, T. M., C. P. Kalberer, H. Hengartner, and R. M. Zinkernagel. 1993. Vaccination with two different vaccinia recombinant viruses: long-term inhibition of secondary vaccination. *Vaccine* 11: 1154-1158.
125. He, Y., J. Zhang, C. Donahue, and L. D. Falo, Jr. 2006. Skin-derived dendritic cells induce potent CD8(+) T cell immunity in recombinant lentivector-mediated genetic immunization. *Immunity* 24: 643-656.
126. Wang, Y., K. A. Kim, J. H. Kim, and H. S. Sul. 2006. Pref-1, a preadipocyte secreted factor that inhibits adipogenesis. *The Journal of nutrition* 136: 2953-2956.
127. Falix, F. A., D. C. Aronson, W. H. Lamers, and I. C. Gaemers. 2012. Possible roles of DLK1 in the Notch pathway during development and disease. *Biochim Biophys Acta* 1822: 988-995.
128. Waddell, J. N., P. Zhang, Y. Wen, S. K. Gupta, A. Yevtodiyenko, J. V. Schmidt, C. A. Bidwell, A. Kumar, and S. Kuang. 2010. Dlk1 is necessary for proper skeletal muscle development and regeneration. *PLoS One* 5: e15055.
129. Raghunandan, R., M. Ruiz-Hidalgo, Y. Jia, R. Ettinger, E. Rudikoff, P. Riggins, R. Farnsworth, A. Tesfaye, J. Laborda, and S. R. Bauer. 2008. Dlk1 influences differentiation and function of B lymphocytes. *Stem cells and development* 17: 495-507.
130. Sanchez-Solana, B., M. L. Nueda, M. D. Ruvira, M. J. Ruiz-Hidalgo, E. M. Monsalve, S. Rivero, J. J. Garcia-Ramirez, M. J. Diaz-Guerra, V. Baladron, and J. Laborda. 2011. The EGF-like proteins DLK1 and DLK2 function as inhibitory non-canonical ligands of NOTCH1 receptor that modulate each other's activities. *Biochim Biophys Acta* 1813: 1153-1164.
131. Begum, A., Y. Kim, Q. Lin, and Z. Yun. 2012. DLK1, delta-like 1 homolog (Drosophila), regulates tumor cell differentiation in vivo. *Cancer letters* 318: 26-33.
132. Ranganathan, P., K. L. Weaver, and A. J. Capobianco. 2011. Notch signalling in solid tumours: a little bit of everything but not all the time. *Nat Rev Cancer* 11: 338-351.
133. Artavanis-Tsakonas, S., K. Matsuno, and M. E. Fortini. 1995. Notch signaling. *Science* 268: 225-232.
134. Lobry, C., P. Oh, and I. Aifantis. 2011. Oncogenic and tumor suppressor functions of Notch in cancer: it's NOTCH what you think. *J Exp Med* 208: 1931-1935.
135. Radtke, F., and K. Raj. 2003. The role of Notch in tumorigenesis: oncogene or tumour suppressor? *Nat Rev Cancer* 3: 756-767.
136. Weng, A. P., A. A. Ferrando, W. Lee, J. P. t. Morris, L. B. Silverman, C. Sanchez-Irizarry, S. C. Blacklow, A. T. Look, and J. C. Aster. 2004. Activating mutations of NOTCH1 in human T cell acute lymphoblastic leukemia. *Science* 306: 269-271.

137. Reedijk, M. 2012. Notch signaling and breast cancer. *Advances in experimental medicine and biology* 727: 241-257.
138. Van Vlierberghe, P., and A. Ferrando. 2012. The molecular basis of T cell acute lymphoblastic leukemia. *J Clin Invest* 122: 3398-3406.
139. Zhang, X., T. Chen, J. Zhang, Q. Mao, S. Li, W. Xiong, Y. Qiu, Q. Xie, and J. Ge. 2012. Notch1 promotes glioma cell migration and invasion by stimulating beta-catenin and NF-kappaB signaling via AKT activation. *Cancer Sci* 103: 181-190.
140. Grudzien, P., S. Lo, K. S. Albain, P. Robinson, P. Rajan, P. R. Strack, T. E. Golde, L. Miele, and K. E. Foreman. 2010. Inhibition of Notch signaling reduces the stem-like population of breast cancer cells and prevents mammosphere formation. *Anticancer research* 30: 3853-3867.
141. Sikandar, S. S., K. T. Pate, S. Anderson, D. Dizon, R. A. Edwards, M. L. Waterman, and S. M. Lipkin. 2010. NOTCH signaling is required for formation and self-renewal of tumor-initiating cells and for repression of secretory cell differentiation in colon cancer. *Cancer Res* 70: 1469-1478.
142. Pietras, A., D. Gisselsson, I. Ora, R. Noguera, S. Beckman, S. Navarro, and S. Pahlman. 2008. High levels of HIF-2alpha highlight an immature neural crest-like neuroblastoma cell cohort located in a perivascular niche. *The Journal of pathology* 214: 482-488.
143. Nicolas, M., A. Wolfer, K. Raj, J. A. Kummer, P. Mill, M. van Noort, C. C. Hui, H. Clevers, G. P. Dotto, and F. Radtke. 2003. Notch1 functions as a tumor suppressor in mouse skin. *Nature genetics* 33: 416-421.
144. Demehri, S., A. Turkoz, and R. Kopan. 2009. Epidermal Notch1 loss promotes skin tumorigenesis by impacting the stromal microenvironment. *Cancer cell* 16: 55-66.
145. Viatour, P., U. Ehmer, L. A. Saddic, C. Dorrell, J. B. Andersen, C. Lin, A. F. Zmoos, P. K. Mazur, B. E. Schaffer, A. Ostermeier, H. Vogel, K. G. Sylvester, S. S. Thorgeirsson, M. Grompe, and J. Sage. 2011. Notch signaling inhibits hepatocellular carcinoma following inactivation of the RB pathway. *J Exp Med* 208: 1963-1976.
146. Klinakis, A., C. Lobry, O. Abdel-Wahab, P. Oh, H. Haeno, S. Buonamici, I. van De Walle, S. Cathelin, T. Trimarchi, E. Araldi, C. Liu, S. Ibrahim, M. Beran, J. Zavadil, A. Efstratiadis, T. Taghon, F. Michor, R. L. Levine, and I. Aifantis. 2011. A novel tumour-suppressor function for the Notch pathway in myeloid leukaemia. *Nature* 473: 230-233.
147. Dumont, A. G., Y. Yang, D. Reynoso, D. Katz, J. C. Trent, and D. P. Hughes. 2012. Anti-tumor effects of the Notch pathway in gastrointestinal stromal tumors. *Carcinogenesis* 33: 1674-1683.
148. Jonusiene, V., A. Sasnauskiene, N. Lachej, D. Kanopiene, D. Dabkeviciene, S. Sasnauskiene, B. Kazbariene, and J. Didziapetriene. 2013. Down-regulated expression of Notch signaling molecules in human endometrial cancer. *Med Oncol* 30: 438.
149. Noguera-Troise, I., C. Daly, N. J. Papadopoulos, S. Coetzee, P. Boland, N. W. Gale, H. C. Lin, G. D. Yancopoulos, and G. Thurston. 2006. Blockade of Dll4 inhibits tumour growth by promoting non-productive angiogenesis. *Nature* 444: 1032-1037.
150. Ridgway, J., G. Zhang, Y. Wu, S. Stawicki, W. C. Liang, Y. Chanthery, J. Kowalski, R. J. Watts, C. Callahan, I. Kasman, M. Singh, M. Chien, C. Tan, J. A. Hongo, F. de Sauvage, G. Plowman, and M. Yan. 2006. Inhibition of Dll4 signalling inhibits tumour growth by deregulating angiogenesis. *Nature* 444: 1083-1087.

151. Yan, M., C. A. Callahan, J. C. Beyer, K. P. Allamneni, G. Zhang, J. B. Ridgway, K. Niessen, and G. D. Plowman. 2010. Chronic DLL4 blockade induces vascular neoplasms. *Nature* 463: E6-7.
152. Purow, B. 2012. Notch inhibition as a promising new approach to cancer therapy. *Advances in experimental medicine and biology* 727: 305-319.
153. Zhou, B. B., M. Peyton, B. He, C. Liu, L. Girard, E. Caudler, Y. Lo, F. Baribaud, I. Mikami, N. Reguart, G. Yang, Y. Li, W. Yao, K. Vaddi, A. F. Gazdar, S. M. Friedman, D. M. Jablons, R. C. Newton, J. S. Fridman, J. D. Minna, and P. A. Scherle. 2006. Targeting ADAM-mediated ligand cleavage to inhibit HER3 and EGFR pathways in non-small cell lung cancer. *Cancer cell* 10: 39-50.
154. Ostrand-Rosenberg, S. 2008. Immune surveillance: a balance between protumor and antitumor immunity. *Current opinion in genetics & development* 18: 11-18.
155. Reiman, J. M., M. Kmieciak, M. H. Manjili, and K. L. Knutson. 2007. Tumor immunoediting and immunosculpting pathways to cancer progression. *Seminars in cancer biology* 17: 275-287.
156. Bui, J. D., and R. D. Schreiber. 2007. Cancer immunosurveillance, immunoediting and inflammation: independent or interdependent processes? *Current opinion in immunology* 19: 203-208.
157. Slingluff, C. L., Jr., K. A. Chianese-Bullock, T. N. Bullock, W. W. Grosh, D. W. Mullins, L. Nichols, W. Olson, G. Petroni, M. Smolkin, and V. H. Engelhard. 2006. Immunity to melanoma antigens: from self-tolerance to immunotherapy. *Advances in immunology* 90: 243-295.
158. Yu, Z., and N. P. Restifo. 2002. Cancer vaccines: progress reveals new complexities. *J Clin Invest* 110: 289-294.
159. Singh, R., and Y. Paterson. 2007. Immunoediting sculpts tumor epitopes during immunotherapy. *Cancer Res* 67: 1887-1892.
160. Gajewski, T. F., F. Fallarino, A. Ashikari, and M. Sherman. 2001. Immunization of HLA-A2+ melanoma patients with MAGE-3 or MelanA peptide-pulsed autologous peripheral blood mononuclear cells plus recombinant human interleukin 12. *Clin Cancer Res* 7: 895s-901s.
161. Feltkamp, M. C., H. L. Smits, M. P. Vierboom, R. P. Minnaar, B. M. de Jongh, J. W. Drijfhout, J. ter Schegget, C. J. Melief, and W. M. Kast. 1993. Vaccination with cytotoxic T lymphocyte epitope-containing peptide protects against a tumor induced by human papillomavirus type 16-transformed cells. *Eur J Immunol* 23: 2242-2249.
162. Hofmeister, V., D. Schrama, and J. C. Becker. 2008. Anti-cancer therapies targeting the tumor stroma. *Cancer Immunol Immunother* 57: 1-17.
163. Zhang, B., N. A. Bowerman, J. K. Salama, H. Schmidt, M. T. Spiotto, A. Schietinger, P. Yu, Y. X. Fu, R. R. Weichselbaum, D. A. Rowley, D. M. Kranz, and H. Schreiber. 2007. Induced sensitization of tumor stroma leads to eradication of established cancer by T cells. *J Exp Med* 204: 49-55.
164. Loberg, R. D., B. A. Gayed, K. B. Olson, and K. J. Pienta. 2005. A paradigm for the treatment of prostate cancer bone metastases based on an understanding of tumor cell-microenvironment interactions. *J Cell Biochem* 96: 439-446.
165. Firat, H., M. Cochet, P. S. Rohrlich, F. Garcia-Pons, S. Darche, O. Danos, F. A. Lemonnier, and P. Langlade-Demoyen. 2002. Comparative analysis of the CD8(+) T cell

repertoires of H-2 class I wild-type/HLA-A2.1 and H-2 class I knockout/HLA-A2.1 transgenic mice. *International immunology* 14: 925-934.

166. Hatano, M., N. Kuwashima, T. Tatsumi, J. E. Dusak, F. Nishimura, K. M. Reilly, W. J. Storkus, and H. Okada. 2004. Vaccination with EphA2-derived T cell-epitopes promotes immunity against both EphA2-expressing and EphA2-negative tumors. *Journal of translational medicine* 2: 40.
167. Burg, M. A., R. Pasqualini, W. Arap, E. Ruoslahti, and W. B. Stallcup. 1999. NG2 proteoglycan-binding peptides target tumor neovasculature. *Cancer Res* 59: 2869-2874.
168. Tatsumi, T., J. Huang, W. E. Gooding, A. Gambotto, P. D. Robbins, N. L. Vujanovic, S. M. Alber, S. C. Watkins, H. Okada, and W. J. Storkus. 2003. Intratumoral delivery of dendritic cells engineered to secrete both interleukin (IL)-12 and IL-18 effectively treats local and distant disease in association with broadly reactive Tc1-type immunity. *Cancer Res* 63: 6378-6386.
169. Mittendorf, E. A., C. E. Storrer, C. D. Shriver, S. Ponniah, and G. E. Peoples. 2005. Evaluation of the CD107 cytotoxicity assay for the detection of cytolytic CD8+ cells recognizing HER2/neu vaccine peptides. *Breast cancer research and treatment* 92: 85-93.
170. Maciag, P. C., M. M. Seavey, Z. K. Pan, S. Ferrone, and Y. Paterson. 2008. Cancer immunotherapy targeting the high molecular weight melanoma-associated antigen protein results in a broad antitumor response and reduction of pericytes in the tumor vasculature. *Cancer Res* 68: 8066-8075.
171. Ishizaki, H., T. Tsunoda, S. Wada, M. Yamauchi, M. Shibuya, and H. Tahara. 2006. Inhibition of tumor growth with antiangiogenic cancer vaccine using epitope peptides derived from human vascular endothelial growth factor receptor 1. *Clin Cancer Res* 12: 5841-5849.
172. Wada, S., T. Tsunoda, T. Baba, F. J. Primus, H. Kuwano, M. Shibuya, and H. Tahara. 2005. Rationale for antiangiogenic cancer therapy with vaccination using epitope peptides derived from human vascular endothelial growth factor receptor 2. *Cancer Res* 65: 4939-4946.
173. Kaplan, C. D., J. A. Kruger, H. Zhou, Y. Luo, R. Xiang, and R. A. Reisfeld. 2006. A novel DNA vaccine encoding PDGFRbeta suppresses growth and dissemination of murine colon, lung and breast carcinoma. *Vaccine* 24: 6994-7002.
174. Liu, W., A. A. Parikh, O. Stoeltzing, F. Fan, M. F. McCarty, J. Wey, D. J. Hicklin, and L. M. Ellis. 2005. Upregulation of neuropilin-1 by basic fibroblast growth factor enhances vascular smooth muscle cell migration in response to VEGF. *Cytokine* 32: 206-212.
175. Silver, D. A., I. Pellicer, W. R. Fair, W. D. Heston, and C. Cordon-Cardo. 1997. Prostate-specific membrane antigen expression in normal and malignant human tissues. *Clin Cancer Res* 3: 81-85.
176. Harada, M., S. Matsueda, A. Yao, R. Ogata, M. Noguchi, and K. Itoh. 2004. Prostate-related antigen-derived new peptides having the capacity of inducing prostate cancer-reactive CTLs in HLA-A2+ prostate cancer patients. *Oncology reports* 12: 601-607.
177. Boss, C. N., F. Grunebach, K. Brauer, M. Hantschel, V. Mirakaj, T. Weinschenk, S. Stevanovic, H. G. Rammensee, and P. Brossart. 2007. Identification and characterization of T-cell epitopes deduced from RGS5, a novel broadly expressed tumor antigen. *Clin Cancer Res* 13: 3347-3355.

178. Christian, S., R. Winkler, I. Helfrich, A. M. Boos, E. Besemfelder, D. Schadendorf, and H. G. Augustin. 2008. Endosialin (Tem1) is a marker of tumor-associated myofibroblasts and tumor vessel-associated mural cells. *Am J Pathol* 172: 486-494.
179. Kuball, J., F. W. Schmitz, R. H. Voss, E. A. Ferreira, R. Engel, P. Guillaume, S. Strand, P. Romero, C. Huber, L. A. Sherman, and M. Theobald. 2005. Cooperation of human tumor-reactive CD4+ and CD8+ T cells after redirection of their specificity by a high-affinity p53A2.1-specific TCR. *Immunity* 22: 117-129.
180. Woodland, D. L., and R. W. Dutton. 2003. Heterogeneity of CD4(+) and CD8(+) T cells. *Current opinion in immunology* 15: 336-342.
181. !!! INVALID CITATION !!!
182. Jain, R. K. 2005. Antiangiogenic therapy for cancer: current and emerging concepts. *Oncology* 19: 7-16.
183. Manzur, M., J. Hamzah, and R. Ganss. 2008. Modulation of the "blood-tumor" barrier improves immunotherapy. *Cell cycle* 7: 2452-2455.
184. Krupnick, A. S., D. Kreisel, S. H. Popma, K. R. Balsara, W. Y. Szeto, A. M. Krasinskas, M. Riha, A. D. Wells, L. A. Turka, and B. R. Rosengard. 2002. Mechanism of T cell-mediated endothelial apoptosis. *Transplantation* 74: 871-876.
185. Suidan, G. L., J. R. McDole, Y. Chen, I. Pirko, and A. J. Johnson. 2008. Induction of blood brain barrier tight junction protein alterations by CD8 T cells. *PLoS One* 3: e3037.
186. Suzuki, H., K. Shibano, M. Okane, I. Kono, Y. Matsui, K. Yamane, and H. Kashiwagi. 1989. Interferon-gamma modulates messenger RNA levels of c-sis (PDGF-B chain), PDGF-A chain, and IL-1 beta genes in human vascular endothelial cells. *Am J Pathol* 134: 35-43.
187. Molander, C., A. Kallin, H. Izumi, L. Ronnstrand, and K. Funa. 2000. TNF-alpha suppresses the PDGF beta-receptor kinase. *Experimental cell research* 258: 65-71.
188. Strehl, B., U. Seifert, E. Kruger, S. Heink, U. Kuckelkorn, and P. M. Kloetzel. 2005. Interferon-gamma, the functional plasticity of the ubiquitin-proteasome system, and MHC class I antigen processing. *Immunological reviews* 207: 19-30.
189. Sun, Y., S. Stevanovic, M. Song, A. Schwantes, C. J. Kirkpatrick, D. Schadendorf, and K. Cichutek. 2006. The kinase insert domain-containing receptor is an angiogenesis-associated antigen recognized by human cytotoxic T lymphocytes. *Blood* 107: 1476-1483.
190. van der Most, R. G., A. Currie, B. W. Robinson, and R. A. Lake. 2006. Cranking the immunologic engine with chemotherapy: using context to drive tumor antigen cross-presentation towards useful antitumor immunity. *Cancer Res* 66: 601-604.
191. Butterfield, L. H., A. Ribas, V. B. Dissette, S. N. Amarnani, H. T. Vu, D. Oseguera, H. J. Wang, R. M. Elashoff, W. H. McBride, B. Mukherji, A. J. Cochran, J. A. Glaspy, and J. S. Economou. 2003. Determinant spreading associated with clinical response in dendritic cell-based immunotherapy for malignant melanoma. *Clin Cancer Res* 9: 998-1008.
192. Ranieri, E., L. S. Kierstead, H. Zarour, J. M. Kirkwood, M. T. Lotze, T. Whiteside, and W. J. Storkus. 2000. Dendritic cell/peptide cancer vaccines: clinical responsiveness and epitope spreading. *Immunological investigations* 29: 121-125.
193. Lehmann, P. V., E. E. Sercarz, T. Forsthuber, C. M. Dayan, and G. Gammon. 1993. Determinant spreading and the dynamics of the autoimmune T-cell repertoire. *Immunology today* 14: 203-208.

194. Jandus, C., D. Speiser, and P. Romero. 2009. Recent advances and hurdles in melanoma immunotherapy. *Pigment cell & melanoma research* 22: 711-723.
195. Seliger, B., M. J. Maeurer, and S. Ferrone. 2000. Antigen-processing machinery breakdown and tumor growth. *Immunology today* 21: 455-464.
196. Atkins, D., S. Ferrone, G. E. Schmahl, S. Storkel, and B. Seliger. 2004. Down-regulation of HLA class I antigen processing molecules: an immune escape mechanism of renal cell carcinoma? *The Journal of urology* 171: 885-889.
197. Seliger, B., R. Stoehr, D. Handke, A. Mueller, S. Ferrone, B. Wullich, A. Tannapfel, F. Hofstaedter, and A. Hartmann. 2010. Association of HLA class I antigen abnormalities with disease progression and early recurrence in prostate cancer. *Cancer Immunol Immunother* 59: 529-540.
198. Li, Y., M. N. Wang, H. Li, K. D. King, R. Bassi, H. Sun, A. Santiago, A. T. Hooper, P. Bohlen, and D. J. Hicklin. 2002. Active immunization against the vascular endothelial growth factor receptor flk1 inhibits tumor angiogenesis and metastasis. *J Exp Med* 195: 1575-1584.
199. Niethammer, A. G., R. Xiang, J. C. Becker, H. Wodrich, U. Pertl, G. Karsten, B. P. Eliceiri, and R. A. Reisfeld. 2002. A DNA vaccine against VEGF receptor 2 prevents effective angiogenesis and inhibits tumor growth. *Nature medicine* 8: 1369-1375.
200. Nair, S., D. Boczkowski, B. Moeller, M. Dewhirst, J. Vieweg, and E. Gilboa. 2003. Synergy between tumor immunotherapy and antiangiogenic therapy. *Blood* 102: 964-971.
201. Yu, P., D. A. Rowley, Y. X. Fu, and H. Schreiber. 2006. The role of stroma in immune recognition and destruction of well-established solid tumors. *Current opinion in immunology* 18: 226-231.
202. Singer, C. F., D. Gschwantler-Kaulich, A. Fink-Retter, C. Haas, G. Hudelist, K. Czerwenka, and E. Kubista. 2008. Differential gene expression profile in breast cancer-derived stromal fibroblasts. *Breast cancer research and treatment* 110: 273-281.
203. Ghilardi, C., G. Chiorino, R. Dossi, Z. Nagy, R. Giavazzi, and M. Bani. 2008. Identification of novel vascular markers through gene expression profiling of tumor-derived endothelium. *BMC genomics* 9: 201.
204. Hanson, J. A., J. W. Gillespie, A. Grover, M. A. Tangrea, R. F. Chuaqui, M. R. Emmert-Buck, J. A. Tangrea, S. K. Libutti, W. M. Linehan, and K. G. Woodson. 2006. Gene promoter methylation in prostate tumor-associated stromal cells. *Journal of the National Cancer Institute* 98: 255-261.
205. Luo, Y., D. Markowitz, R. Xiang, H. Zhou, and R. A. Reisfeld. 2007. FLK-1-based minigene vaccines induce T cell-mediated suppression of angiogenesis and tumor protective immunity in syngeneic BALB/c mice. *Vaccine* 25: 1409-1415.
206. Dong, Y., J. Qian, R. Ibrahim, J. A. Berzofsky, and S. N. Khleif. 2006. Identification of H-2Db-specific CD8+ T-cell epitopes from mouse VEGFR2 that can inhibit angiogenesis and tumor growth. *Journal of immunotherapy* 29: 32-40.
207. Firat, H., F. Garcia-Pons, S. Tourdot, S. Pascolo, A. Scardino, Z. Garcia, M. L. Michel, R. W. Jack, G. Jung, K. Kosmatopoulos, L. Mateo, A. Suhrbier, F. A. Lemonnier, and P. Langlade-Demoyen. 1999. H-2 class I knockout, HLA-A2.1-transgenic mice: a versatile animal model for preclinical evaluation of antitumor immunotherapeutic strategies. *Eur J Immunol* 29: 3112-3121.
208. Zhao, X., A. Bose, H. Komita, J. L. Taylor, M. Kawabe, N. Chi, L. Spokas, D. B. Lowe, C. Goldbach, S. Alber, S. C. Watkins, L. H. Butterfield, P. Kalinski, J. M. Kirkwood, and

W. J. Storkus. 2011. Intratumoral IL-12 gene therapy results in the crosspriming of Tc1 cells reactive against tumor-associated stromal antigens. *Mol Ther* 19: 805-814.

209. Yamaguchi, S., T. Tatsumi, T. Takehara, R. Sakamori, A. Uemura, T. Mizushima, K. Ohkawa, W. J. Storkus, and N. Hayashi. 2007. Immunotherapy of murine colon cancer using receptor tyrosine kinase EphA2-derived peptide-pulsed dendritic cell vaccines. *Cancer* 110: 1469-1477.
210. Stuber, G., G. H. Leder, W. T. Storkus, M. T. Lotze, S. Modrow, L. Szekely, H. Wolf, E. Klein, K. Karre, and G. Klein. 1994. Identification of wild-type and mutant p53 peptides binding to HLA-A2 assessed by a peptide loading-deficient cell line assay and a novel major histocompatibility complex class I peptide binding assay. *Eur J Immunol* 24: 765-768.
211. Teng, M. W., J. B. Swann, C. M. Koebel, R. D. Schreiber, and M. J. Smyth. 2008. Immune-mediated dormancy: an equilibrium with cancer. *Journal of leukocyte biology* 84: 988-993.
212. Ossowski, L., and J. A. Aguirre-Ghiso. 2010. Dormancy of metastatic melanoma. *Pigment cell & melanoma research* 23: 41-56.
213. Brown, C. E., R. Starr, C. Martinez, B. Aguilar, M. D'Apuzzo, I. Todorov, C. C. Shih, B. Badie, M. Hudecek, S. R. Riddell, and M. C. Jensen. 2009. Recognition and killing of brain tumor stem-like initiating cells by CD8+ cytolytic T cells. *Cancer Res* 69: 8886-8893.
214. Dubinett, S., and S. Sharma. 2009. Towards effective immunotherapy for lung cancer: simultaneous targeting of tumor-initiating cells and immune pathways in the tumor microenvironment. *Immunotherapy* 1: 721-725.
215. Inoda, S., Y. Hirohashi, T. Torigoe, R. Morita, A. Takahashi, H. Asanuma, M. Nakatsugawa, S. Nishizawa, Y. Tamura, T. Tsuruma, T. Terui, T. Kondo, K. Ishitani, T. Hasegawa, K. Hirata, and N. Sato. 2011. Cytotoxic T lymphocytes efficiently recognize human colon cancer stem-like cells. *Am J Pathol* 178: 1805-1813.
216. Haanen, J. B., A. Baars, R. Gomez, P. Weder, M. Smits, T. D. de Gruijl, B. M. von Blomberg, E. Bloemena, R. J. Scheper, S. M. van Ham, H. M. Pinedo, and A. J. van den Eertwegh. 2006. Melanoma-specific tumor-infiltrating lymphocytes but not circulating melanoma-specific T cells may predict survival in resected advanced-stage melanoma patients. *Cancer Immunol Immunother* 55: 451-458.
217. Balabanov, R., T. Beaumont, and P. Dore-Duffy. 1999. Role of central nervous system microvascular pericytes in activation of antigen-primed splenic T-lymphocytes. *Journal of neuroscience research* 55: 578-587.
218. Fabry, Z., M. Sandor, T. F. Gajewski, J. A. Herlein, M. M. Waldschmidt, R. G. Lynch, and M. N. Hart. 1993. Differential activation of Th1 and Th2 CD4+ cells by murine brain microvessel endothelial cells and smooth muscle/pericytes. *J Immunol* 151: 38-47.
219. Buckanovich, R. J., A. Facciabene, S. Kim, F. Benencia, D. Sasaroli, K. Balint, D. Katsaros, A. O'Brien-Jenkins, P. A. Gimotty, and G. Coukos. 2008. Endothelin B receptor mediates the endothelial barrier to T cell homing to tumors and disables immune therapy. *Nature medicine* 14: 28-36.
220. Helfrich, I., I. Scheffrahn, S. Bartling, J. Weis, V. von Felbert, M. Middleton, M. Kato, S. Ergun, and D. Schadendorf. 2010. Resistance to antiangiogenic therapy is directed by vascular phenotype, vessel stabilization, and maturation in malignant melanoma. *J Exp Med* 207: 491-503.

221. Gaengel, K., G. Genove, A. Armulik, and C. Betsholtz. 2009. Endothelial-mural cell signaling in vascular development and angiogenesis. *Arterioscler Thromb Vasc Biol* 29: 630-638.
222. Finke, J. H., R. Tubbs, B. Connelly, E. Pontes, and J. Montie. 1988. Tumor-infiltrating lymphocytes in patients with renal-cell carcinoma. *Ann N Y Acad Sci* 532: 387-394.
223. Muul, L. M., P. J. Spiess, E. P. Director, and S. A. Rosenberg. 1987. Identification of specific cytolytic immune responses against autologous tumor in humans bearing malignant melanoma. *J Immunol* 138: 989-995.
224. Lokich, J. 1997. Spontaneous regression of metastatic renal cancer. Case report and literature review. *Am J Clin Oncol* 20: 416-418.
225. Najjar, Y. G., and B. I. Rini. 2012. Novel agents in renal carcinoma: a reality check. *Therapeutic advances in medical oncology* 4: 183-194.
226. Murphy, G. P., and W. J. Hrushesky. 1973. A murine renal cell carcinoma. *Journal of the National Cancer Institute* 50: 1013-1025.
227. Klungsoyr, L., and K. F. Stoa. 1954. Spectrophotometric determination of hemoglobin oxygen saturation: the method of Drabkin & Schmidt as modified for its use in clinical routine analysis. *Scand J Clin Lab Invest* 6: 270-276.
228. Stallcup, W. B. 2002. The NG2 proteoglycan: past insights and future prospects. *J Neurocytol* 31: 423-435.
229. Trevino-Villarreal, J. H., D. A. Cotanche, R. Sepulveda, M. E. Bortoni, O. Manneberg, T. Udagawa, and R. A. Rogers. 2011. Host-derived pericytes and Sca-1+ cells predominate in the MART-1- stroma fraction of experimentally induced melanoma. *The journal of histochemistry and cytochemistry : official journal of the Histochemistry Society* 59: 1060-1075.
230. Sasaki, K., X. Zhu, C. Vasquez, F. Nishimura, J. E. Dusak, J. Huang, M. Fujita, A. Wesa, D. M. Potter, P. R. Walker, W. J. Storkus, and H. Okada. 2007. Preferential expression of very late antigen-4 on type 1 CTL cells plays a critical role in trafficking into central nervous system tumors. *Cancer Res* 67: 6451-6458.
231. Huang, Y., S. Goel, D. G. Duda, D. Fukumura, and R. K. Jain. 2013. Vascular normalization as an emerging strategy to enhance cancer immunotherapy. *Cancer Res* 73: 2943-2948.
232. Matsumoto, S., H. Yasui, S. Batra, Y. Kinoshita, M. Bernardo, J. P. Munasinghe, H. Utsumi, R. Choudhuri, N. Devasahayam, S. Subramanian, J. B. Mitchell, and M. C. Krishna. 2009. Simultaneous imaging of tumor oxygenation and microvascular permeability using Overhauser enhanced MRI. *Proc Natl Acad Sci U S A* 106: 17898-17903.
233. Wilson, W. R., and M. P. Hay. 2011. Targeting hypoxia in cancer therapy. *Nat Rev Cancer* 11: 393-410.
234. Cabarcas, S. M., L. A. Mathews, and W. L. Farrar. 2011. The cancer stem cell niche--there goes the neighborhood? *Int J Cancer* 129: 2315-2327.
235. Levesque, J. P., I. G. Winkler, J. Hendy, B. Williams, F. Helwani, V. Barbier, B. Nowlan, and S. K. Nilsson. 2007. Hematopoietic progenitor cell mobilization results in hypoxia with increased hypoxia-inducible transcription factor-1 alpha and vascular endothelial growth factor A in bone marrow. *Stem Cells* 25: 1954-1965.
236. Roesch, A., M. Fukunaga-Kalabis, E. C. Schmidt, S. E. Zabierowski, P. A. Brafford, A. Vultur, D. Basu, P. Gimotty, T. Vogt, and M. Herlyn. 2010. A temporarily distinct

subpopulation of slow-cycling melanoma cells is required for continuous tumor growth. *Cell* 141: 583-594.
237. Mathieu, J., Z. Zhang, W. Zhou, A. J. Wang, J. M. Heddleston, C. M. Pinna, A. Hubaud, B. Stadler, M. Choi, M. Bar, M. Tewari, A. Liu, R. Vessella, R. Rostomily, D. Born, M. Horwitz, C. Ware, C. A. Blau, M. A. Cleary, J. N. Rich, and H. Ruohola-Baker. 2011. HIF induces human embryonic stem cell markers in cancer cells. *Cancer Res* 71: 4640-4652.
238. Liang, D., Y. Ma, J. Liu, C. G. Trope, R. Holm, J. M. Nesland, and Z. Suo. 2012. The hypoxic microenvironment upgrades stem-like properties of ovarian cancer cells. *BMC Cancer* 12: 201.
239. Espinoza, I., and L. Miele. 2013. Notch inhibitors for cancer treatment. *Pharmacology & therapeutics* 139: 95-110.
240. Neish, A. S., A. J. Williams, H. J. Palmer, M. Z. Whitley, and T. Collins. 1992. Functional analysis of the human vascular cell adhesion molecule 1 promoter. *J Exp Med* 176: 1583-1593.
241. Saha, B., S. Jyothi Prasanna, B. Chandrasekar, and D. Nandi. 2010. Gene modulation and immunoregulatory roles of interferon gamma. *Cytokine* 50: 1-14.
242. Reis, M., C. J. Czupalla, N. Ziegler, K. Devraj, J. Zinke, S. Seidel, R. Heck, S. Thom, J. Macas, E. Bockamp, M. Fruttiger, M. M. Taketo, S. Dimmeler, K. H. Plate, and S. Liebner. 2012. Endothelial Wnt/beta-catenin signaling inhibits glioma angiogenesis and normalizes tumor blood vessels by inducing PDGF-B expression. *J Exp Med* 209: 1611-1627.
243. Abdallah, B. M., and M. Kassem. 2012. New factors controlling the balance between osteoblastogenesis and adipogenesis. *Bone* 50: 540-545.
244. Ueno, K., H. Hirata, Y. Hinoda, and R. Dahiya. 2013. Frizzled homolog proteins, microRNAs and Wnt signaling in cancer. *Int J Cancer* 132: 1731-1740.
245. Wang, Y., and H. S. Sul. 2006. Ectodomain shedding of preadipocyte factor 1 (Pref-1) by tumor necrosis factor alpha converting enzyme (TACE) and inhibition of adipocyte differentiation. *Molecular and cellular biology* 26: 5421-5435.
246. Zhang, J., S. Fukuhara, K. Sako, T. Takenouchi, H. Kitani, T. Kume, G. Y. Koh, and N. Mochizuki. 2011. Angiopoietin-1/Tie2 signal augments basal Notch signal controlling vascular quiescence by inducing delta-like 4 expression through AKT-mediated activation of beta-catenin. *The Journal of biological chemistry* 286: 8055-8066.
247. Perez-Cabezas, B., M. Naranjo-Gomez, P. Bastos-Amador, G. Requena-Fernandez, R. Pujol-Borrell, and F. E. Borras. 2011. Ligation of Notch receptors in human conventional and plasmacytoid dendritic cells differentially regulates cytokine and chemokine secretion and modulates Th cell polarization. *J Immunol* 186: 7006-7015.
248. Rini, B. I., and M. B. Atkins. 2009. Resistance to targeted therapy in renal-cell carcinoma. *Lancet Oncol* 10: 992-1000.
249. Chi, N., J. K. Maranchie, L. J. Appleman, and W. J. Storkus. 2010. Update on vaccine development for renal cell cancer. *Research and Reports in Urology* 2010: 125-141.
250. Siekmann, A. F., and N. D. Lawson. 2007. Notch signalling and the regulation of angiogenesis. *Cell Adh Migr* 1: 104-106.
251. Maraver, A., P. J. Fernandez-Marcos, D. Herranz, M. Canamero, M. Munoz-Martin, G. Gomez-Lopez, F. Mulero, D. Megias, M. Sanchez-Carbayo, J. Shen, M. Sanchez-Cespedes, T. Palomero, A. Ferrando, and M. Serrano. 2012. Therapeutic effect of

gamma-secretase inhibition in KrasG12V-driven non-small cell lung carcinoma by derepression of DUSP1 and inhibition of ERK. *Cancer cell* 22: 222-234.
252. Krebs, L. T., Y. Xue, C. R. Norton, J. R. Shutter, M. Maguire, J. P. Sundberg, D. Gallahan, V. Closson, J. Kitajewski, R. Callahan, G. H. Smith, K. L. Stark, and T. Gridley. 2000. Notch signaling is essential for vascular morphogenesis in mice. *Genes & development* 14: 1343-1352.
253. Glomski, K., S. Monette, K. Manova, B. De Strooper, P. Saftig, and C. P. Blobel. 2011. Deletion of Adam10 in endothelial cells leads to defects in organ-specific vascular structures. *Blood* 118: 1163-1174.
254. Bugeon, L., L. M. Gardner, A. Rose, M. Gentle, and M. J. Dallman. 2008. Cutting edge: Notch signaling induces a distinct cytokine profile in dendritic cells that supports T cell-mediated regulation and IL-2-dependent IL-17 production. *J Immunol* 181: 8189-8193.
255. Ohishi, K., B. Varnum-Finney, R. E. Serda, C. Anasetti, and I. D. Bernstein. 2001. The Notch ligand, Delta-1, inhibits the differentiation of monocytes into macrophages but permits their differentiation into dendritic cells. *Blood* 98: 1402-1407.
256. Kuijk, L. M., M. I. Verstege, N. V. Rekers, S. C. Bruijns, E. Hooijberg, B. O. Roep, T. D. de Gruijl, Y. van Kooyk, and W. W. Unger. 2013. Notch controls generation and function of human effector CD8+ T cells. *Blood* 121: 2638-2646.
257. Metsuyanim, S., O. Harari-Steinberg, E. Buzhor, D. Omer, N. Pode-Shakked, H. Ben-Hur, R. Halperin, D. Schneider, and B. Dekel. 2009. Expression of stem cell markers in the human fetal kidney. *PLoS One* 4: e6709.
258. Takebe, N., P. J. Harris, R. Q. Warren, and S. P. Ivy. 2009. Targeting cancer stem cells by inhibiting Wnt, Notch, and Hedgehog pathways. *Nat Rev Clin Oncol* 8: 97-106.
259. Ellisen, L. W., J. Bird, D. C. West, A. L. Soreng, T. C. Reynolds, S. D. Smith, and J. Sklar. 1991. TAN-1, the human homolog of the Drosophila notch gene, is broken by chromosomal translocations in T lymphoblastic neoplasms. *Cell* 66: 649-661.
260. Matsuno, Y., A. L. Coelho, G. Jarai, J. Westwick, and C. M. Hogaboam. 2012. Notch signaling mediates TGF-beta1-induced epithelial-mesenchymal transition through the induction of Snai1. *The international journal of biochemistry & cell biology* 44: 776-789.
261. Palagani, V., M. El Khatib, U. Kossatz, P. Bozko, M. R. Muller, M. P. Manns, T. Krech, N. P. Malek, and R. R. Plentz. 2012. Epithelial mesenchymal transition and pancreatic tumor initiating CD44+/EpCAM+ cells are inhibited by gamma-secretase inhibitor IX. *PLoS One* 7: e46514.
262. Xie, M., L. Zhang, C. S. He, F. Xu, J. L. Liu, Z. H. Hu, L. P. Zhao, and Y. Tian. 2012. Activation of Notch-1 enhances epithelial-mesenchymal transition in gefitinib-acquired resistant lung cancer cells. *J Cell Biochem* 113: 1501-1513.
263. Koch, U., R. Lehal, and F. Radtke. 2013. Stem cells living with a Notch. *Development* 140: 689-704.
264. Gu, J. W., P. Rizzo, A. Pannuti, T. Golde, B. Osborne, and L. Miele. 2012. Notch signals in the endothelium and cancer "stem-like" cells: opportunities for cancer therapy. *Vascular cell* 4: 7.
265. Krop, I., T. Demuth, T. Guthrie, P. Y. Wen, W. P. Mason, P. Chinnaiyan, N. Butowski, M. D. Groves, S. Kesari, S. J. Freedman, S. Blackman, J. Watters, A. Loboda, A. Podtelezhnikov, J. Lunceford, C. Chen, M. Giannotti, J. Hing, R. Beckman, and P. Lorusso. 2012. Phase I pharmacologic and pharmacodynamic study of the gamma

secretase (Notch) inhibitor MK-0752 in adult patients with advanced solid tumors. *J Clin Oncol* 30: 2307-2313.

266. Strosberg, J. R., T. Yeatman, J. Weber, D. Coppola, M. J. Schell, G. Han, K. Almhanna, R. Kim, T. Valone, H. Jump, and D. Sullivan. 2012. A phase II study of RO4929097 in metastatic colorectal cancer. *European journal of cancer* 48: 997-1003.
267. Tolcher, A. W., W. A. Messersmith, S. M. Mikulski, K. P. Papadopoulos, E. L. Kwak, D. G. Gibbon, A. Patnaik, G. S. Falchook, A. Dasari, G. I. Shapiro, J. F. Boylan, Z. X. Xu, K. Wang, A. Koehler, J. Song, S. A. Middleton, J. Deutsch, M. Demario, R. Kurzrock, and J. J. Wheler. 2012. Phase I study of RO4929097, a gamma secretase inhibitor of Notch signaling, in patients with refractory metastatic or locally advanced solid tumors. *J Clin Oncol* 30: 2348-2353.
268. Fouladi, M., C. F. Stewart, J. Olson, L. M. Wagner, A. Onar-Thomas, M. Kocak, R. J. Packer, S. Goldman, S. Gururangan, A. Gajjar, T. Demuth, L. E. Kun, J. M. Boyett, and R. J. Gilbertson. 2011. Phase I trial of MK-0752 in children with refractory CNS malignancies: a pediatric brain tumor consortium study. *J Clin Oncol* 29: 3529-3534.
269. Wang, N. J., Z. Sanborn, K. L. Arnett, L. J. Bayston, W. Liao, C. M. Proby, I. M. Leigh, E. A. Collisson, P. B. Gordon, L. Jakkula, S. Pennypacker, Y. Zou, M. Sharma, J. P. North, S. S. Vemula, T. M. Mauro, I. M. Neuhaus, P. E. Leboit, J. S. Hur, K. Park, N. Huh, P. Y. Kwok, S. T. Arron, P. P. Massion, A. E. Bale, D. Haussler, J. E. Cleaver, J. W. Gray, P. T. Spellman, A. P. South, J. C. Aster, S. C. Blacklow, and R. J. Cho. 2011. Loss-of-function mutations in Notch receptors in cutaneous and lung squamous cell carcinoma. *Proc Natl Acad Sci U S A* 108: 17761-17766.
270. Osipo, C., P. Patel, P. Rizzo, A. G. Clementz, L. Hao, T. E. Golde, and L. Miele. 2008. ErbB-2 inhibition activates Notch-1 and sensitizes breast cancer cells to a gamma-secretase inhibitor. *Oncogene* 27: 5019-5032.